

UNCLASSIFIED
UNLIMITED DISTRIBUTION

34442

CRDV RAPPORT 4233/81
DOSSIER: 3633H-039
SEPTEMBRE 1981

DREV REPORT 4233/81
FILE: 3633H-039
SEPTEMBER 1981

(NON-CONTROLLED GOODS)

DMC A

REVIEW:GCEC JUNE 2010

UNLIMITED
DISTRIBUTION
ILLIMITÉE

DETECTION RANGE PROBABILITIES OF
PASSIVE INFRARED SYSTEMS FOR THE NORTH ATLANTIC

A. Laflamme

Centre de Recherches pour la Défense
Defence Research Establishment
Valcartier, Québec

BUREAU - RECHERCHE ET DÉVELOPPEMENT
MINISTÈRE DE LA DÉFENSE NATIONALE
CANADA

NON CLASSIFIÉ
DIFFUSION ILLIMITÉE

RESEARCH AND DEVELOPMENT BRANCH
DEPARTMENT OF NATIONAL DEFENCE
CANADA

CRDV R-4233/81
DOSSIER: 3633H-039

UNCLASSIFIED

DREV R-4233/81
FILE: 3633H-039

DETECTION RANGE PROBABILITIES
OF PASSIVE INFRARED SYSTEMS
FOR THE NORTH ATLANTIC

by

A. Laflamme

CENTRE DE RECHERCHES POUR LA DEFENSE

DEFENCE RESEARCH ESTABLISHMENT

VALCARTIER

Tel: (418) 844-4271

Québec, Canada

October/octobre 1981

NON CLASSIFIE

RESUME

En s'appuyant sur les probabilités d'extinction du rayonnement infrarouge dans l'atmosphère, on présente les probabilités de distance de détection de cibles par les systèmes passifs de surveillance en infrarouge. La zone géographique d'intérêt est l'Atlantique nord. On considère les 2 principales fenêtres atmosphériques dans l'infrarouge, les bandes de 3 à 5 et de 8 à 12 micromètres. Les résultats permettent de prédire et de comparer rapidement la performance des systèmes de détection. (NC)

ABSTRACT

50 // Based on probabilities of extinction of infrared radiation in the atmosphere, range probabilities for target detection by passive infrared surveillance systems are presented. The geographic area covered is the North Atlantic. The two major atmospheric infrared windows, the 3 to 5 and the 8 to 12 micrometer bands, are considered. The results allow to predict and compare readily the performance of detection systems. // (U)

TABLE OF CONTENTS

RESUME/ABSTRACT	i
1.0 INTRODUCTION	1
2.0 MATHEMATICAL FORMULATION	1
3.0 LIMITATIONS	4
4.0 DETECTION RANGE PROBABILITIES	5
5.0 CONCLUSION	7
6.0 ACKNOWLEDGMENTS	8
7.0 REFERENCES	9

TABLE I

FIGURES 1 to 75

1.0 INTRODUCTION

A previous report proposed a simple model for the extinction of infrared radiation in the atmosphere (Ref. 1). This model was used in Ref. 2 with the probability data of the pertinent meteorological variables as derived from measurements made by Ocean Weather Ships to compute probabilities of infrared radiation extinctions in the North Atlantic.

In this report, these extinction probabilities are used to compute range probabilities for detection/tracking with passive systems in both major atmospheric IR windows, the 3.4 to 5.0 micrometer and the 7.75 to 11.75 micrometer bands, hereafter called the 3 to 5 and the 8 to 12 micrometer bands.

This work was performed at DREV between March and June 1981 under PCN 33H39 Electro-Optical Fire-Control Tracking Study.

2.0 MATHEMATICAL FORMULATION

The signal voltage produced by a passive detection system can be described (Ref. 3) as:

$$V_s = \frac{A}{r^2} \int_{\lambda_1}^{\lambda_2} J(\lambda) T_a(\lambda) T_o(\lambda) R(\lambda) d\lambda \quad [1]$$

where V_s is the the peak signal voltage in V,

A is the area of the entrance aperture of the optics in cm^2 ,

r is the range to the target in cm,

$J(\lambda)$ is the spectral radiant intensity of the target in $\text{W sr}^{-1} \mu\text{m}^{-1}$,

$T_a(\lambda)$ is the spectral transmittance of the path (dimensionless),

$T_o(\lambda)$ is the spectral transmittance of the system (dimensionless),
 $R(\lambda)$ is the spectral responsivity of the detector in $V W^{-1} \mu m^{-1}$
 λ_1 and λ_2 are the limits of the spectral interval of the sensor
in μm .

To simplify [1], it is customary to convert the wavelength-dependent terms into their integrated values over the bandpass of the sensor. Effecting this and dividing both sides of the equation by V_n , the rms noise from the sensor system, one obtains:

$$S = \frac{V_s}{V_n} = \left[\frac{A T_o R}{V_n} \right] \left[\frac{J T_a}{r^2} \right] \quad [2]$$

where S is the signal to noise ratio.

By definition, the Noise Equivalent Irradiance (NEI) is the irradiance at the entrance aperture which produces a peak signal equal to the rms noise, i.e. $S = 1$. Since the second bracketed term in [2] is the irradiance from the target, then for $S = 1$,

$$NEI = \frac{V_n}{A T_o R} \quad [3]$$

and [2] can be written

$$S = \frac{J}{NEI} \cdot \frac{T_a}{r^2} \quad [4]$$

in which NEI is the noise equivalent irradiance of the system in $W cm^{-2}$,
 J is the radiant intensity of the target in $W sr^{-1}$,
 S is the required signal to noise ratio.

The transmittance of the path from the target to the sensor has the following form:

$$T_a = e^{-\alpha_t r} \quad [5]$$

where α_t , the total extinction coefficient in km^{-1} , is the sum of 3 components:

$$\alpha_t = \alpha_a + \alpha_r + \alpha_m \quad [6]$$

in which α_a is the extinction due to aerosols, in km^{-1} ,
 α_r is the extinction due to rain, in km^{-1} ,
 α_m is the extinction due to molecular absorption, in km^{-1} .

Both α_a and α_r are relatively independent of λ and their average values can be used readily. On the other hand, α_m varies rapidly with λ and the use of a single average value would introduce appreciable errors in the calculation of T_a for different path lengths. Laflamme and Corriveau (Ref. 2) computed an average value for α_m at a fixed range of 10 km (α_{m10}) and multiplied it by a function of range (FR) as a range correction factor. Thus

$$\alpha_m = \text{FR} \times \alpha_{m10} \quad [7]$$

By substituting [5], [6] and [7] in [4], we obtain

$$1 = \frac{J}{S \bullet \text{NEI} \times 10^{10}} \frac{e^{-(\alpha_a + \alpha_r + \text{FR} \times \alpha_m)r}}{r^2} \quad [8]$$

in which the factor 10^{10} has been introduced to express the range, r , in km rather than in cm. The next equation is easily derived from [8]

$$K = \log_e \left(\frac{J}{S \cdot \text{NEI} \times 10^{10}} \right) = (\alpha_a + \alpha_r + \text{FR} \times \alpha_m)r + 2 \log_e r \quad [9]$$

K is a single number which characterizes the engagement, namely the target by its radiant intensity, J , the sensor by its noise equivalent irradiance, NEI , and by the signal to noise ratio, S , required to obtain a desired false alarm rate.

The extinction probabilities computed in Ref. 2 were used to calculate the probabilities of detection ranges by solving [9] for the range, r , with K as a parameter. The results can thus be applied to any passive system whose operation can be described by the above equations.

3.0 LIMITATIONS

In this previous discussion, the noise has been taken as system noise only and any extraneous noise signal generated by the background (clutter) has been neglected. Supplementary processing performed by the sensor system for the extraction of the target signal from clutter could possibly be assimilated to an increase in the signal to noise ratio, S , required and/or a delay in the target declaration. The detection ranges calculated in this report are then maximum ranges, as obtained against a clutter-free background. The clutter-induced reduction in detection ranges cannot be evaluated properly at this time because of the lack of statistical data on the clutter intensity and spatial distributions. Furthermore, this reduction will depend on the degree of sophistication of the sensor signal processing scheme.

A further restriction is that the model used provides extinction coefficients for horizontal paths near sea level. Since the extinction usually decreases with altitude while the signature of the target may become stronger due to an improved aspect angle, the calculated detection ranges should be even better for slant paths. On the other hand, the higher the target, the greater are the chances that the path between sensor and target will go through clouds, which would shorten ranges considerably. This last effect has not been evaluated, again because suitable statistics on cloud frequency, type, ceiling, etc. are not available presently.

4.0 DETECTION RANGE PROBABILITIES

The extinction probabilities presented in Ref. 2 were based on the measurements of meteorological parameters collected by Ocean Weather Ships. Table I lists the locations of the ships and the period of observation covered. Each location is identified by a letter and all are in the North Atlantic, except for N and P which are in the Pacific. The extinction probabilities were used with equation [9] to compute detection range probabilities with K as a parameter, so that any engagement between a given sensor and a given target can be studied with the curves presented.

The detection range probabilities have been computed for both the 3 to 5 and the 8 to 12 micrometer bands and each figure presents 2 sets of curves, each set applicable to one band in a corresponding location and season.

TABLE I
Weather Ship Locations

OWS Ident	Period of Record	Position Limits
A	1964 - 1971	61.0-63.0 N, 31.0-35.0 W
B	1965 - 1972	55.5-57.5 N, 49.5-52.5 W
C	1965 - 1972	51.5-53.5 N, 34.0-37.0 W
D	1965 - 1972	43.0-45.0 N, 40.0-42.0 W
H	1970-present	35.0-37.0 N, 47.0-49.0 W
I	1964 - 1971	59.0-61.0 N, 18.0-21.0 W
J	1964 - 1971	52.3-54.3 N, 17.8-20.8 W
K	1964 - 1971	44.0-46.0 N, 15.0-17.0 W
M	1964 - 1971	65.0-67.0 N, 0.0 - 4.0 E
N	1965 - 1972	28.5-31.5 N, 138.0-142.0 W
P	1965 - 1971	48.5-51.5 N, 142.6-147.6 W

Figures 1 to 44 show the detection range probabilities for each of the 11 locations and each season. Figures 45 to 55 refer to the same locations but present yearly averages.

The locations have also been grouped in 4 regions:

- locations A, B, C, I and M, North of the Gulf Stream;
- locations D, H, J and K, in the Gulf Stream;
- all locations above, or the North Atlantic;
- locations N and P, Pacific.

Figures 56 to 71 show the detection range probabilities averaged for each region, season by season, while figures 72 to 75 present regional yearly averages.

Each figure is properly identified and should be relatively easy to use. As an example, for a surveillance system having a NEI of $5 \times 10^{-13} \text{ W cm}^{-2}$ working against a target with a radiant intensity, J , of $3 \times 10^2 \text{ W sr}^{-1}$ and requiring a signal to noise ratio, S , of 7, the value of K would be

$$K = \log_e \left(\frac{3 \times 10^2}{7 \times 5 \times 10^{-13} \times 10^{10}} \right) = 9.06$$

The detection range probability for a given location (or region) and season can then be read directly for $K = 9$ on the appropriate figure.

5.0 CONCLUSION

By using IR radiation probabilities derived from meteorological measurements made by weather ships in the North Atlantic, detection range probabilities have been computed which are applicable to most passive IR systems in both the 3 to 5 and the 8 to 12 micrometer bands.

Although the accuracy of the results is limited by some factors such as the adequacy of the extinction model, the presence of intervening clouds, and the effect of background clutter, the curves presented readily supply reasonable estimates of the expected performance of IR surveillance systems and would be even more precise as a tool to establish the relative merits of various systems.

6.0 ACKNOWLEDGMENTS

The author wishes to thank Mr. R. Corriveau for his enlightening comments during the preparation of this report.

7.0 REFERENCES

1. Corriveau, R. and Laflamme, A., "A Simple Atmospheric Extinction Model for Infrared Radiation" (U), to be published.
2. Laflamme, A. and Corriveau, R., "Probabilities of Extinction of Infrared Radiation for the Northern Atlantic" (U), DREV R-4216/81, UNCLASSIFIED
3. Hudson, Richard D. Jr., "Infrared System Engineering", John Wiley & Sons, Inc, New York, 1969.

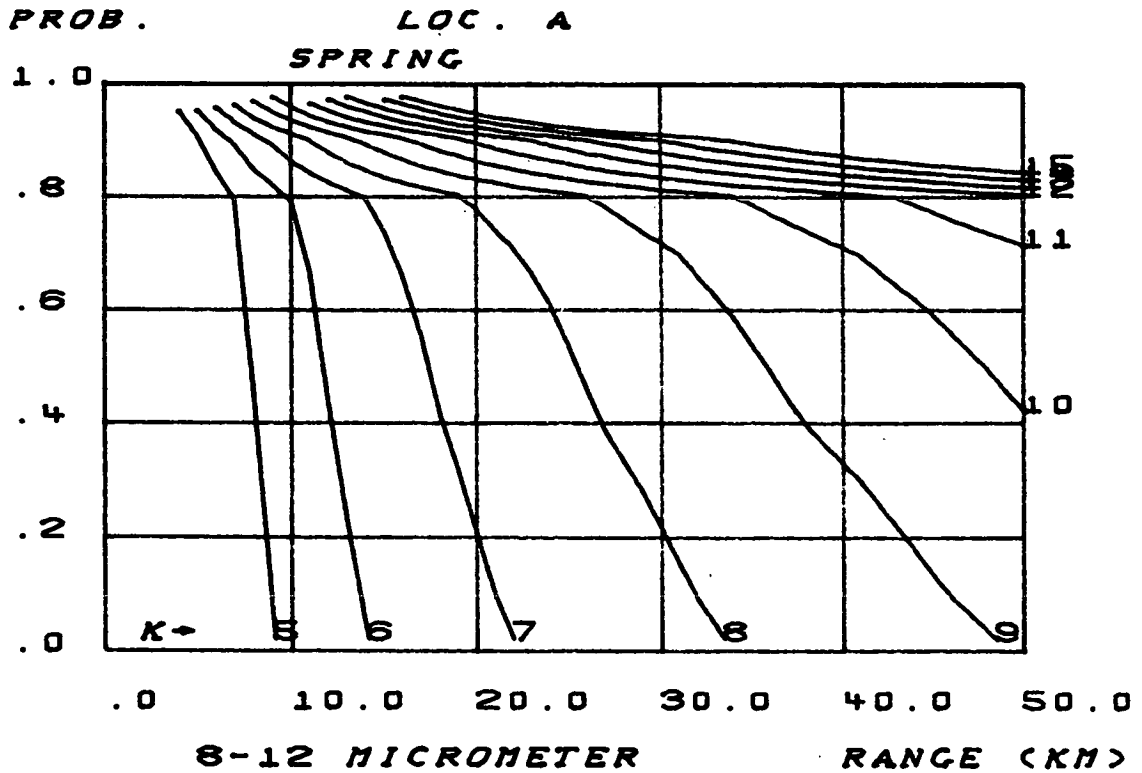
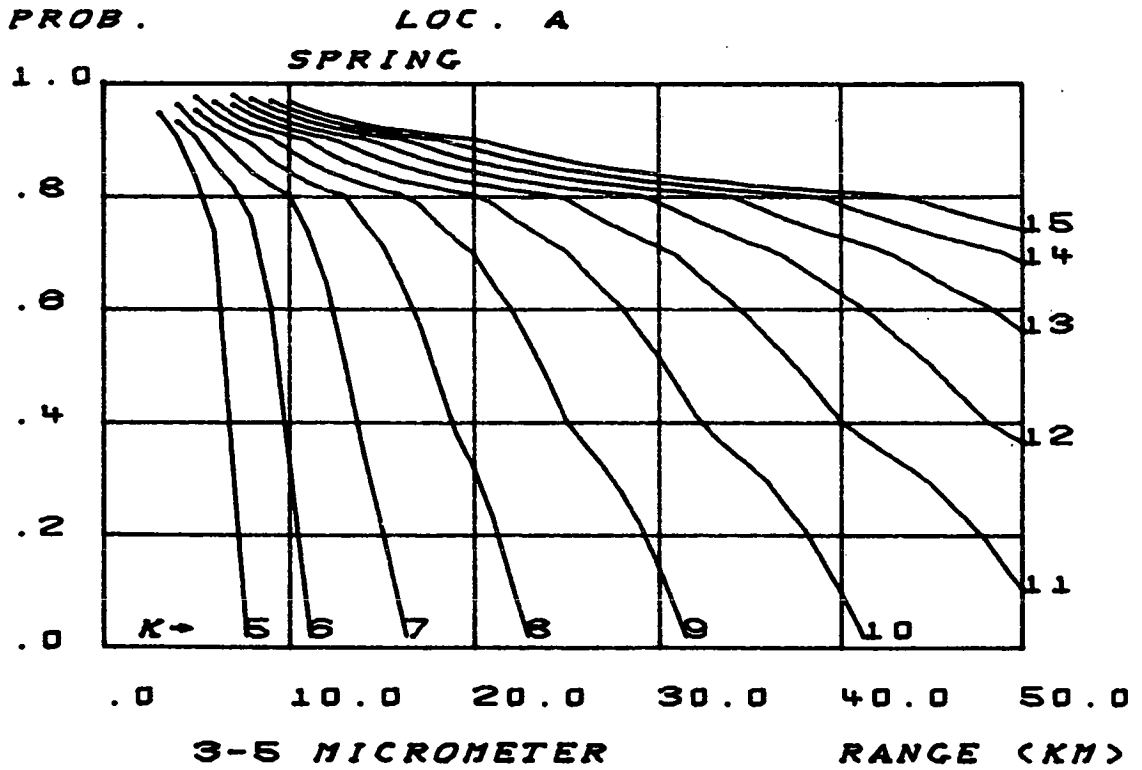


FIGURE - 1

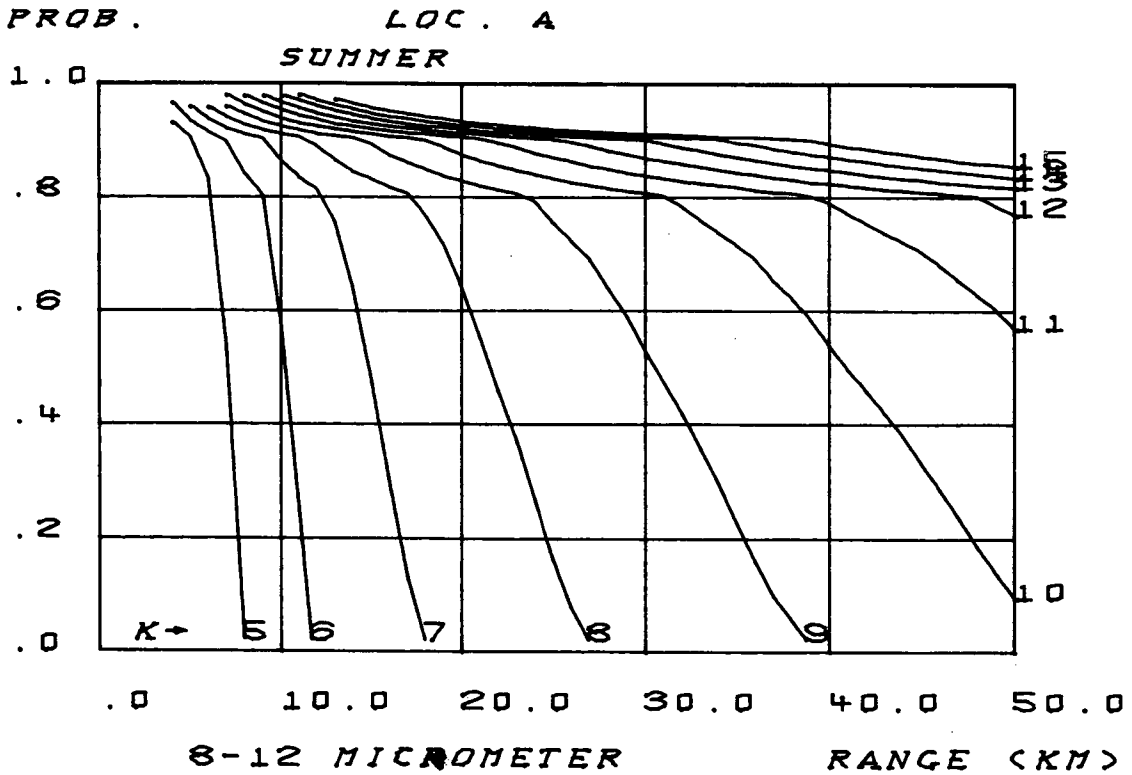
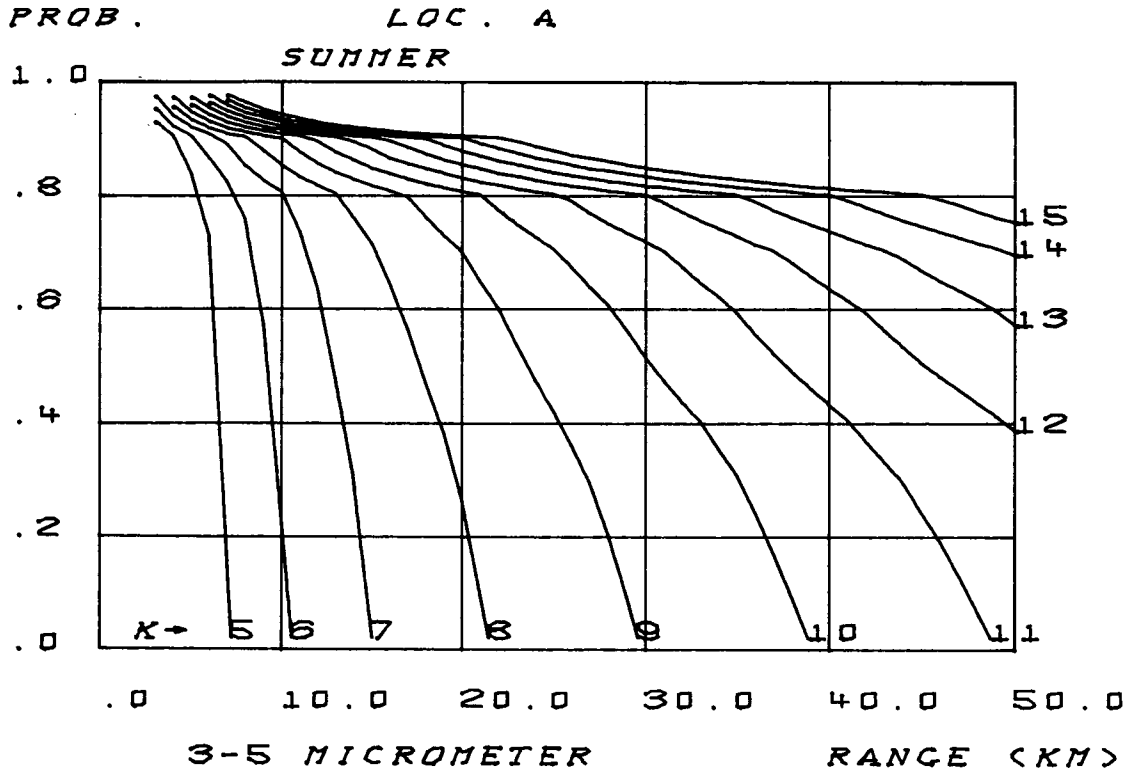


FIGURE - 2

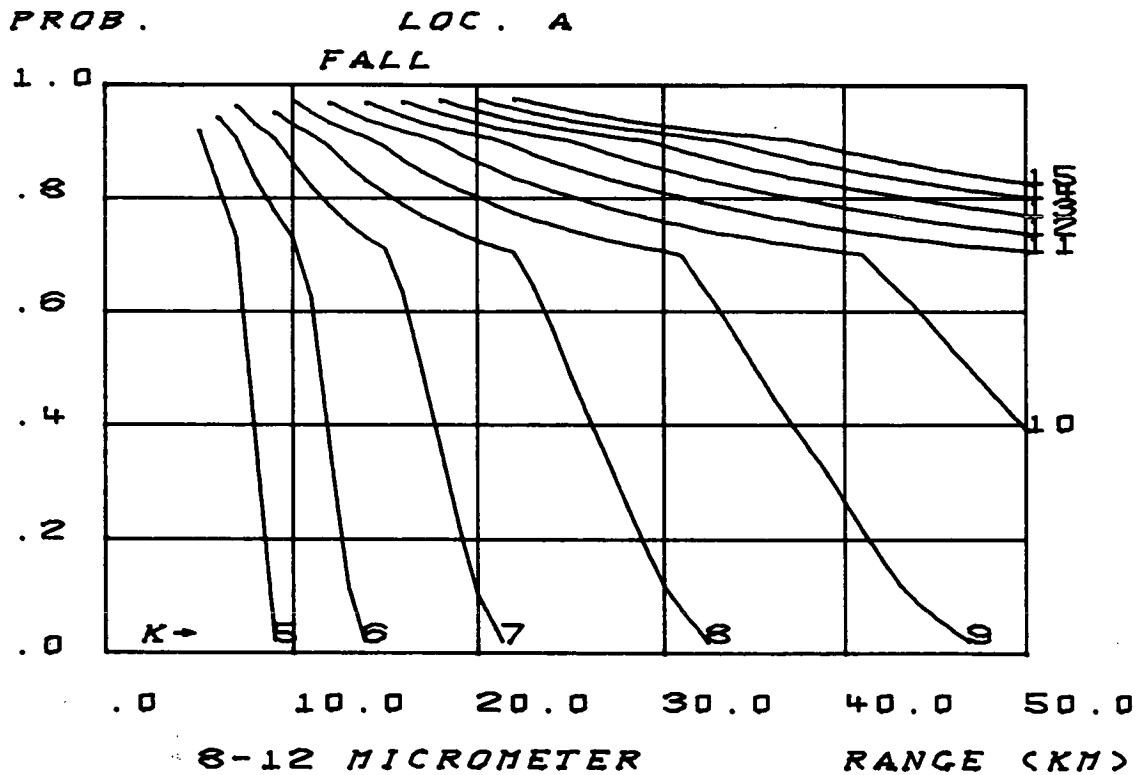
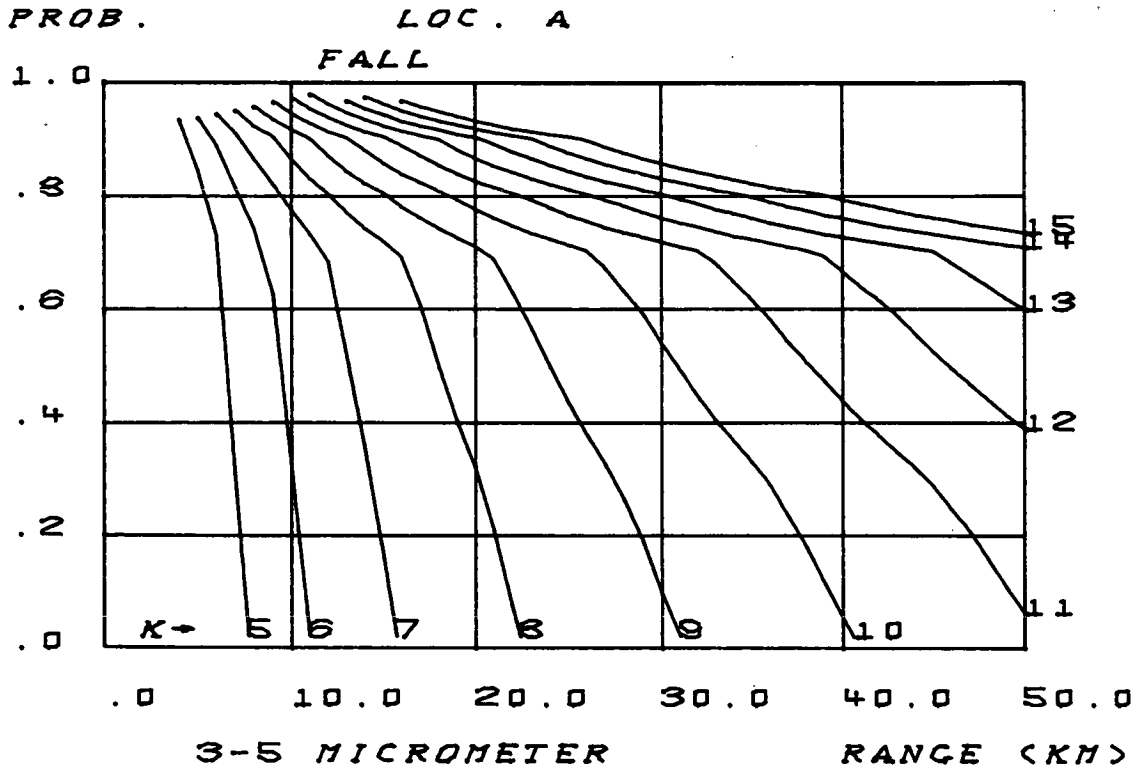


FIGURE - 3

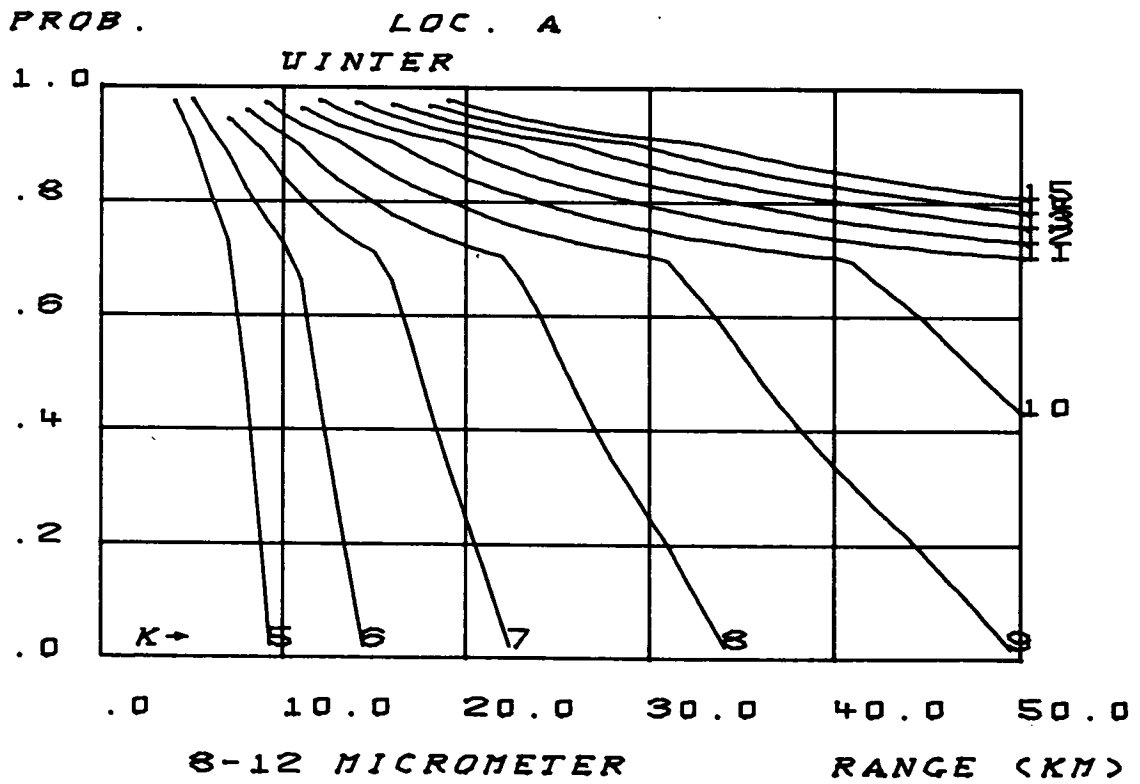
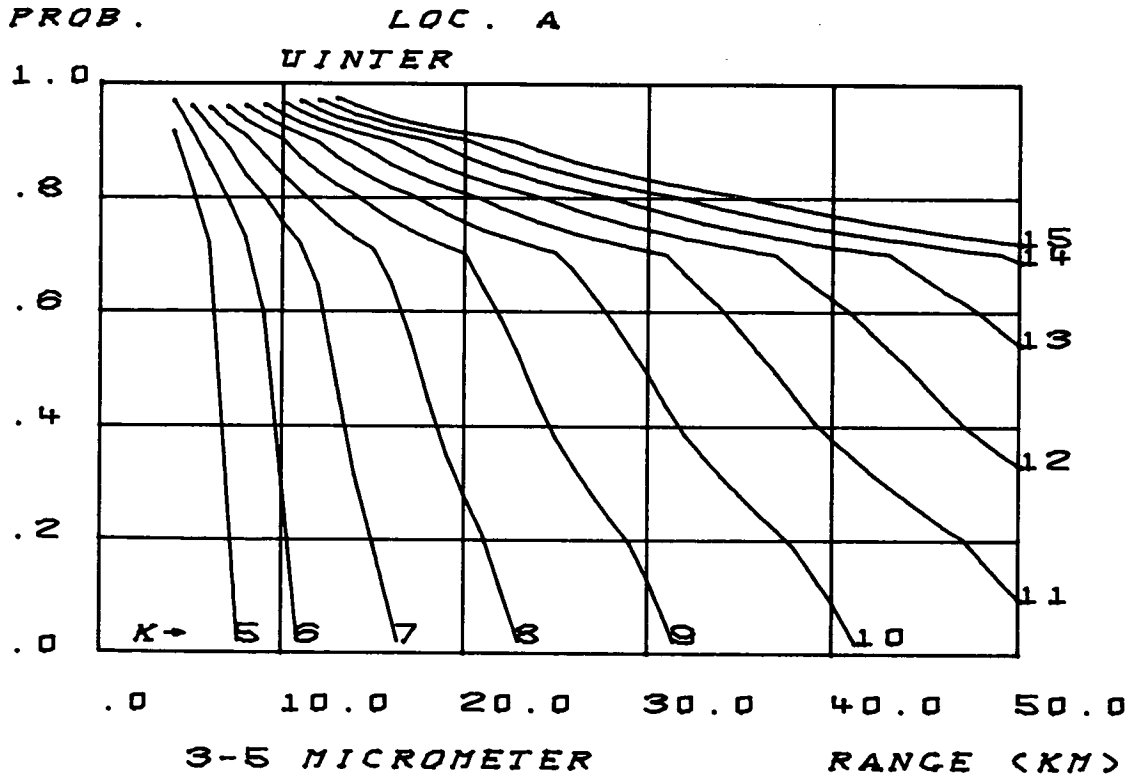


FIGURE - 4

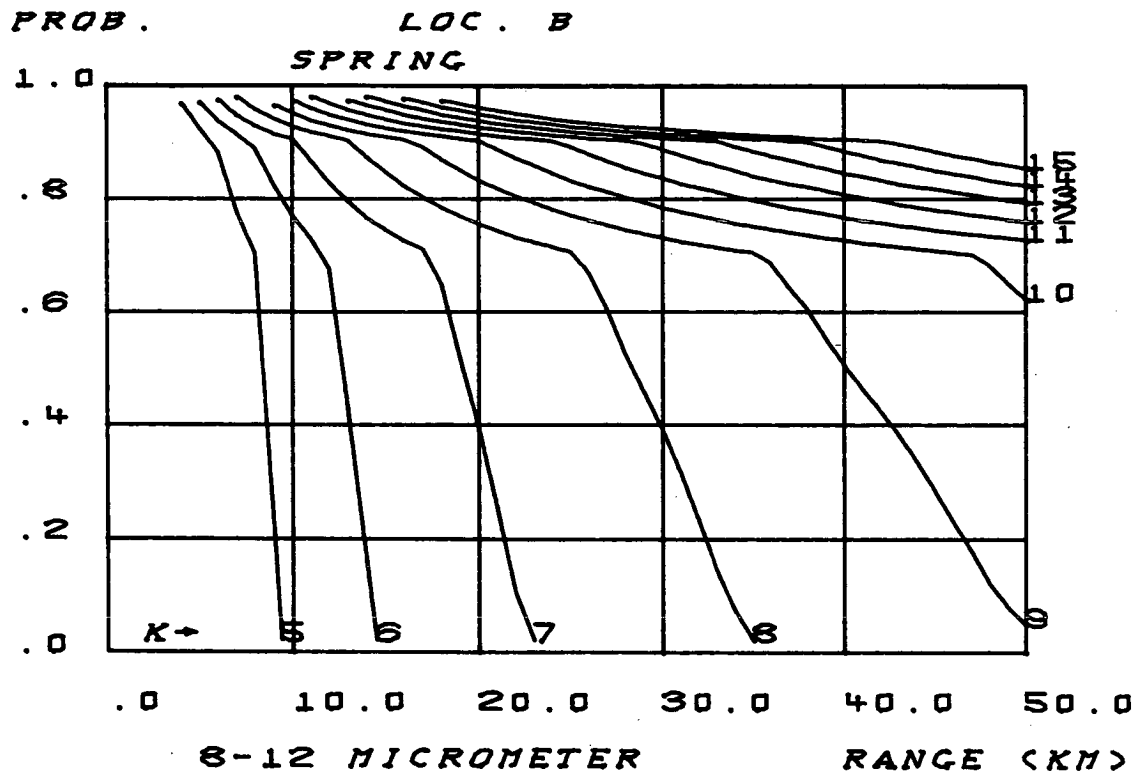
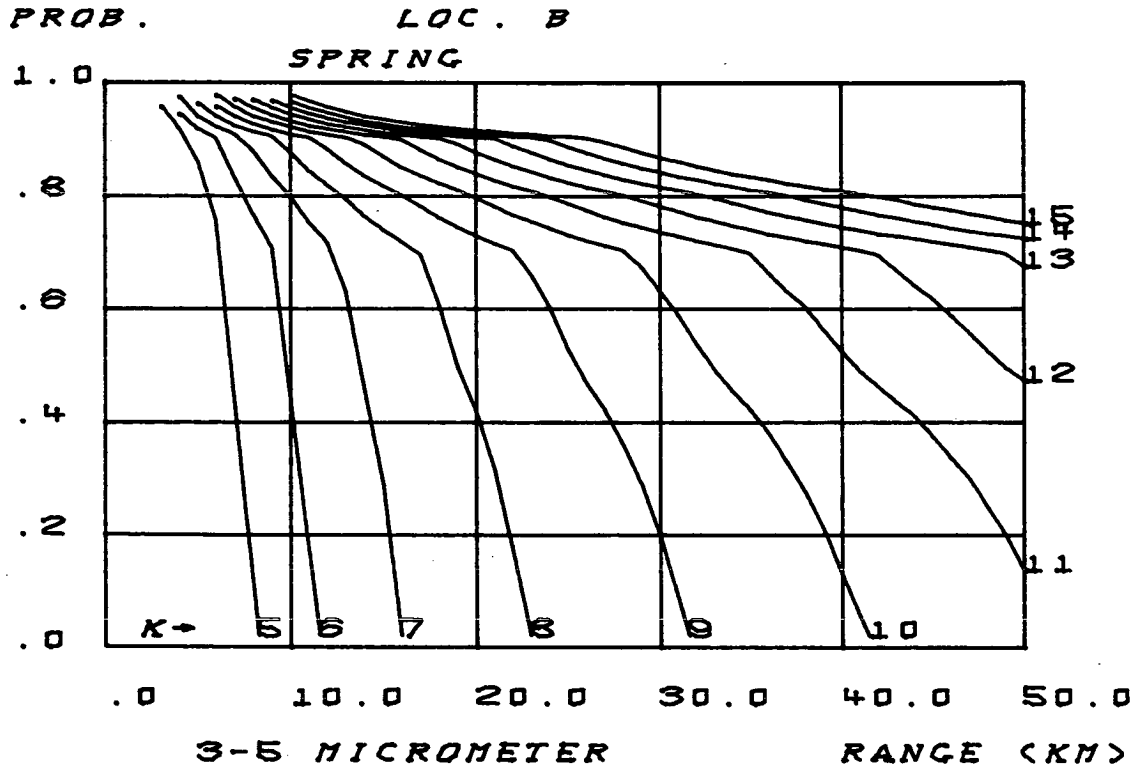


FIGURE - 5

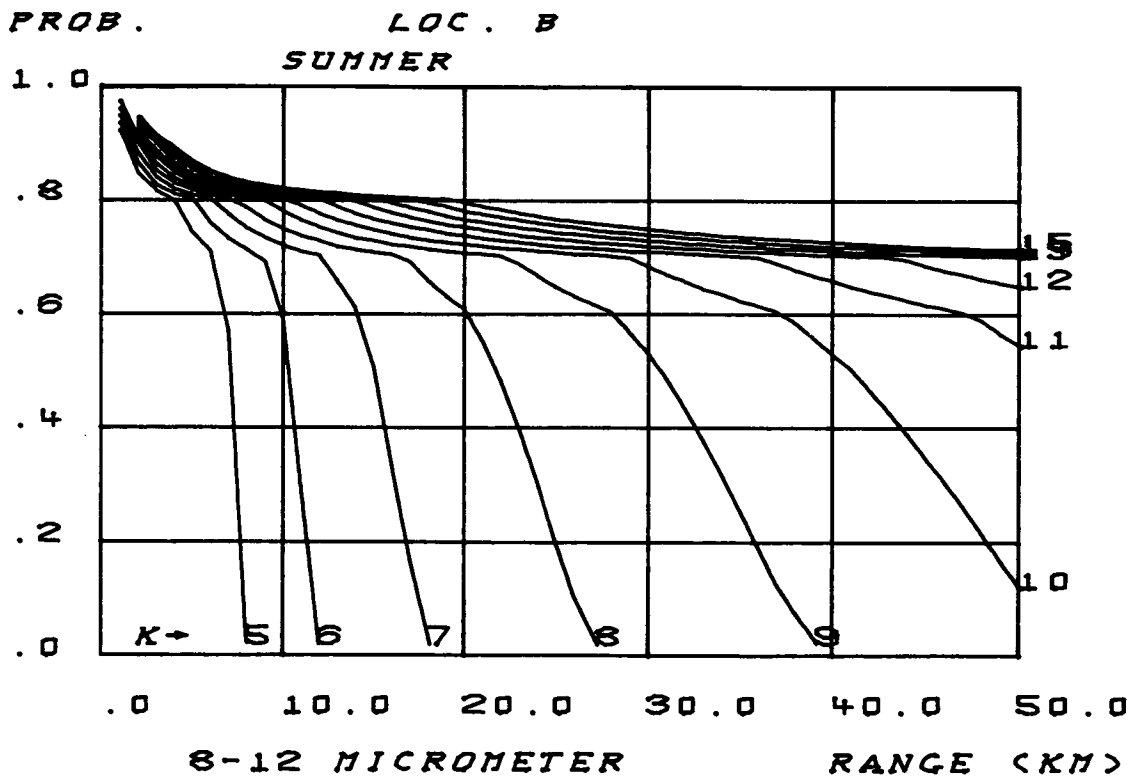
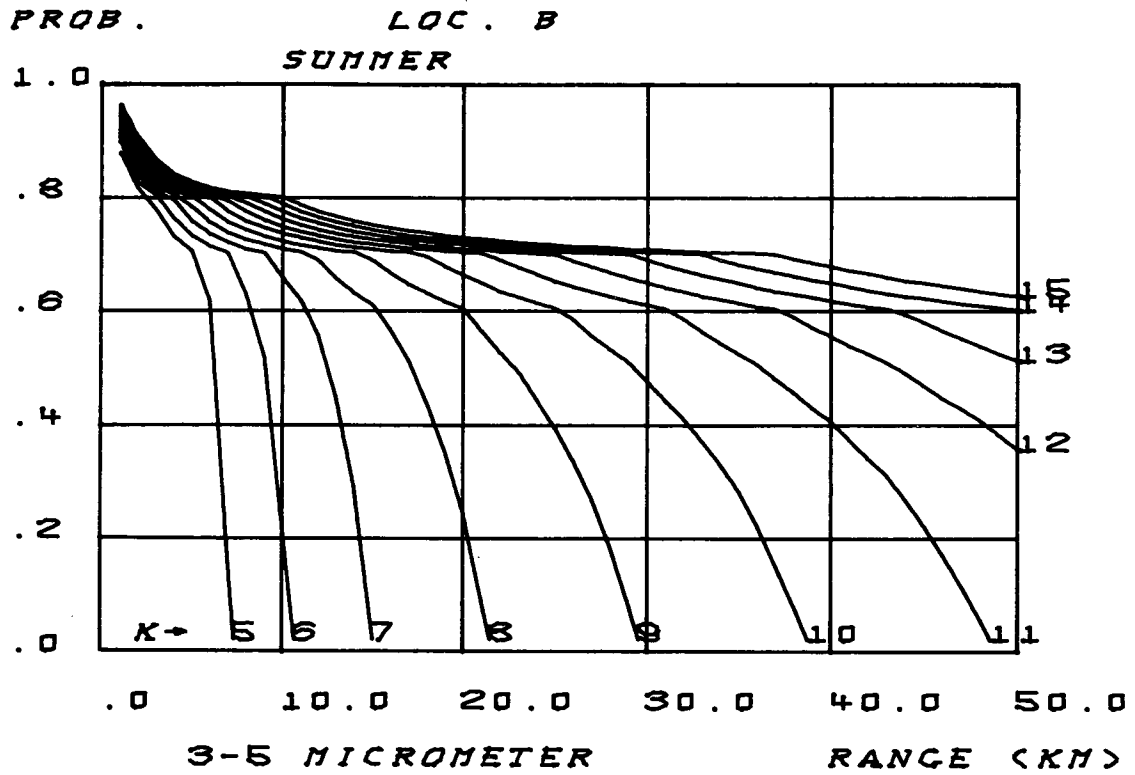


FIGURE - 6

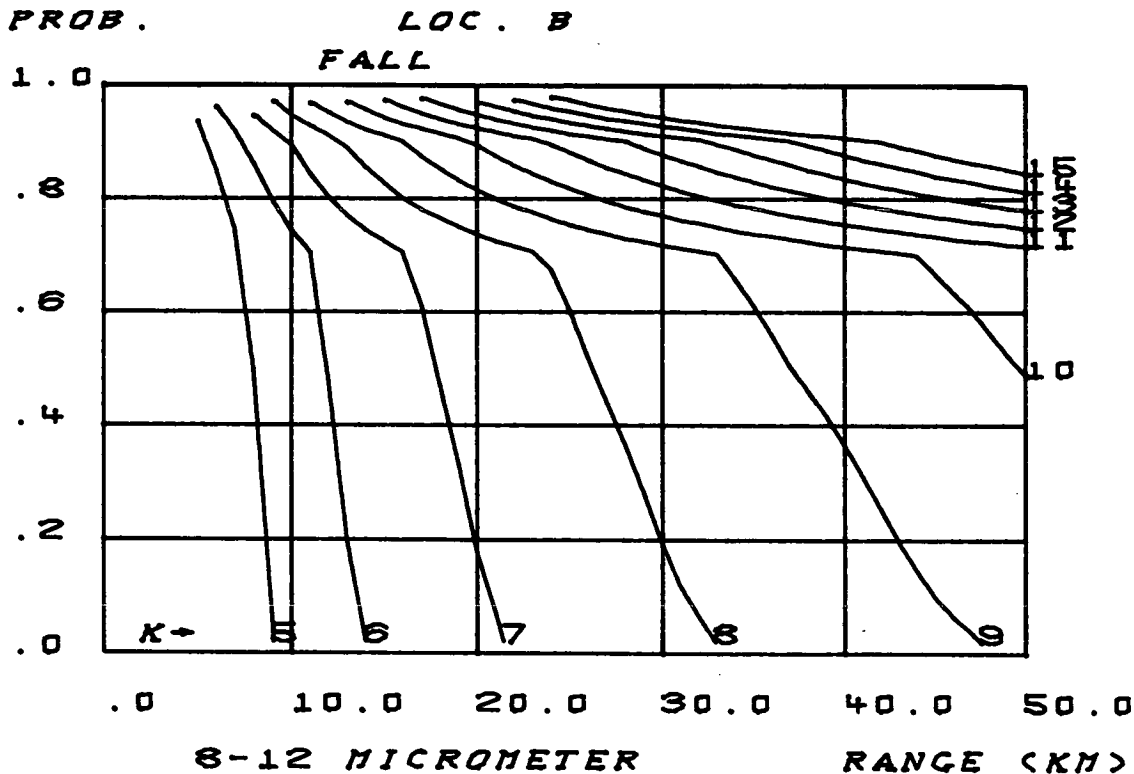
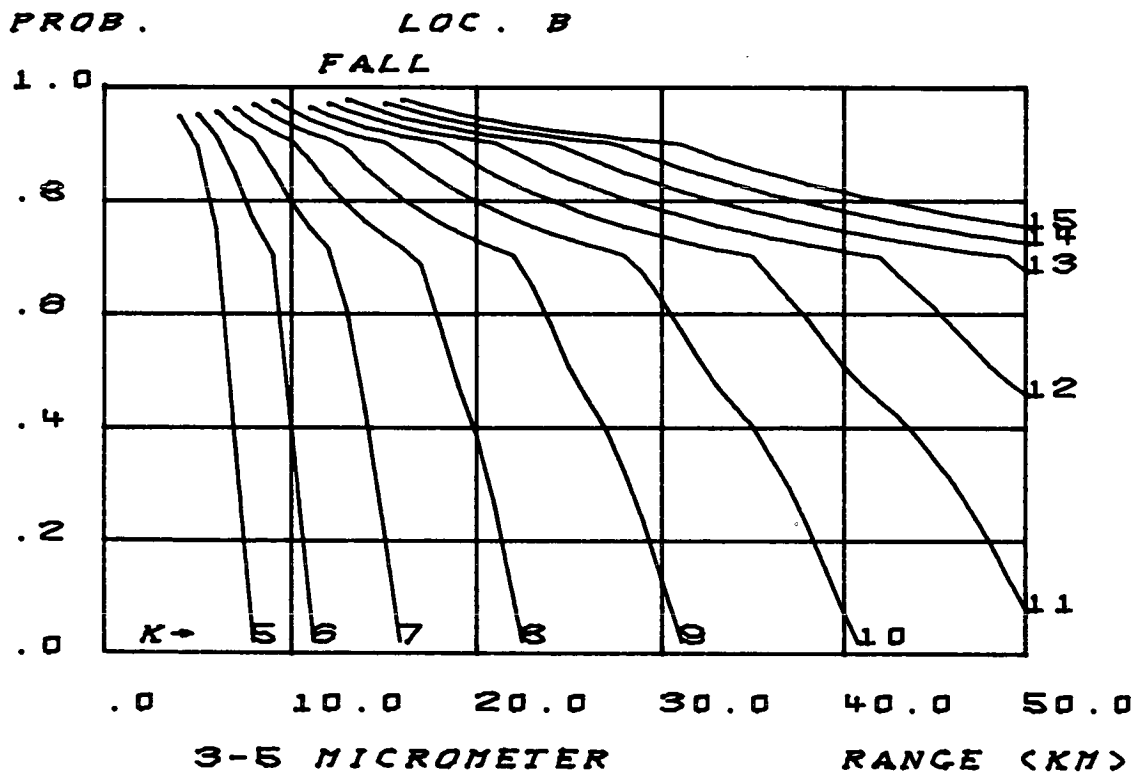


FIGURE - 7

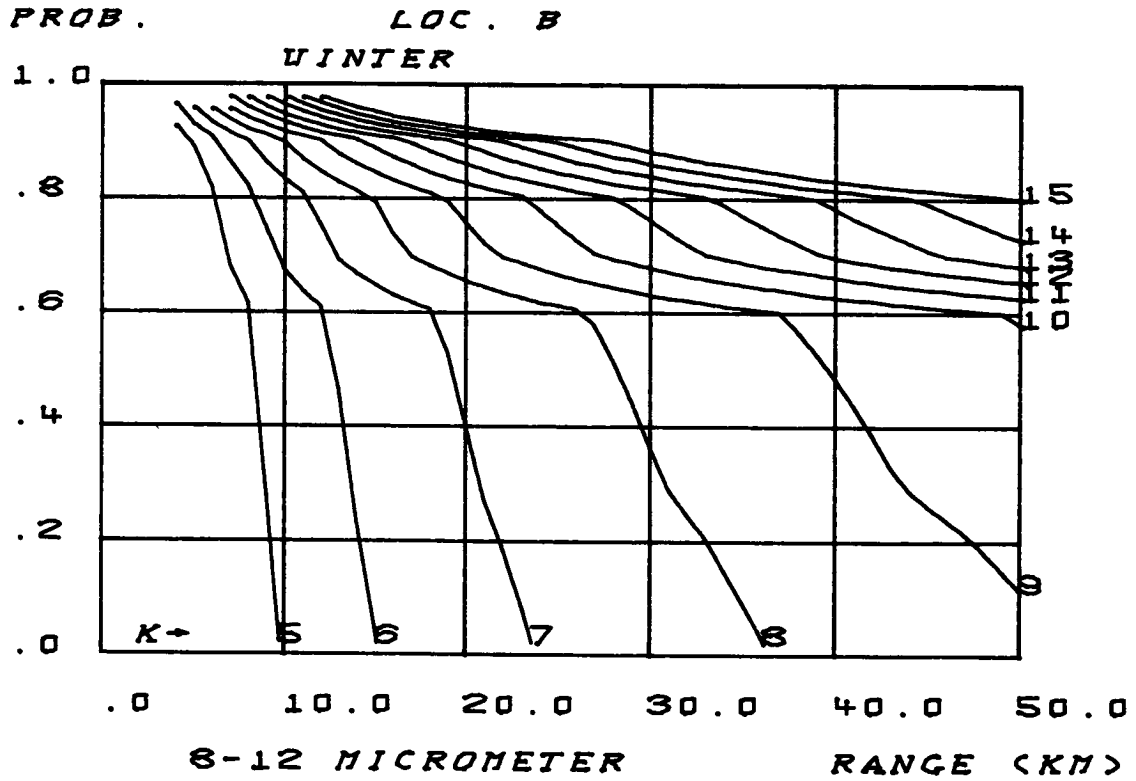
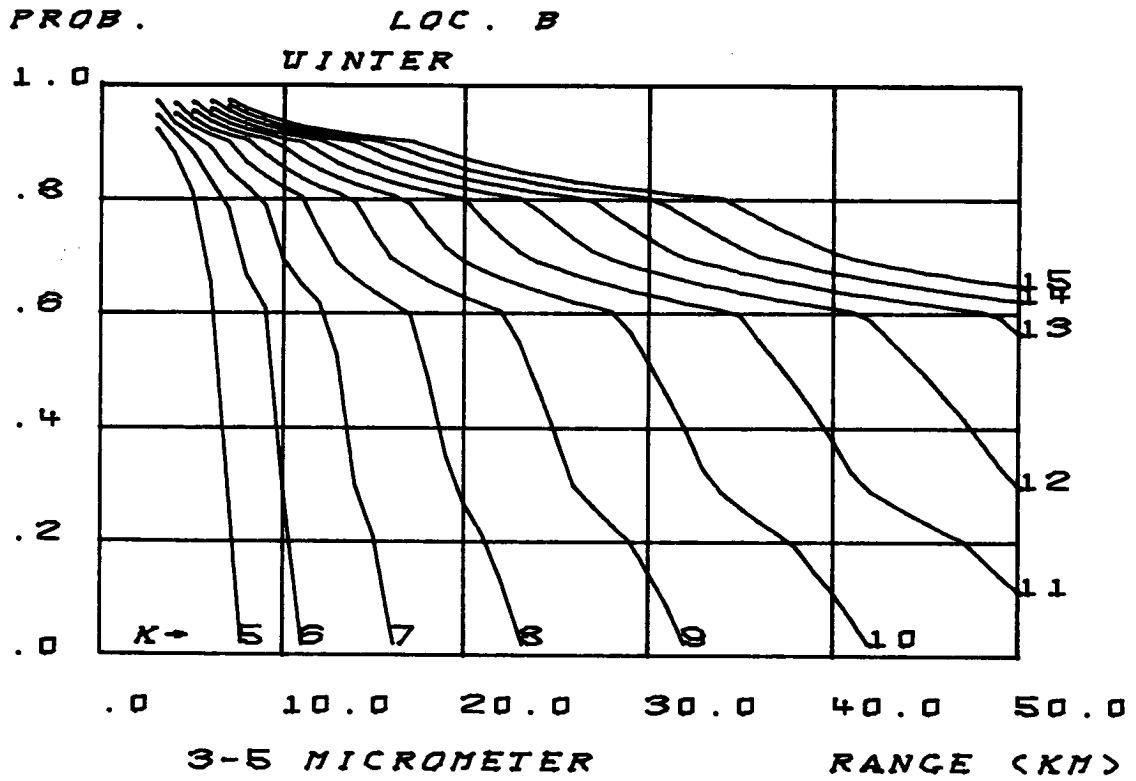


FIGURE - 8

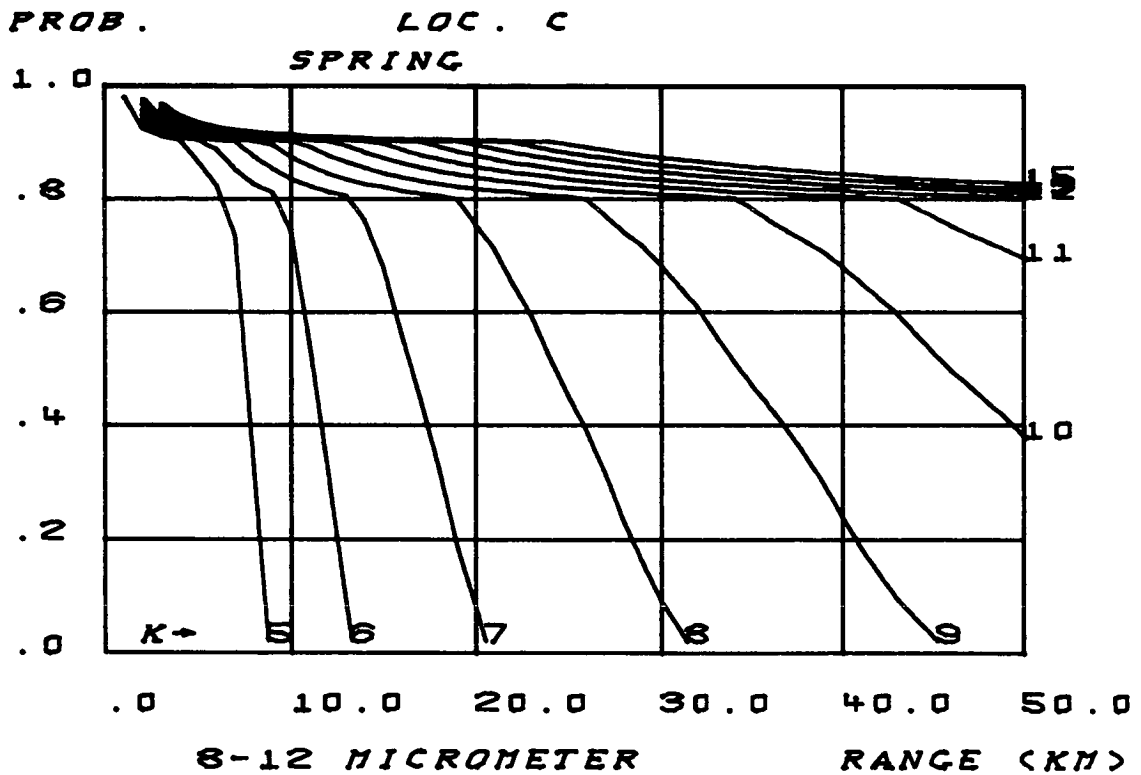
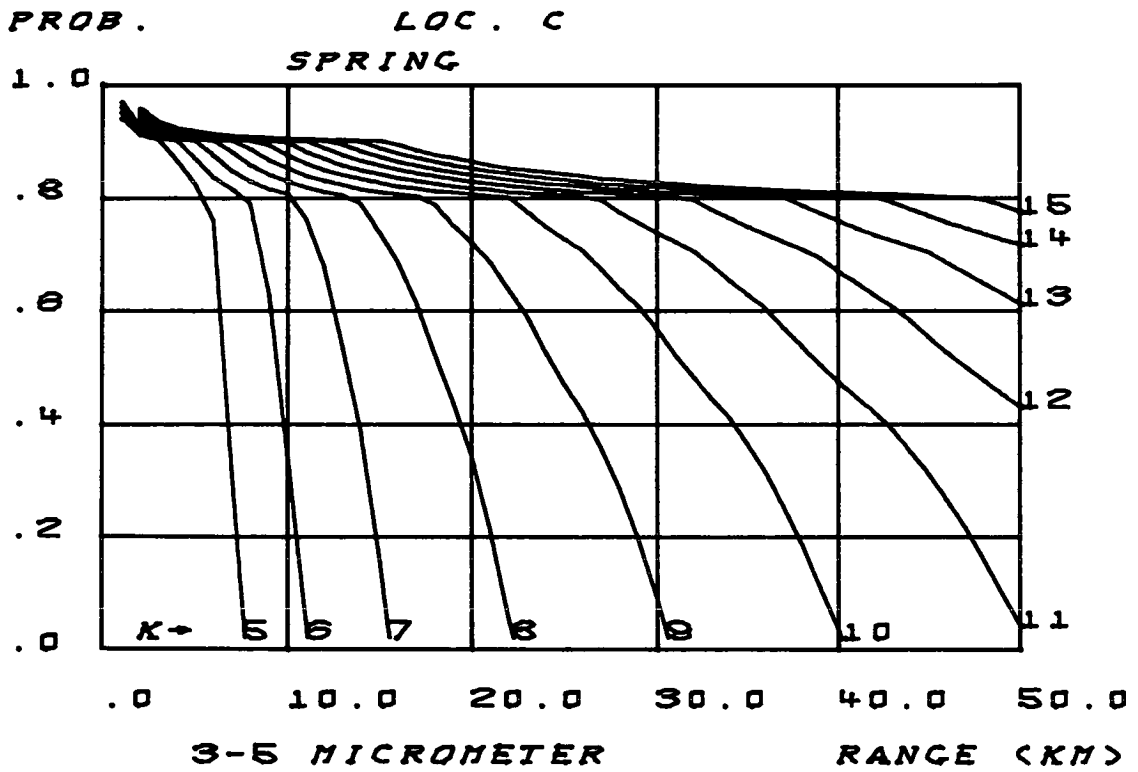


FIGURE - 9

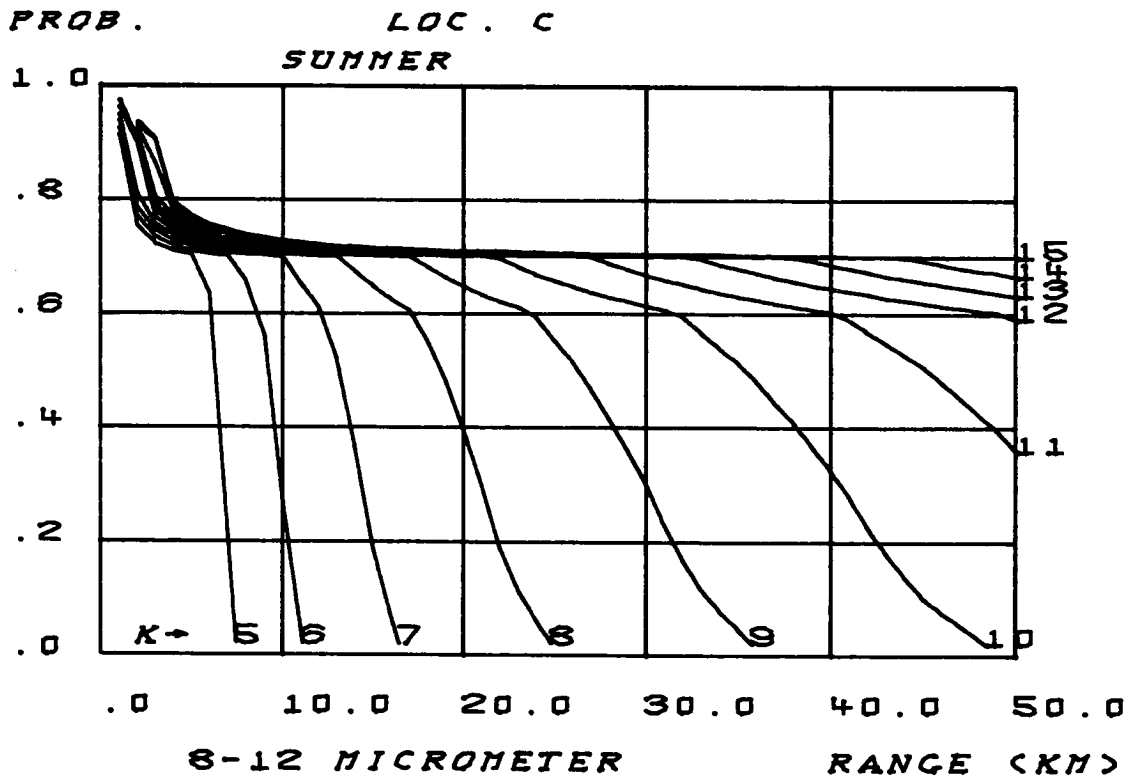
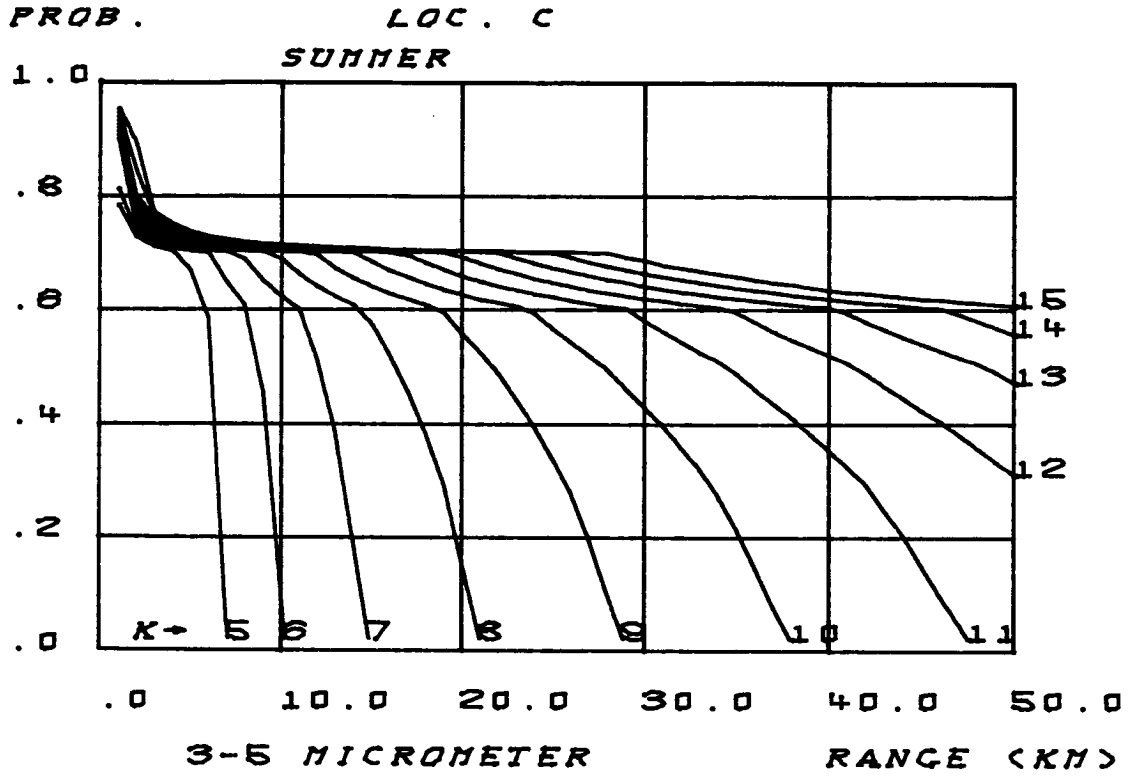


FIGURE - 10

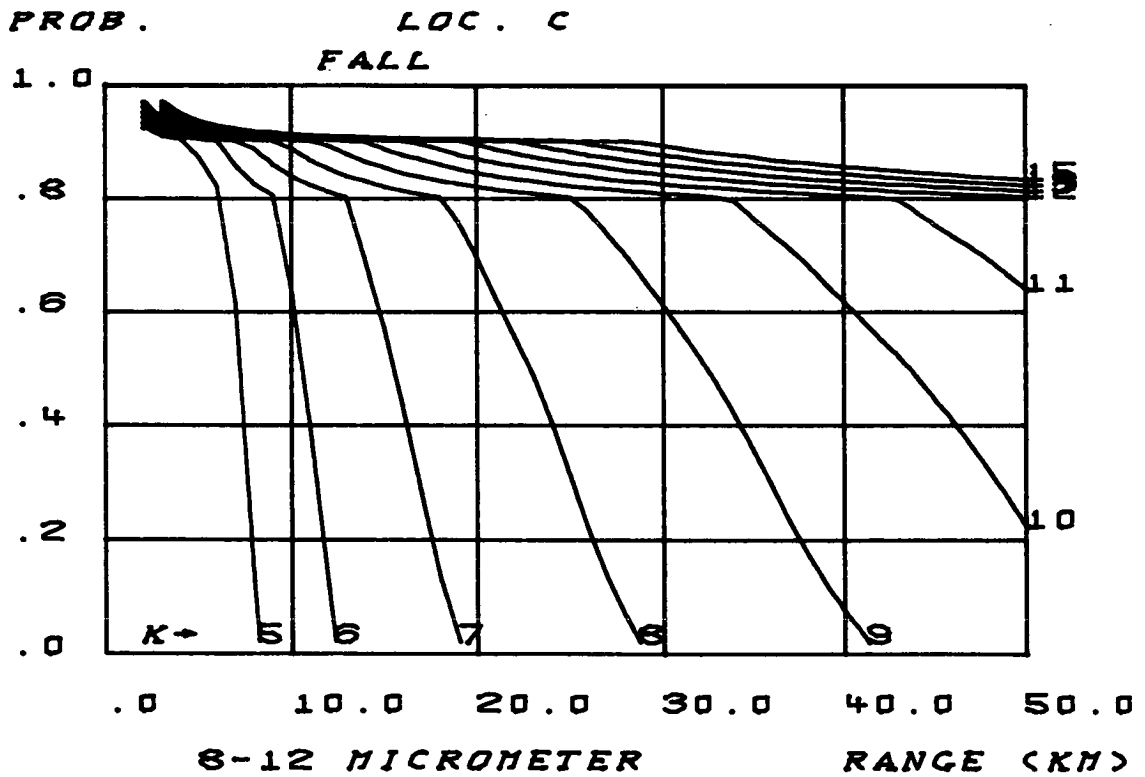
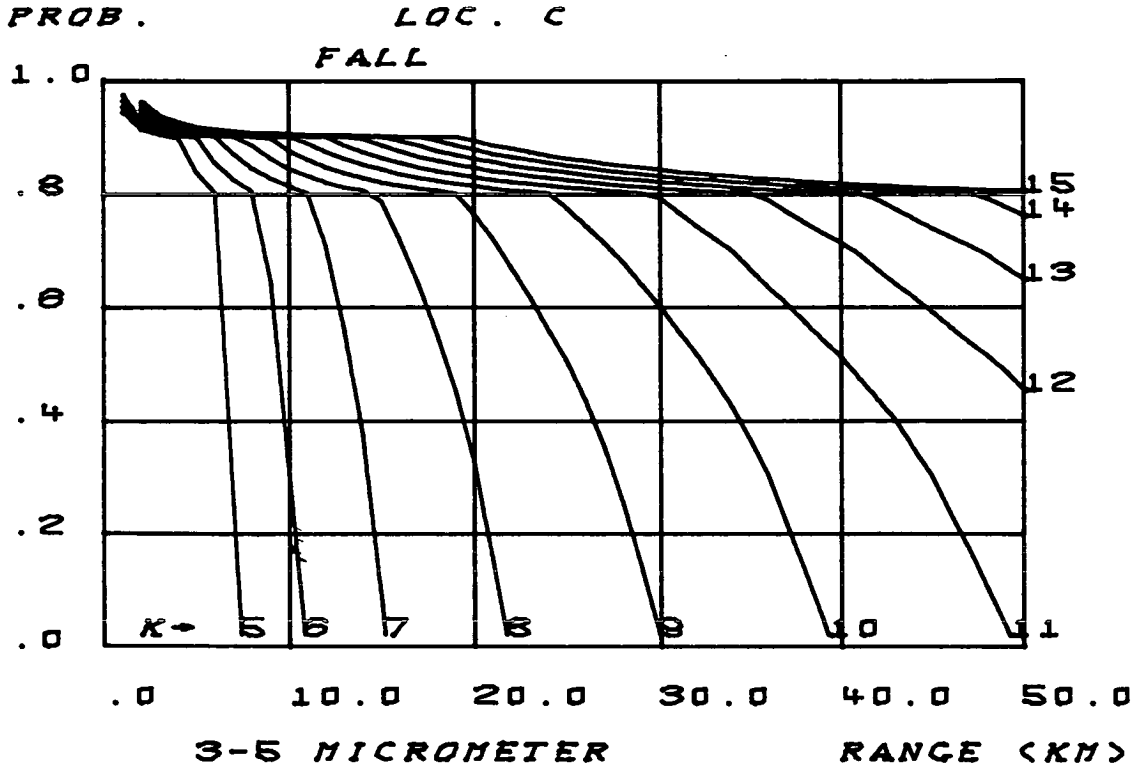


FIGURE - 11

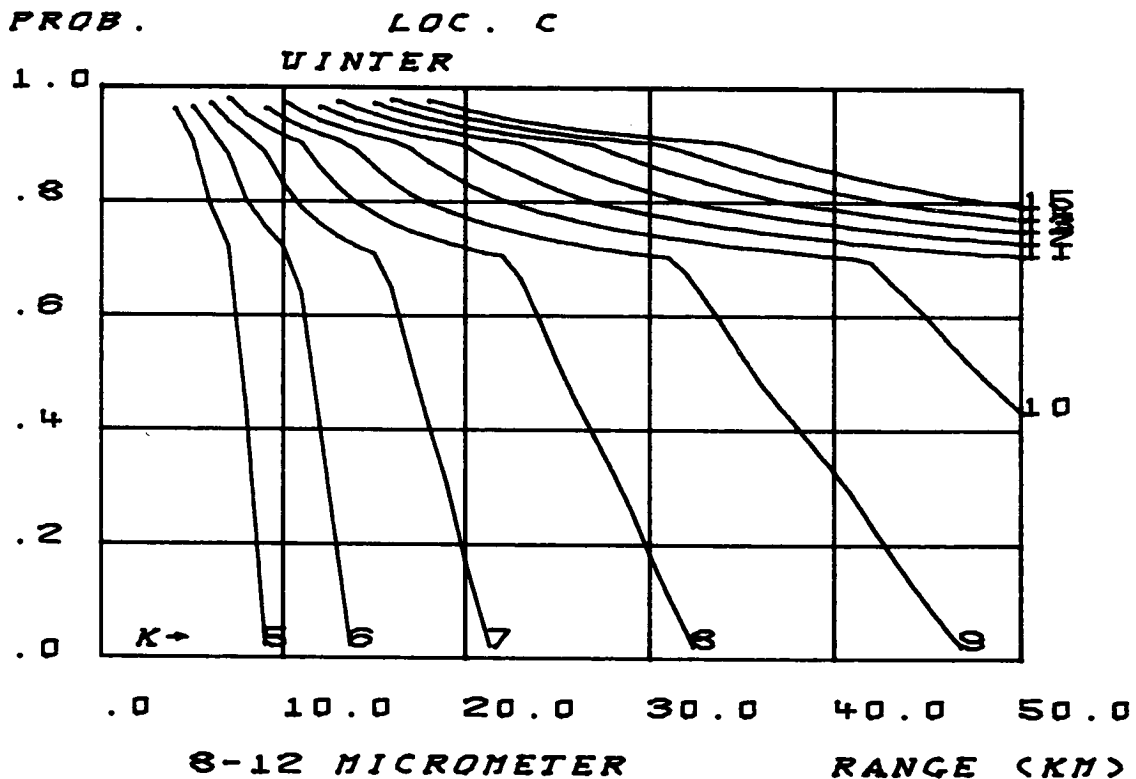
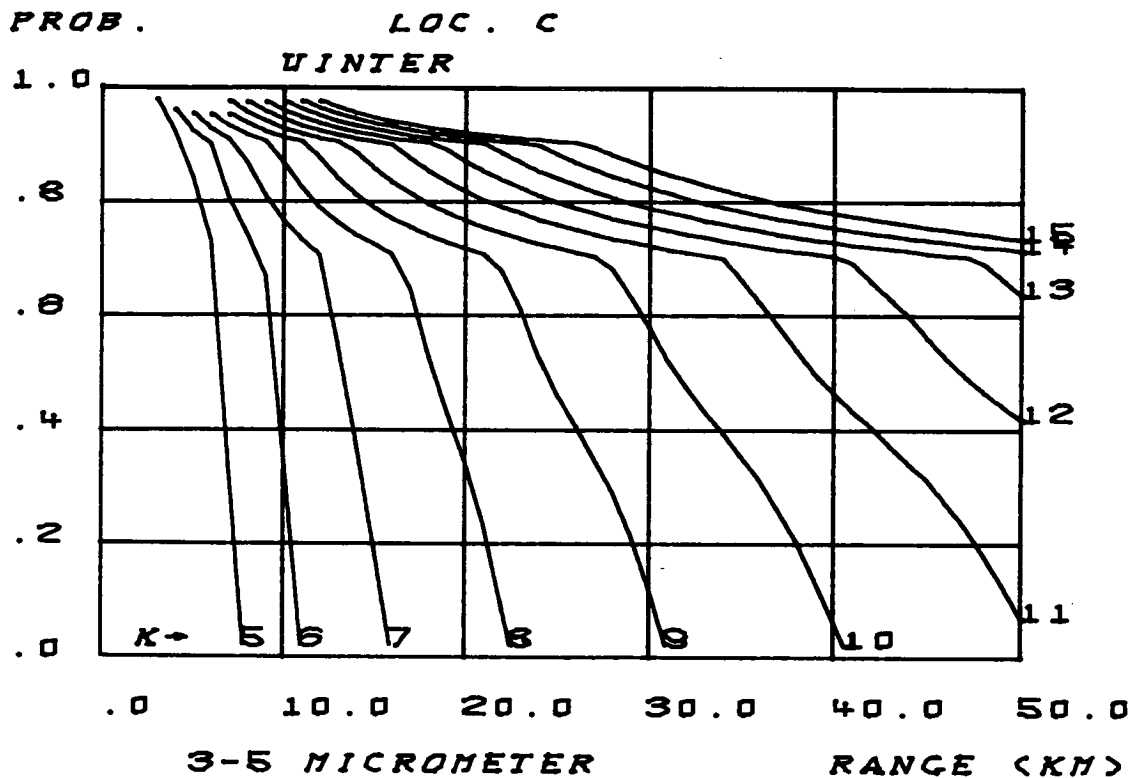


FIGURE - 12

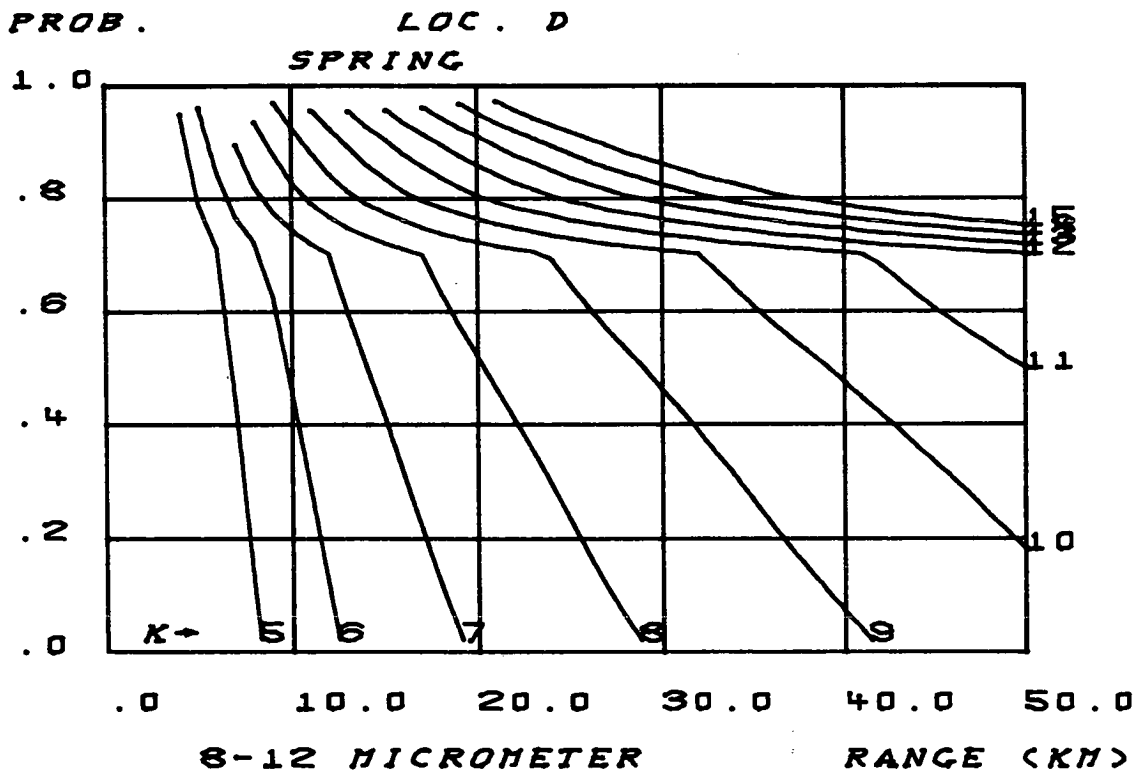
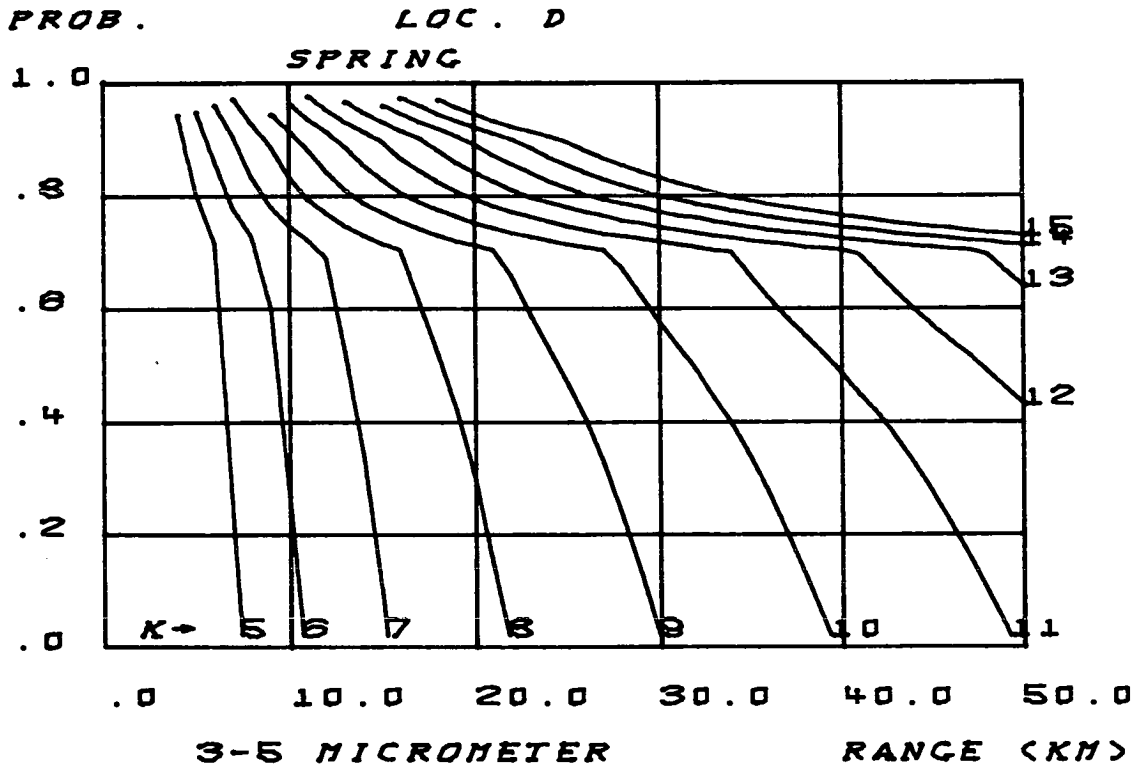


FIGURE - 13

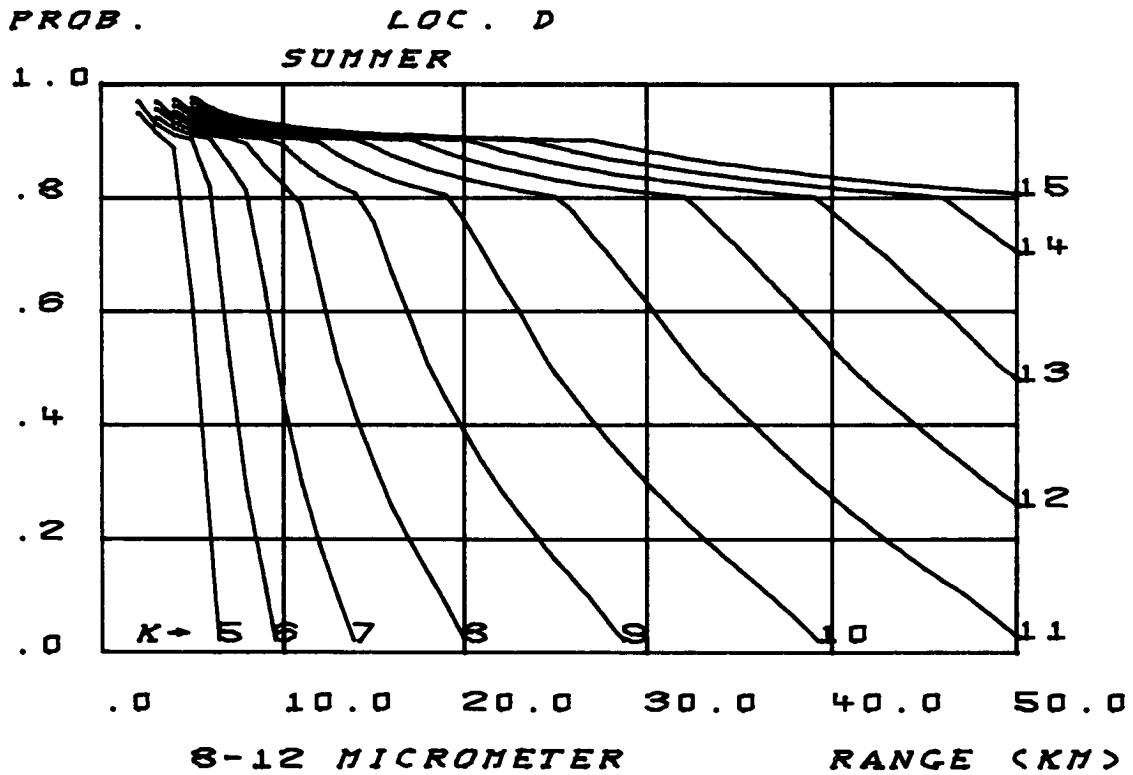
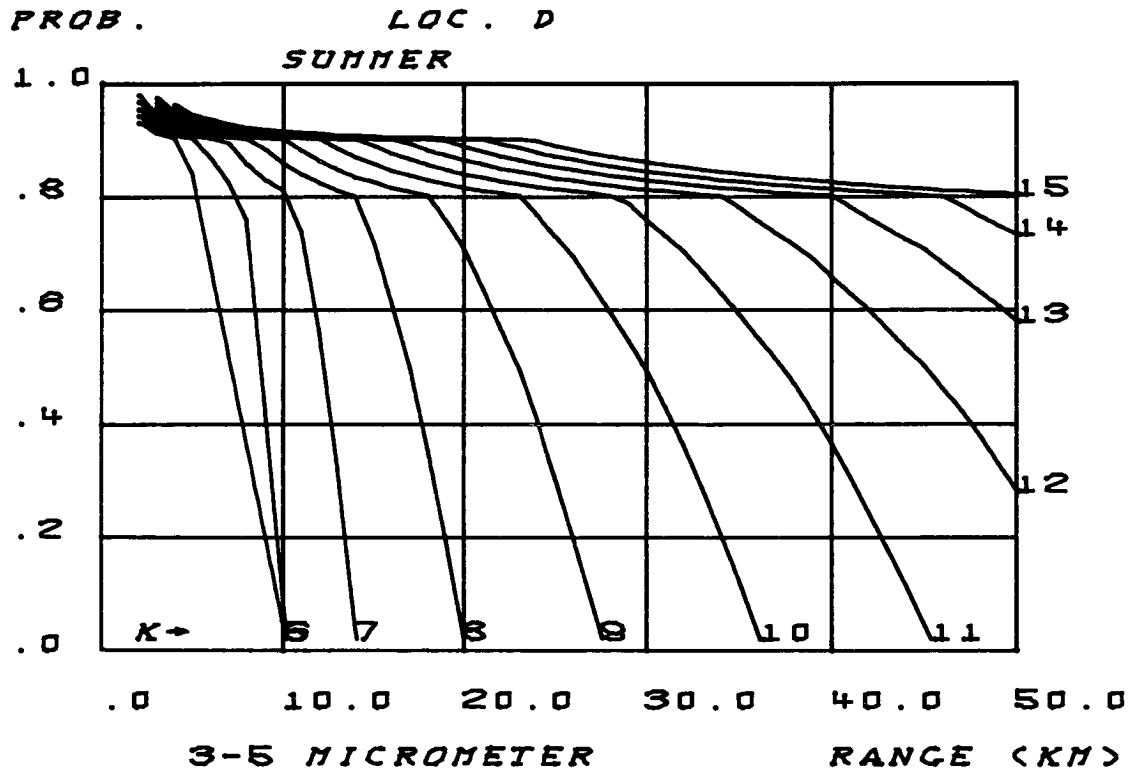
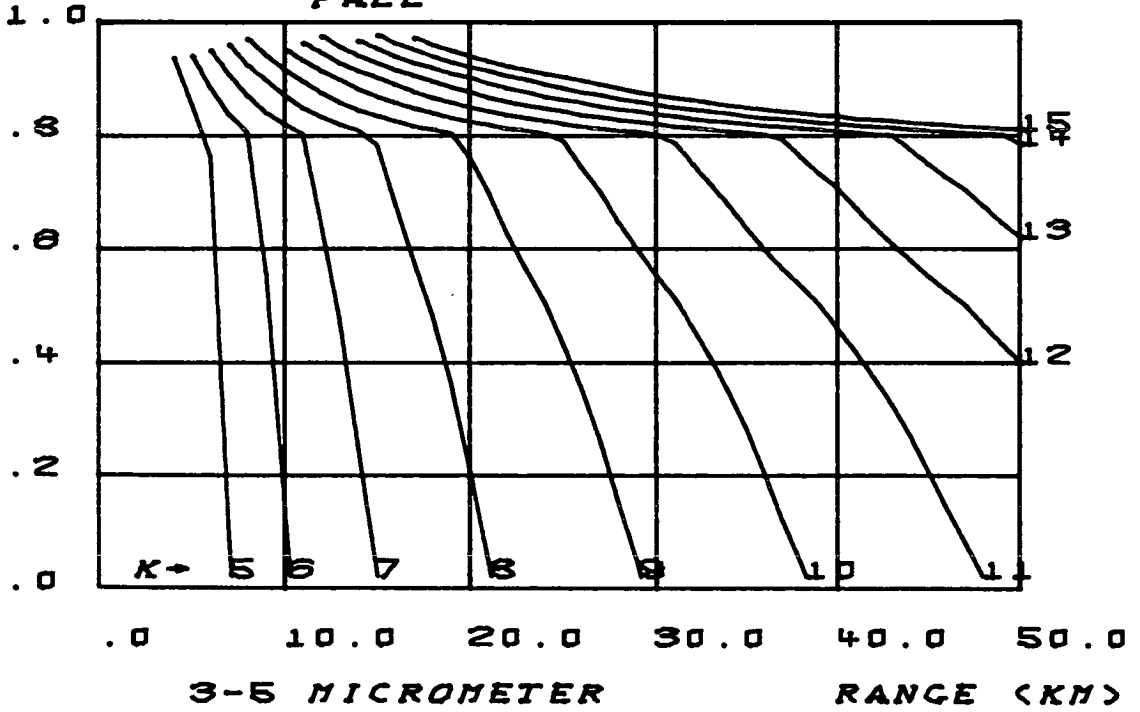


FIGURE - 14

PROB.

LOC. D

FALL



PROB.

LOC. D

FALL

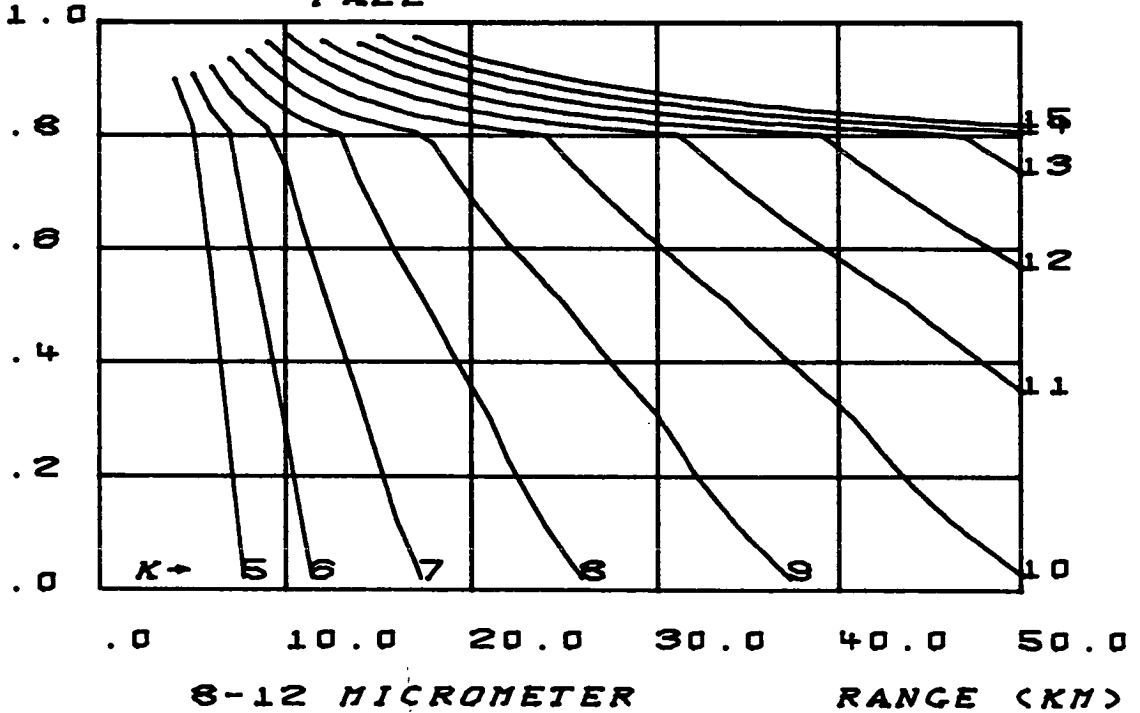


FIGURE - 15

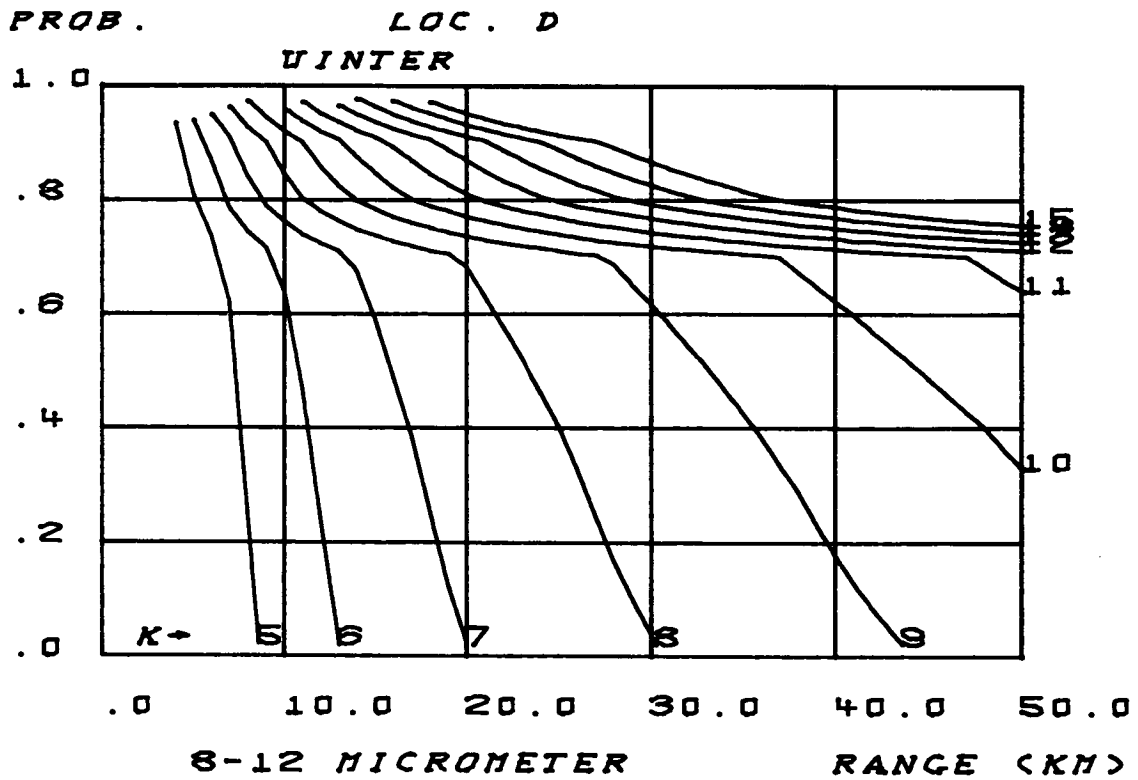
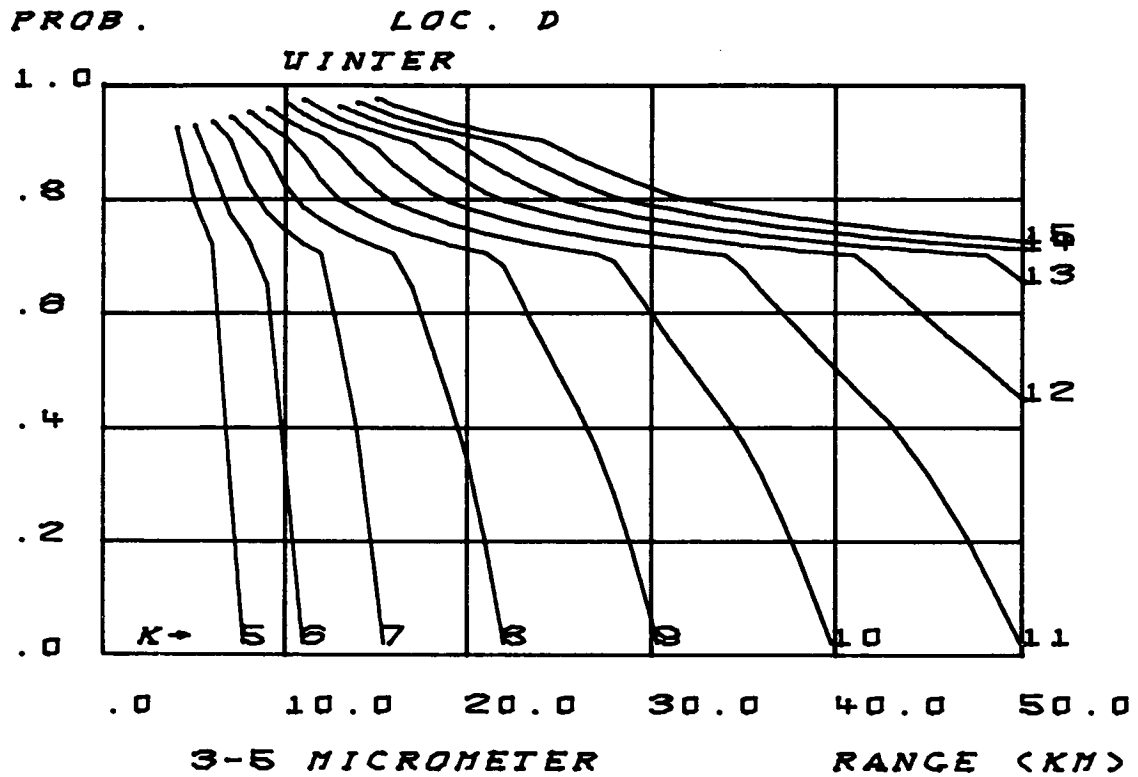


FIGURE - 16

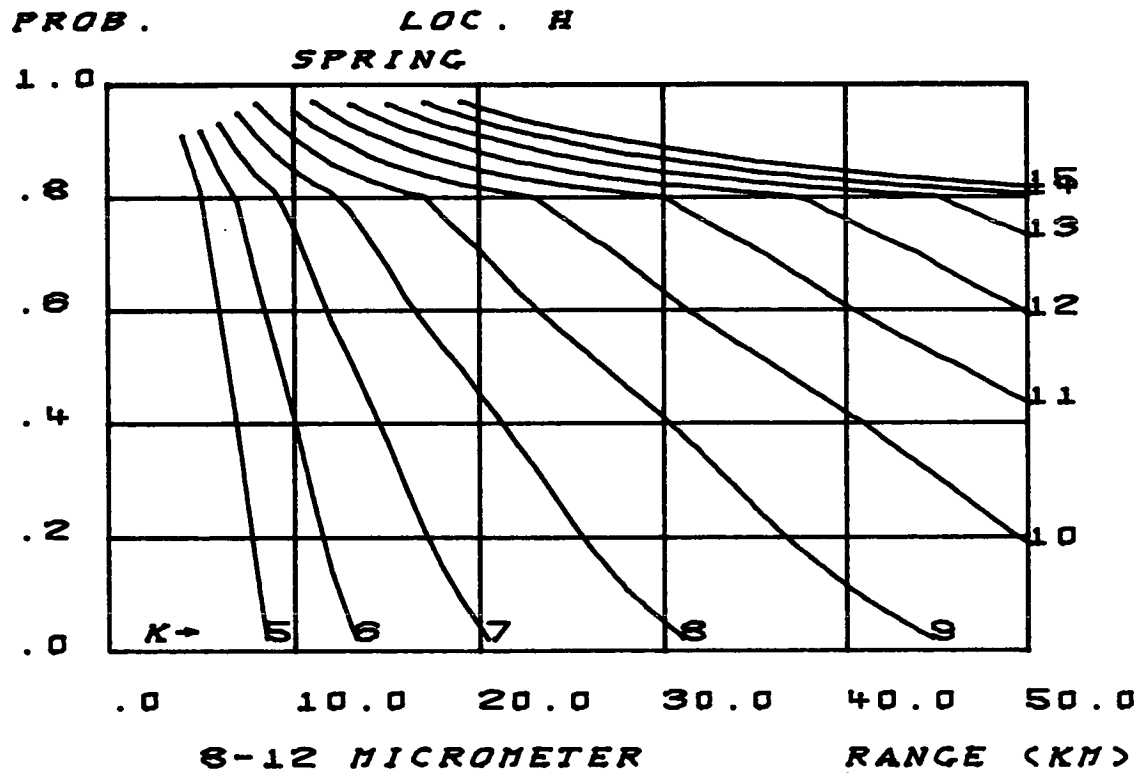
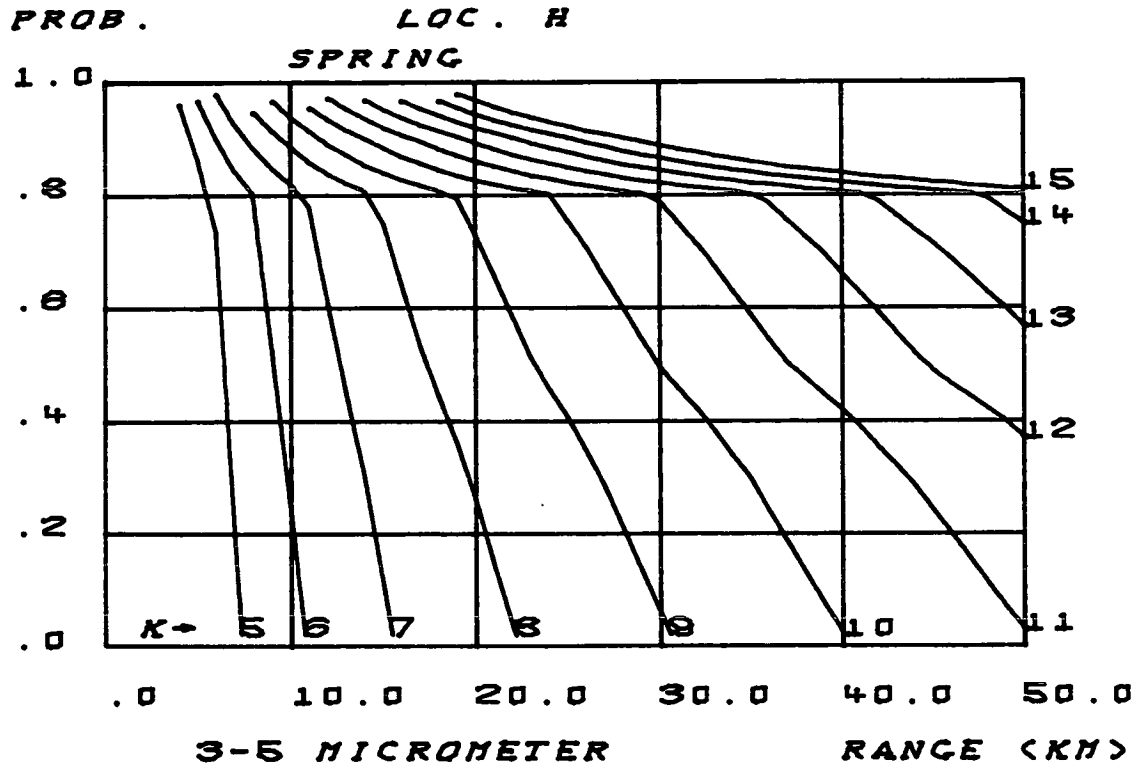


FIGURE - 17

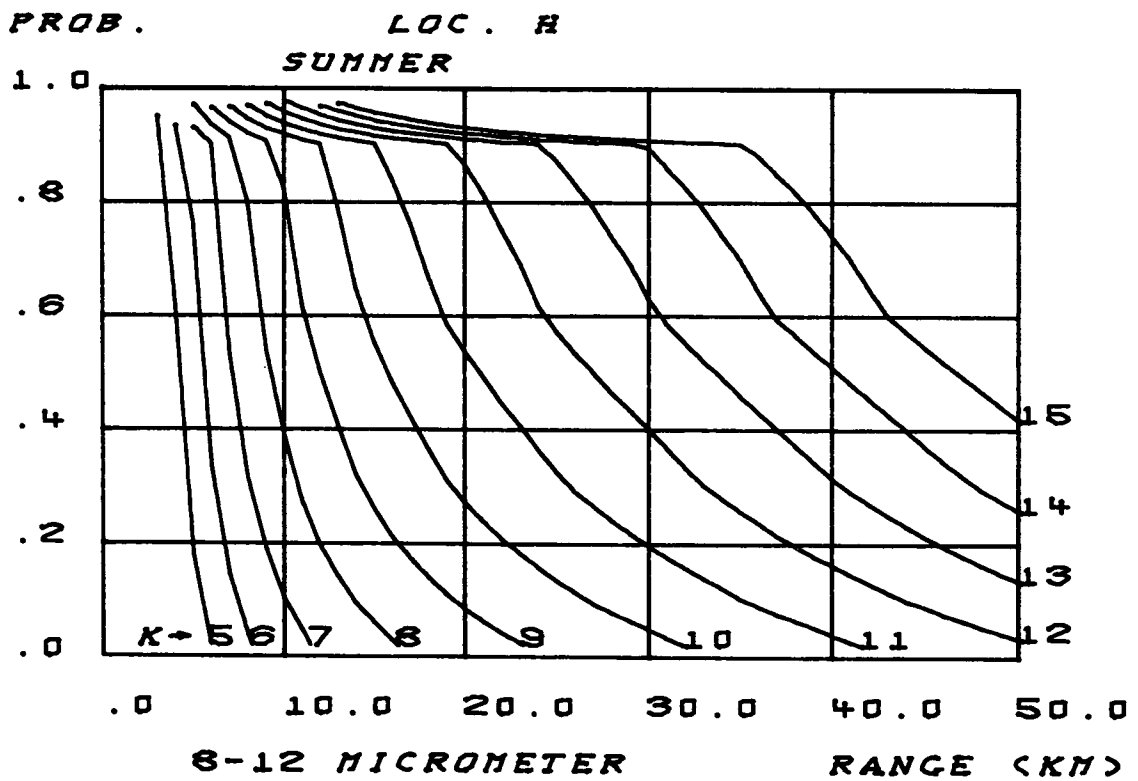
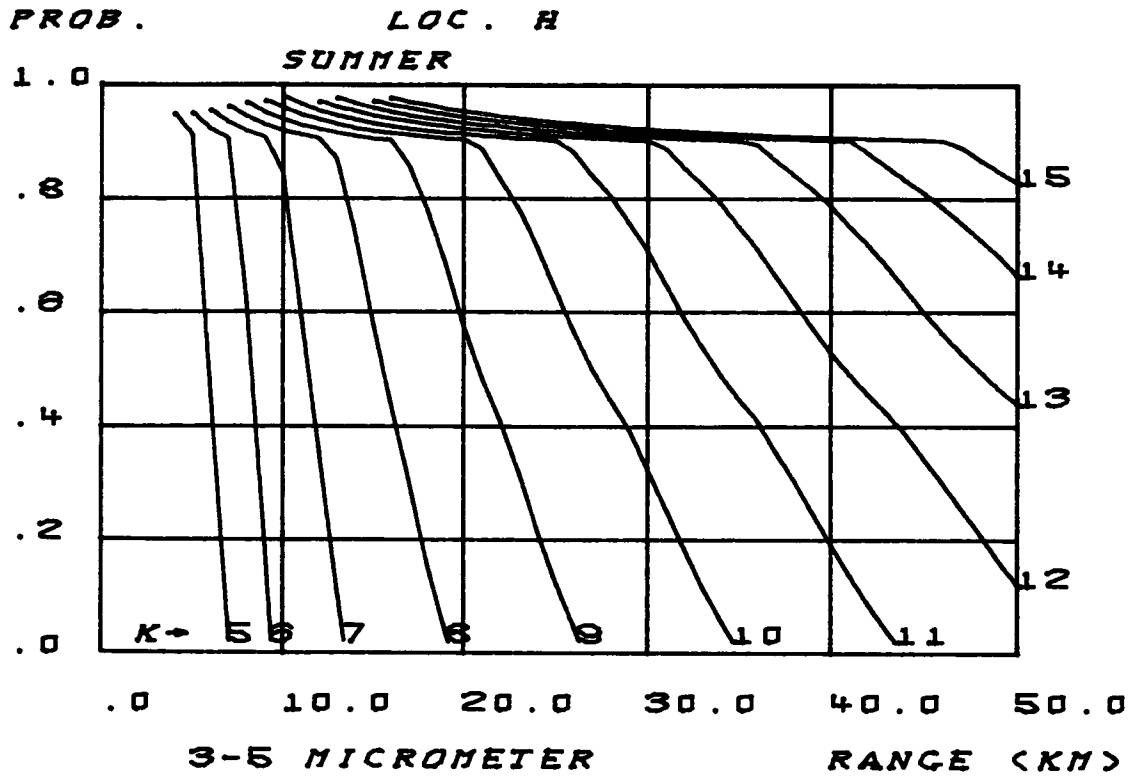


FIGURE - 18

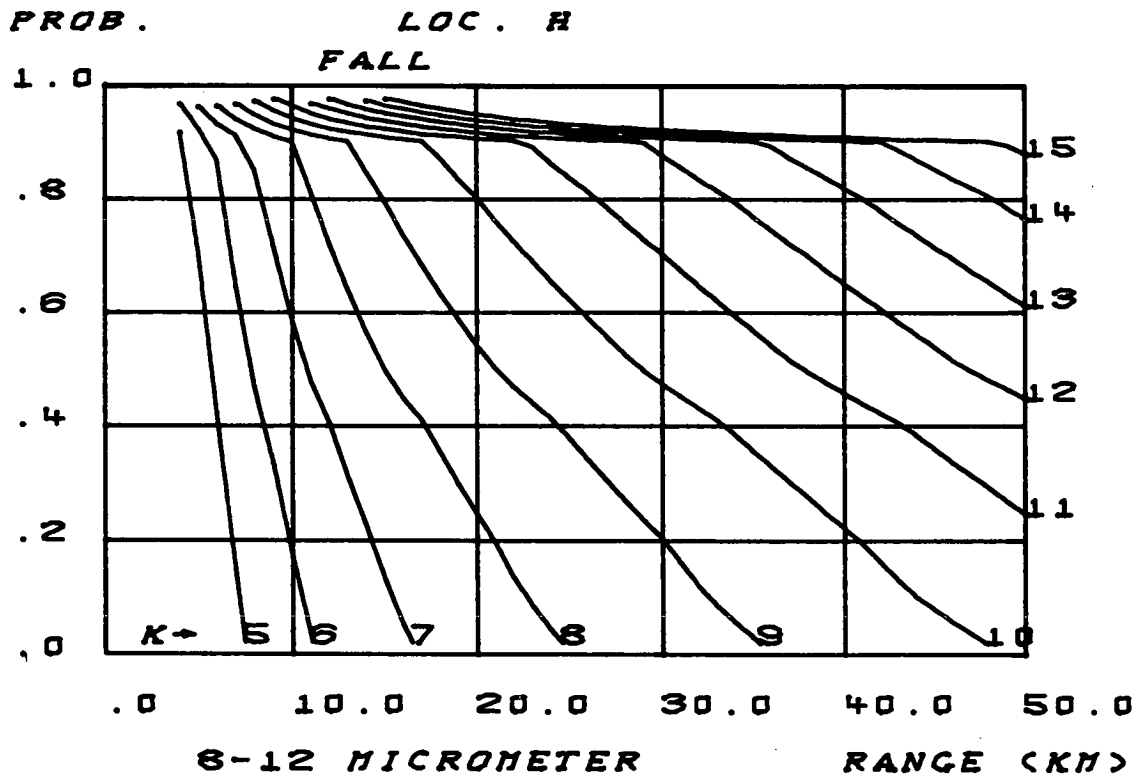
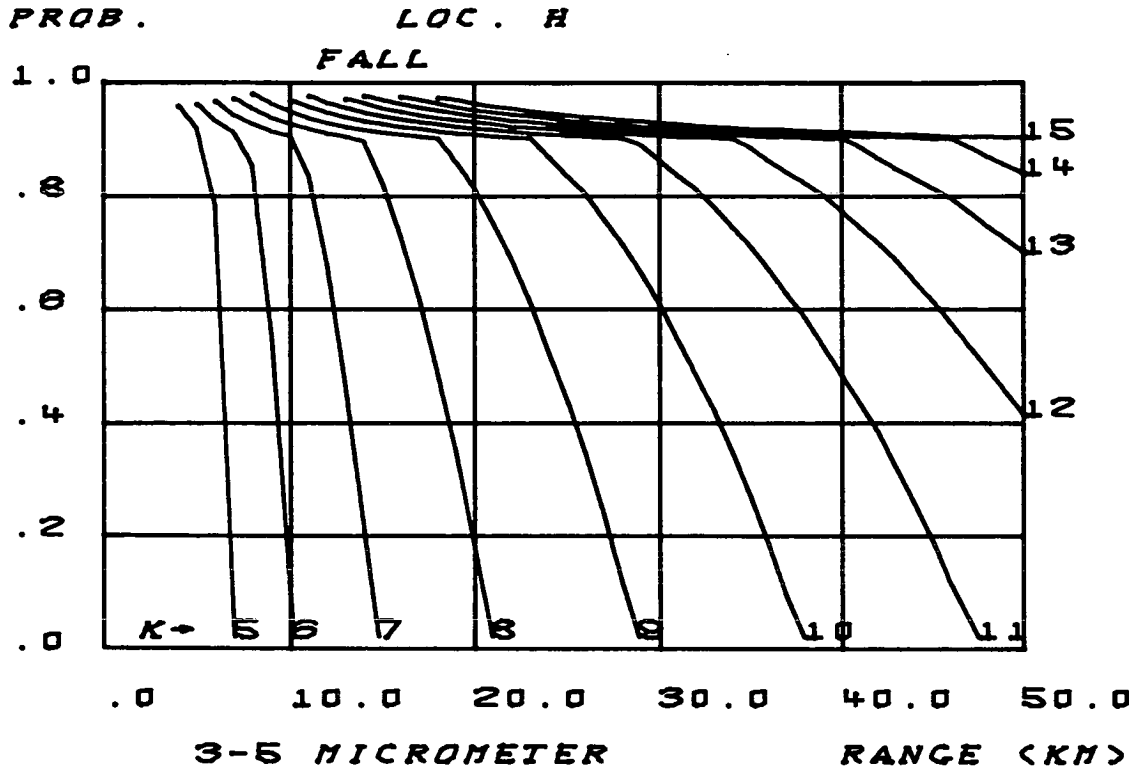


FIGURE - 19

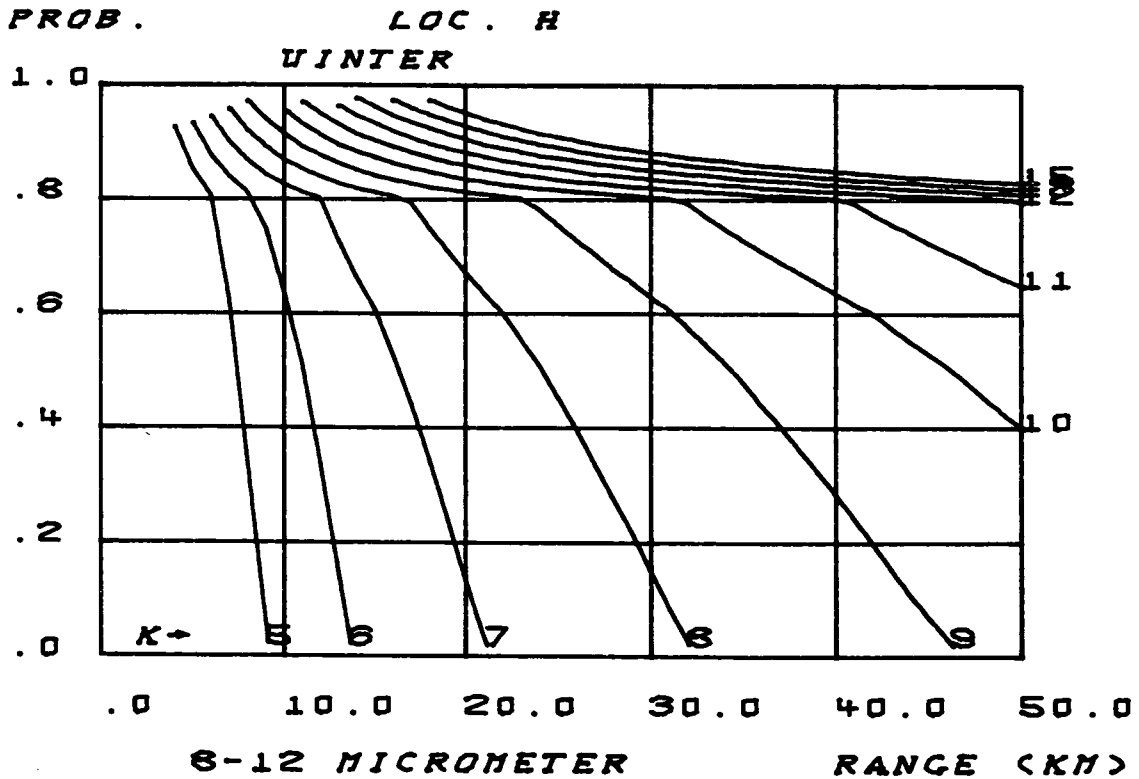
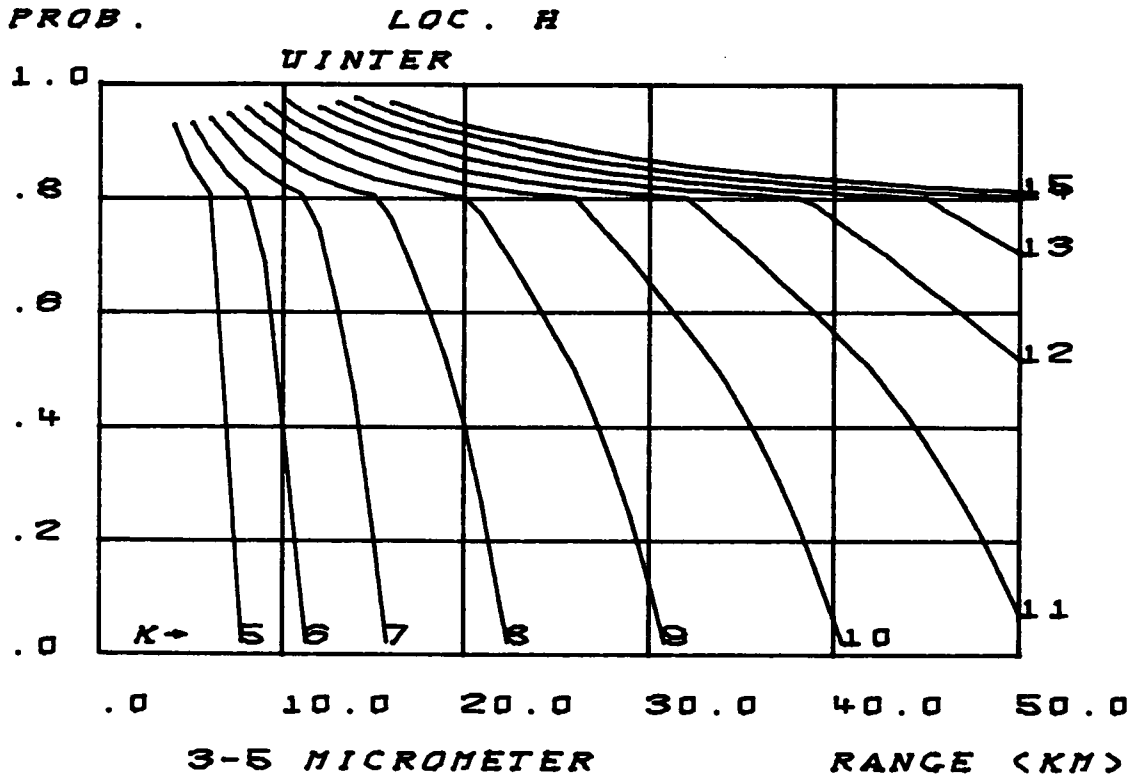


FIGURE - 20

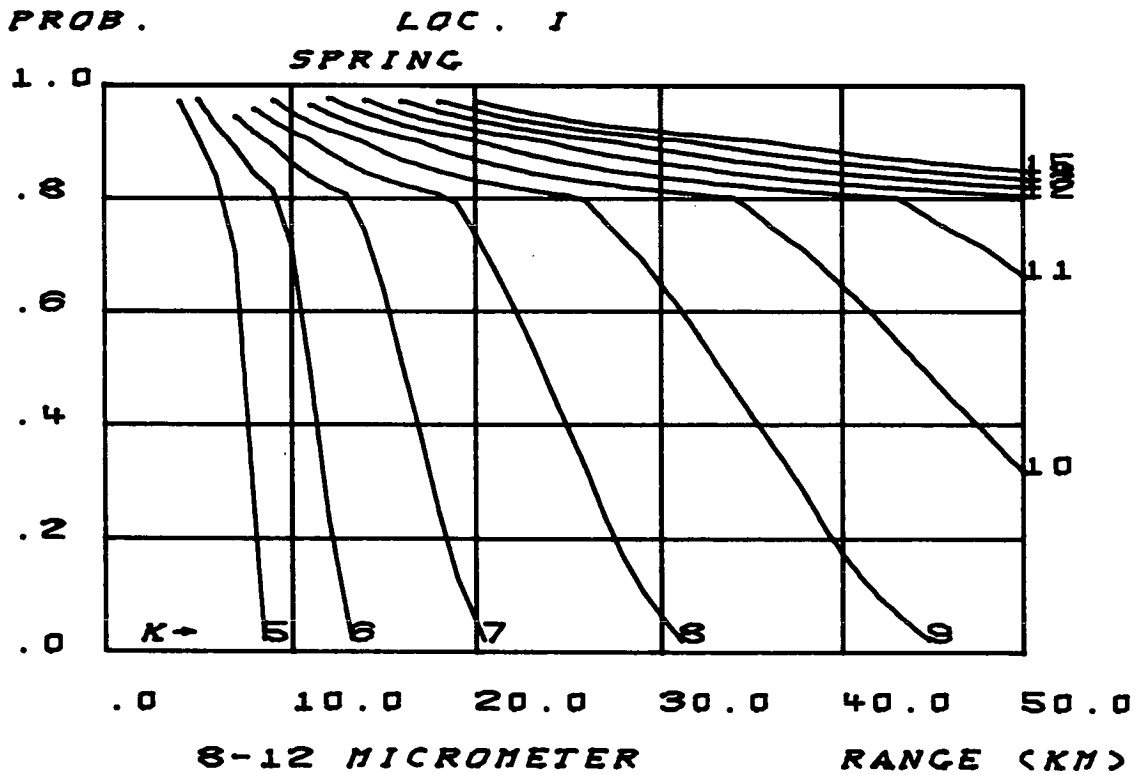
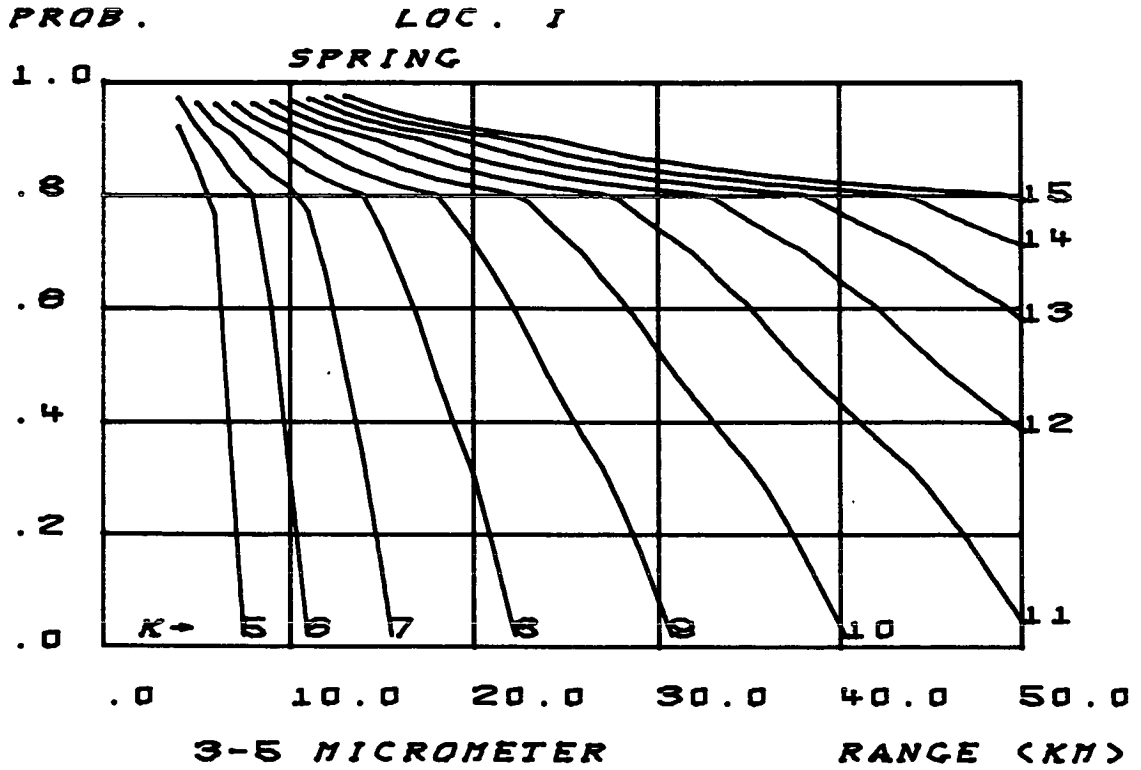


FIGURE - 21

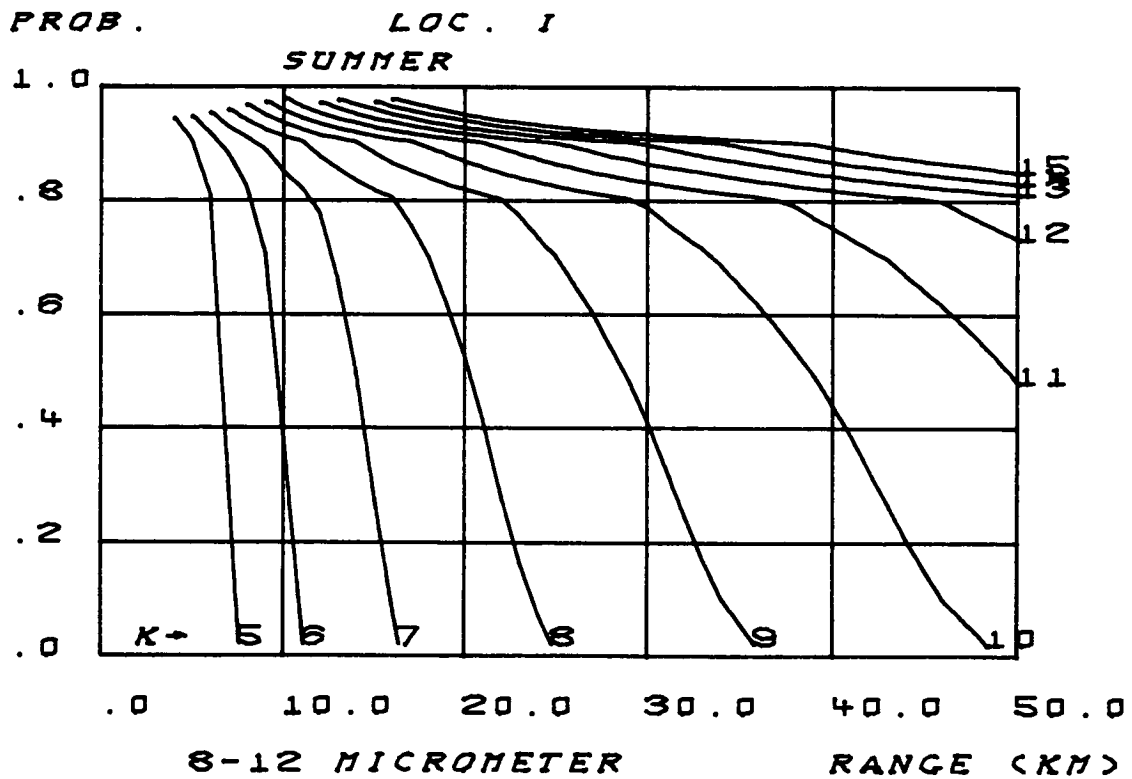
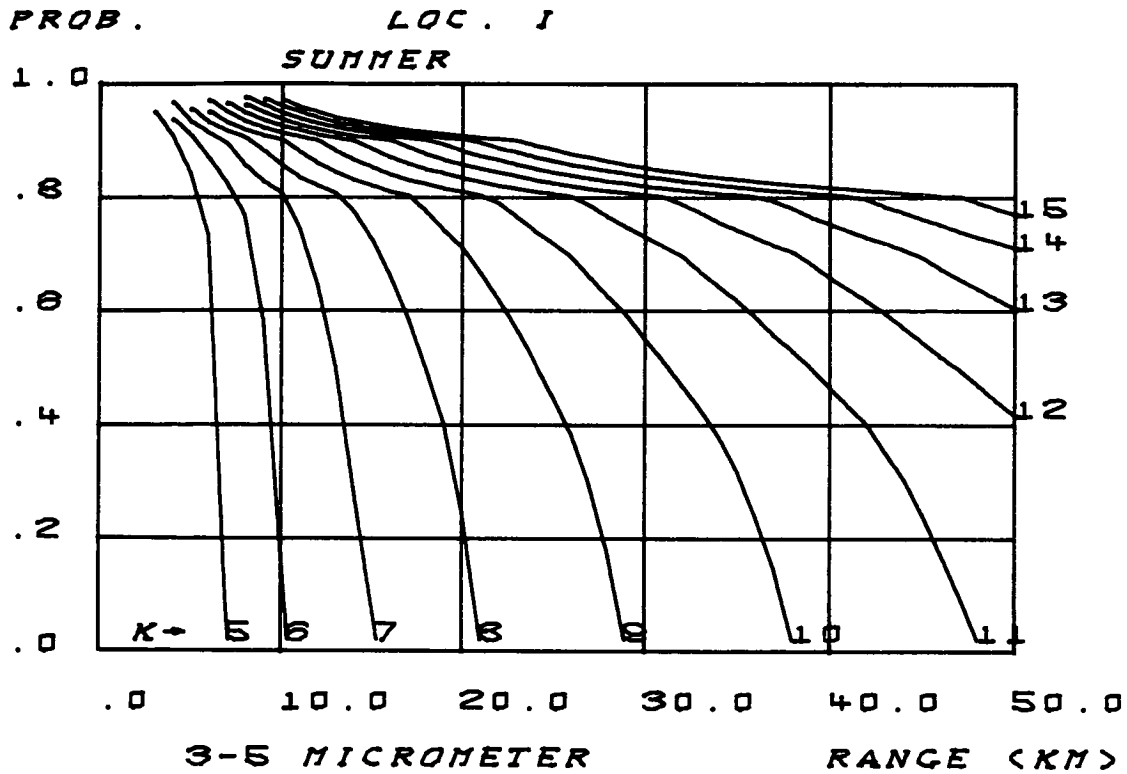


FIGURE - 22

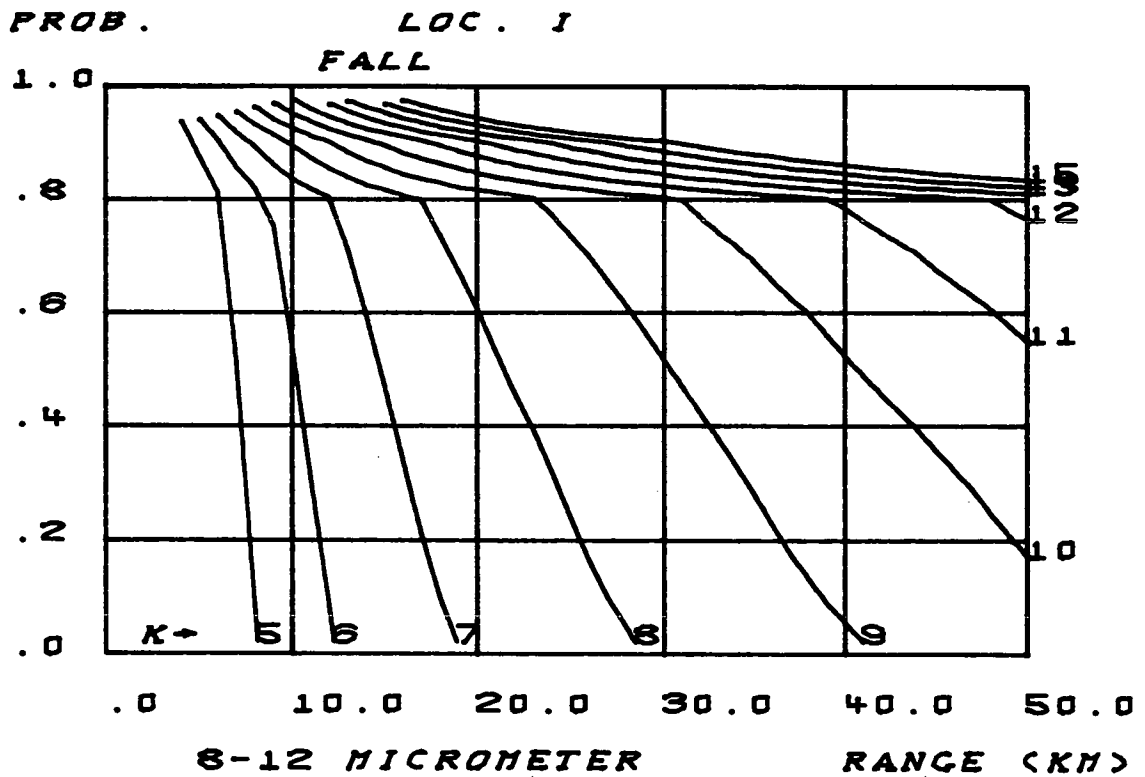
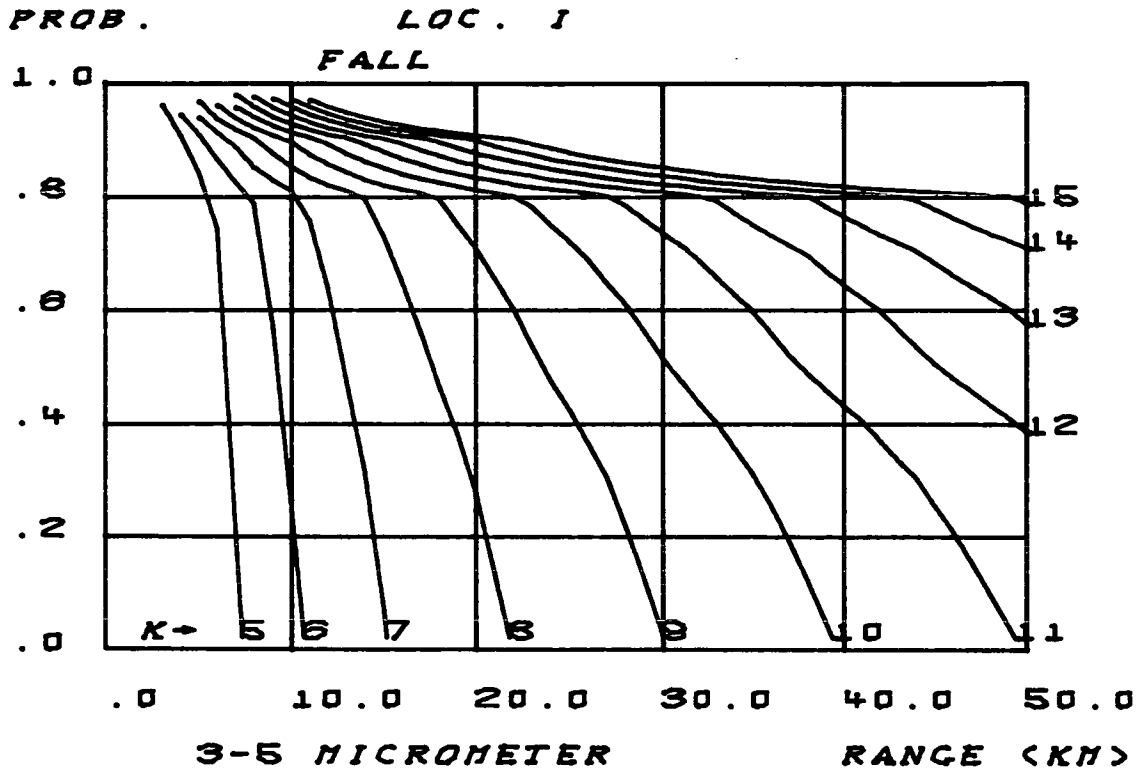


FIGURE - 23

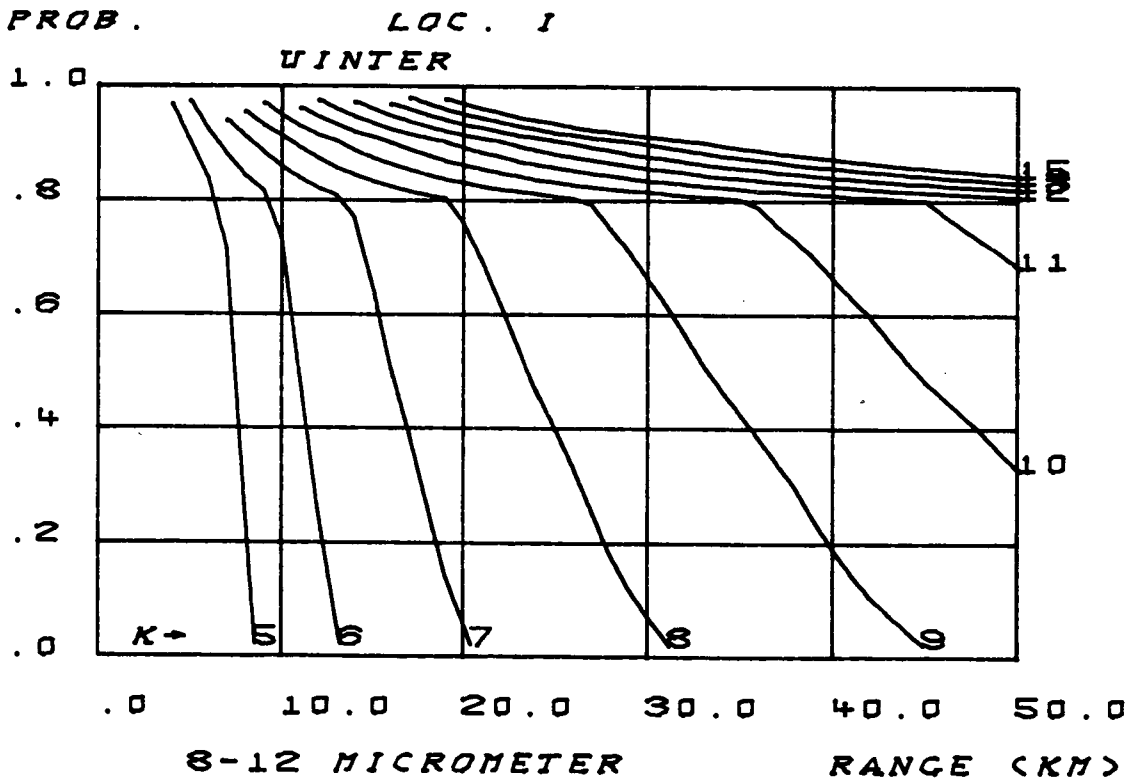
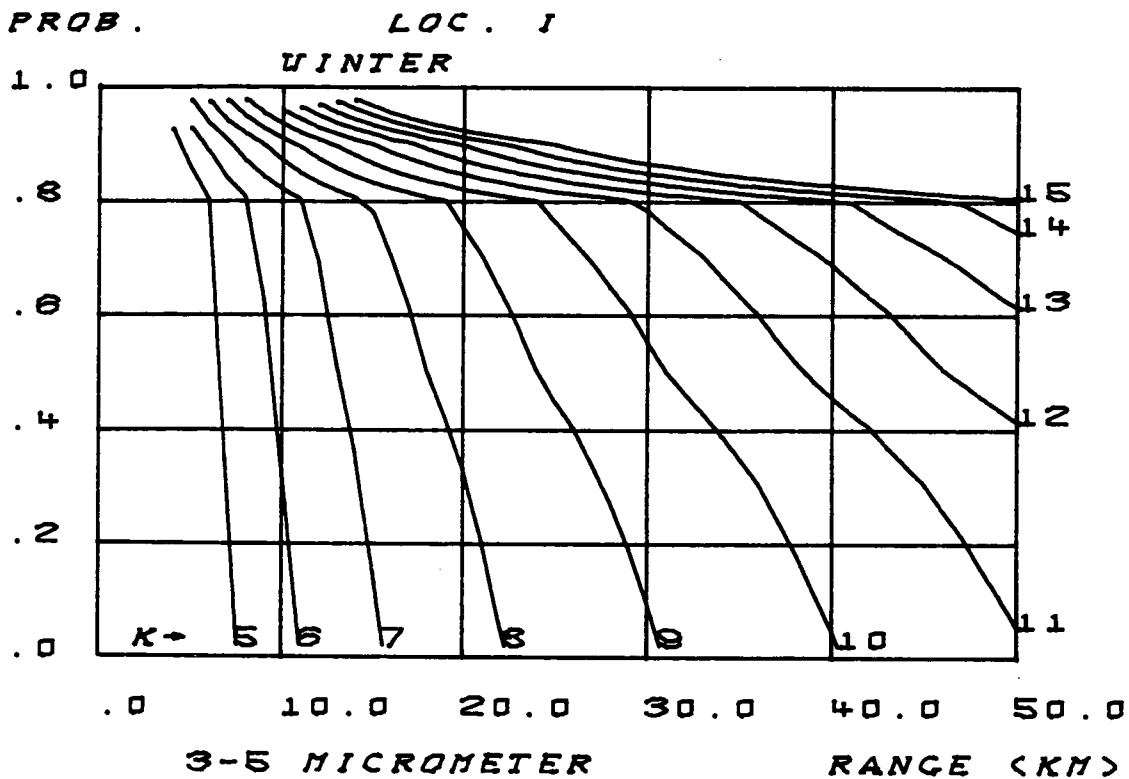


FIGURE - 24

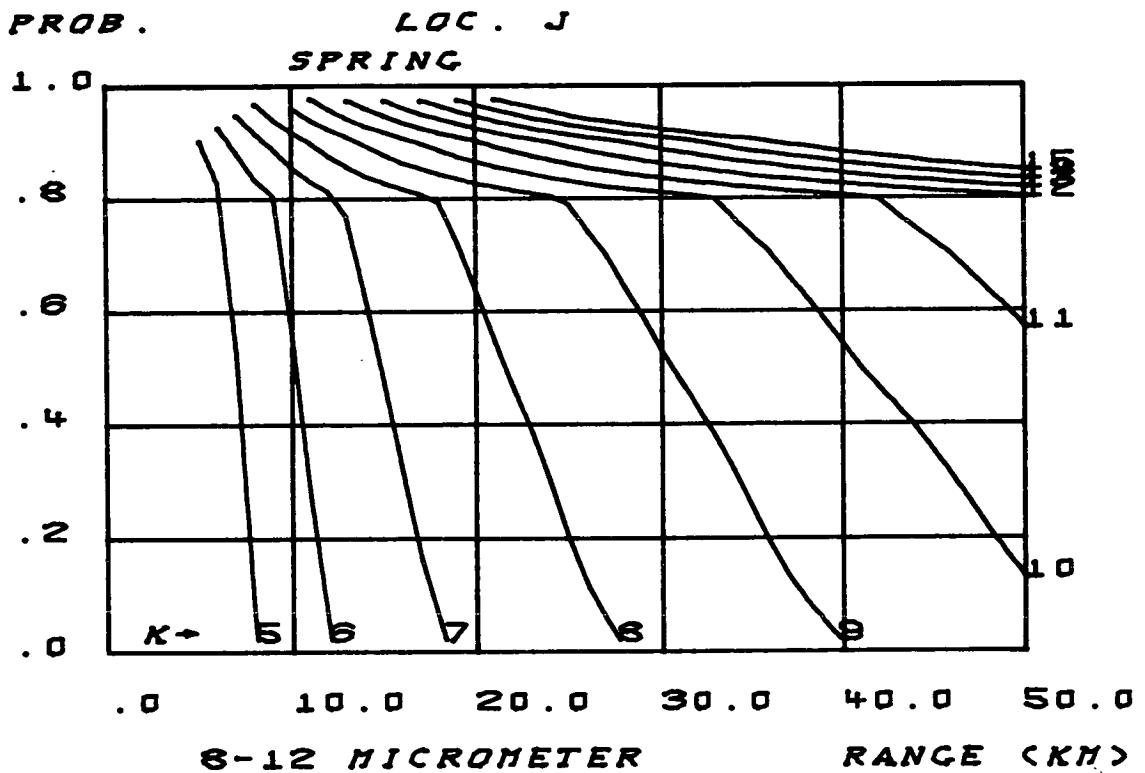
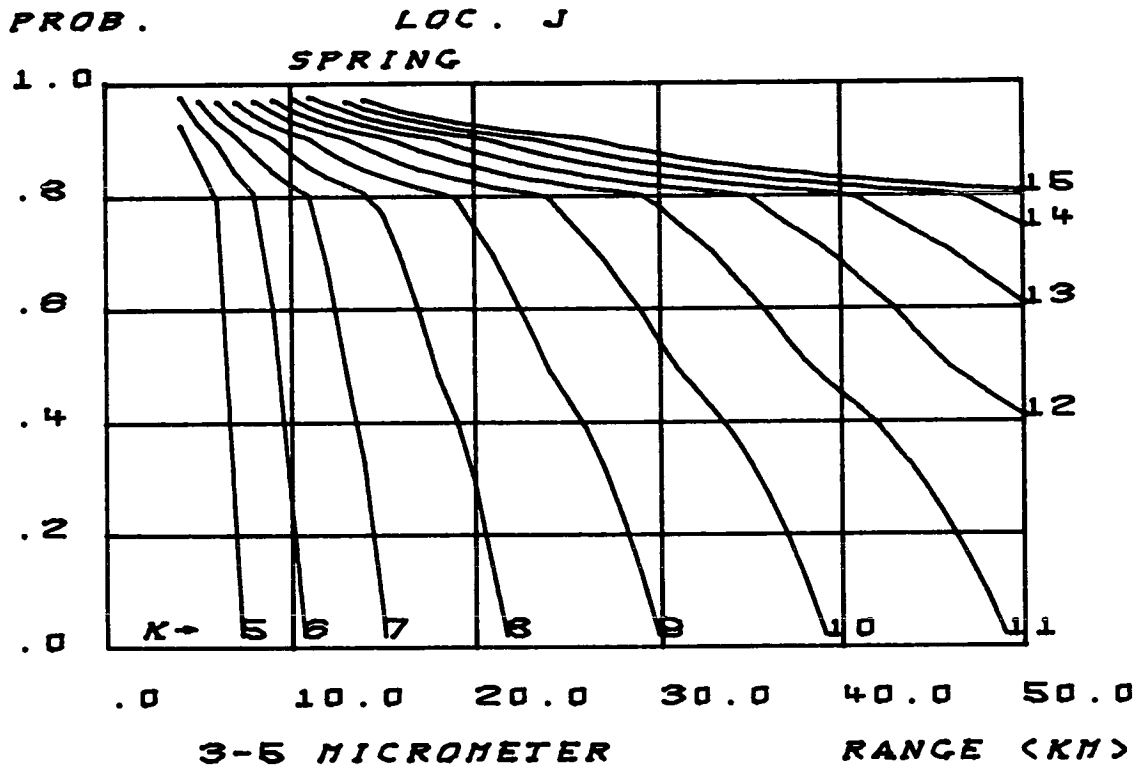


FIGURE - 25

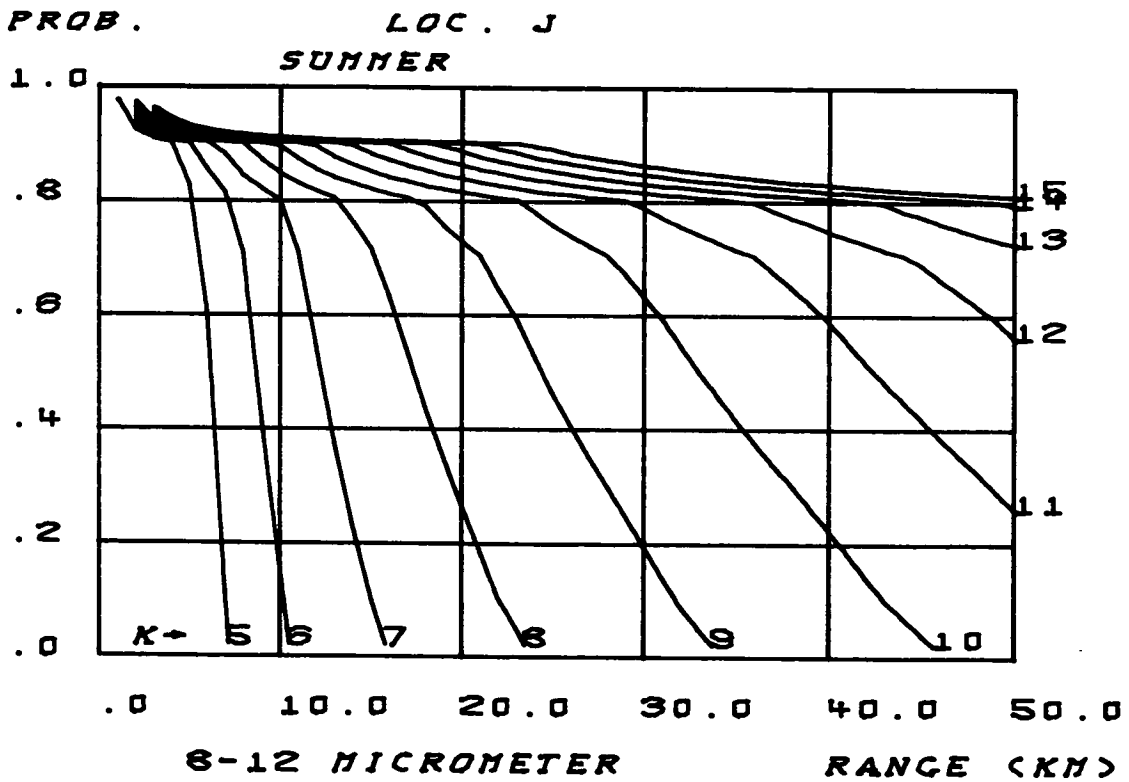
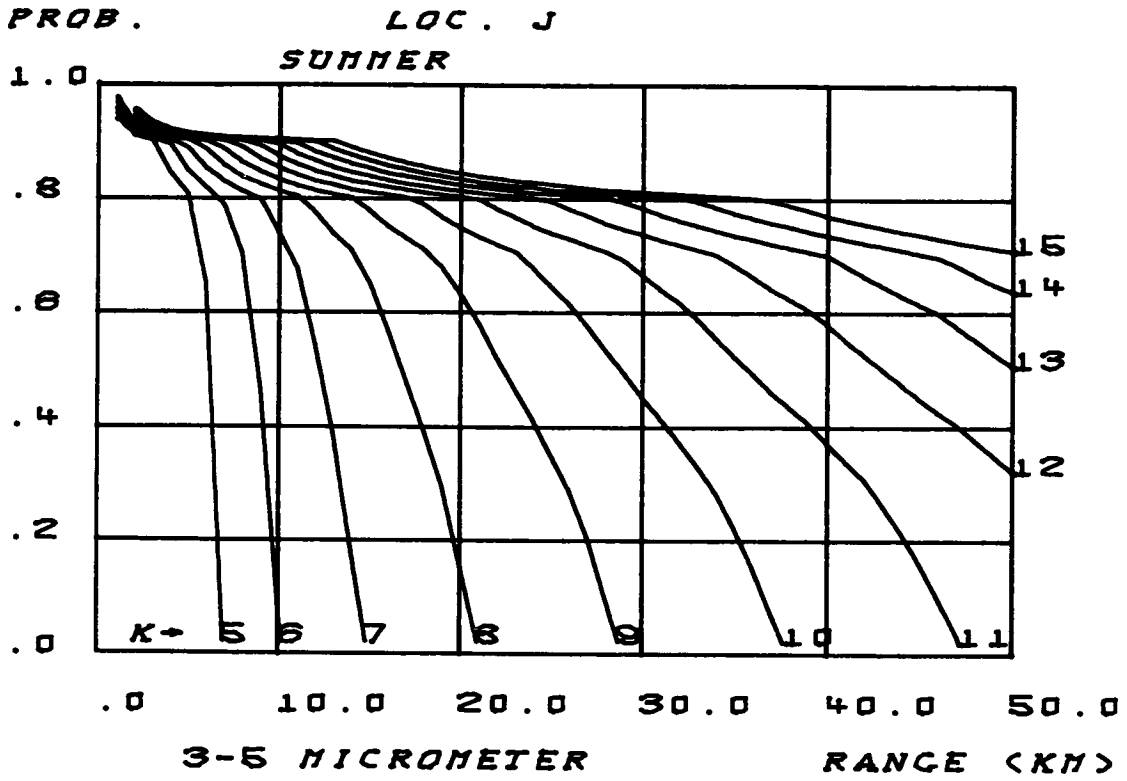


FIGURE - 26

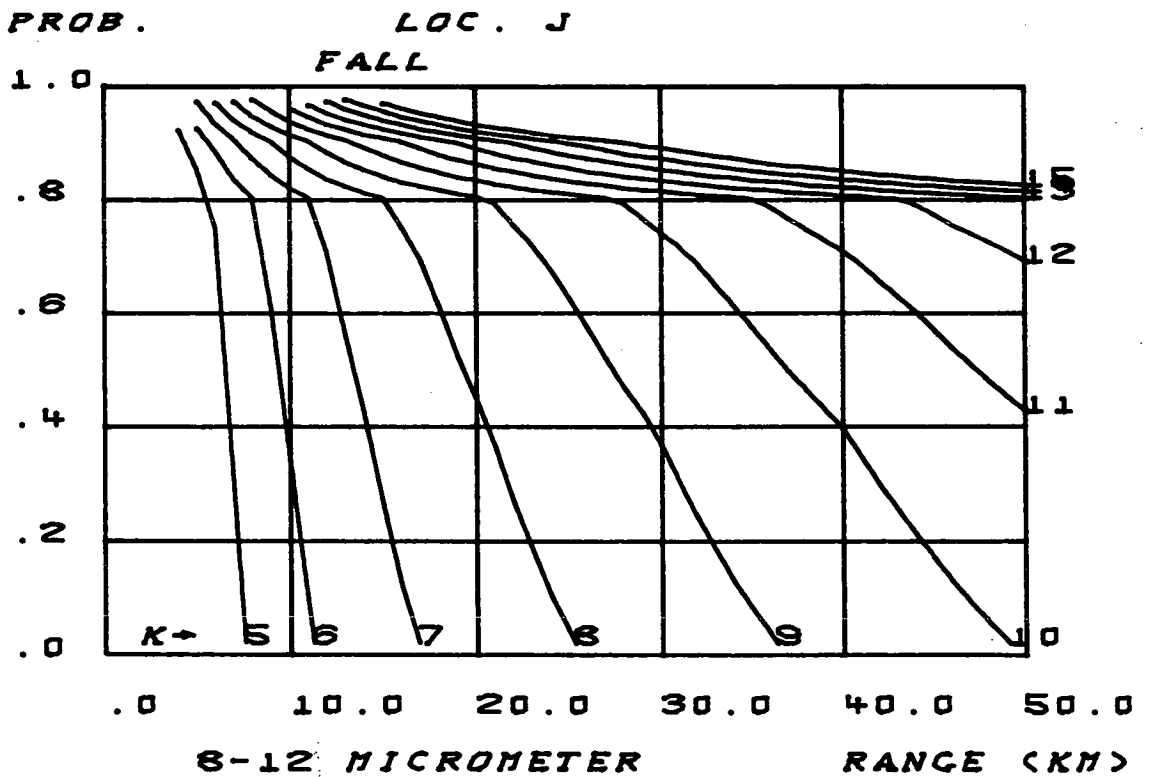
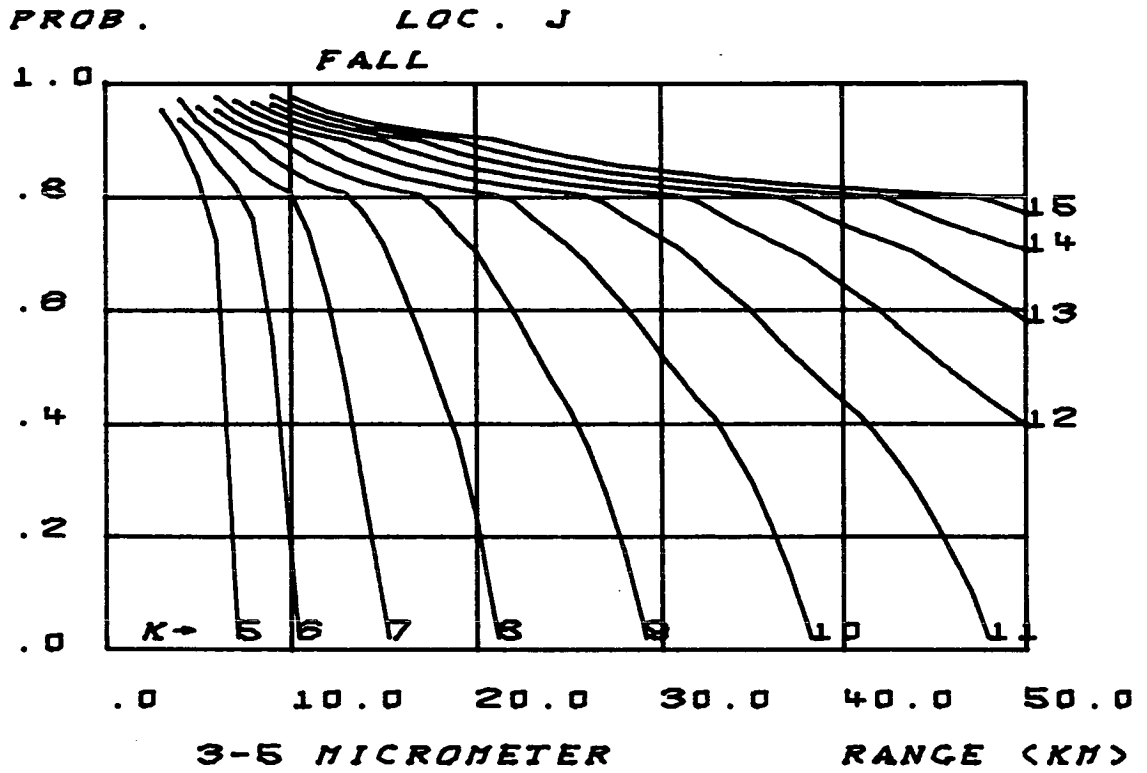


FIGURE - 27

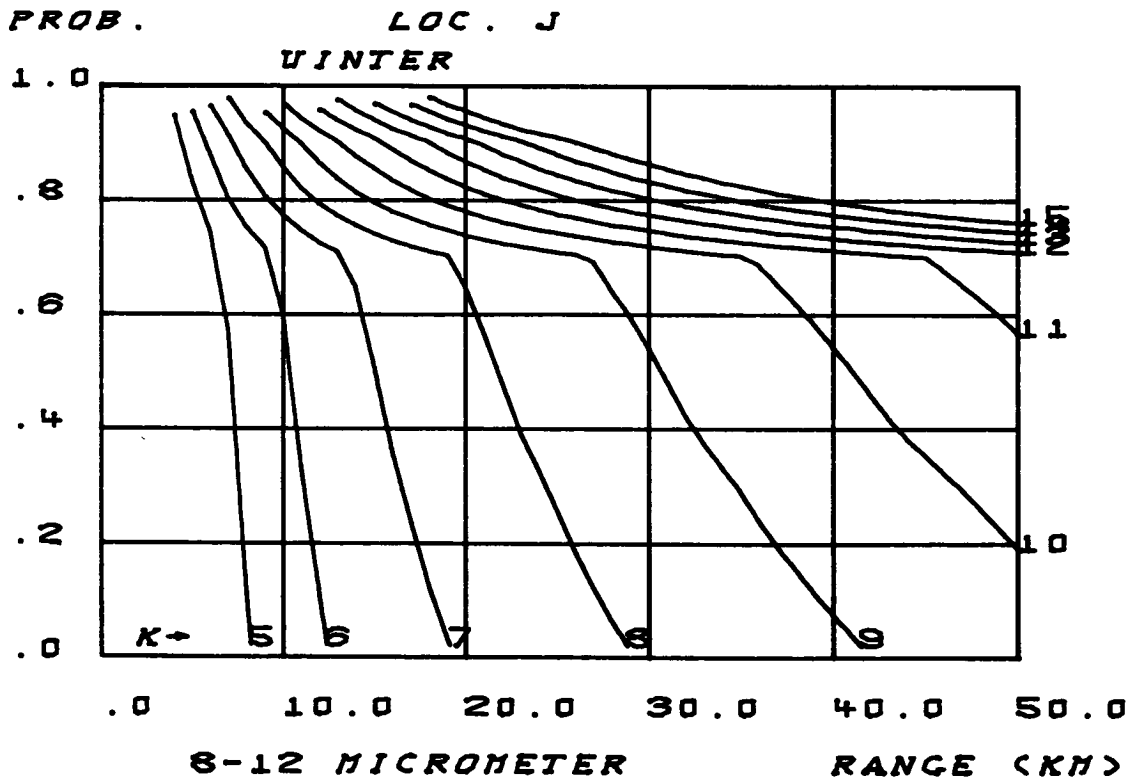
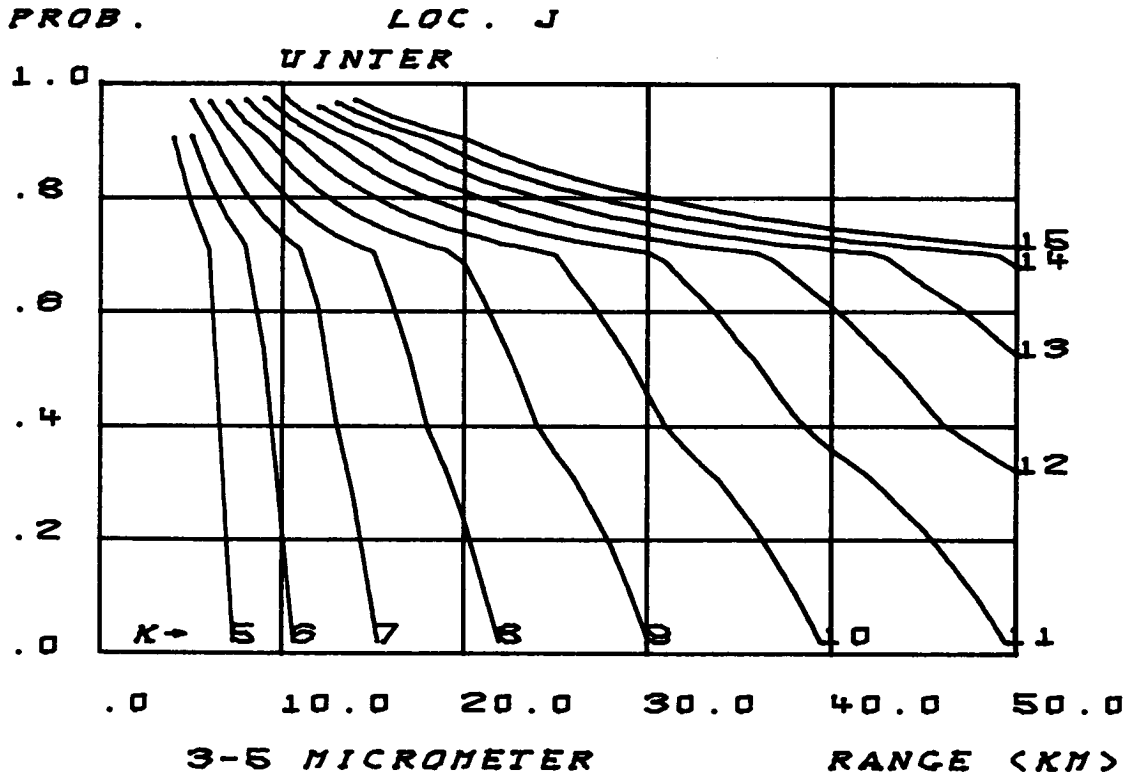


FIGURE - 28

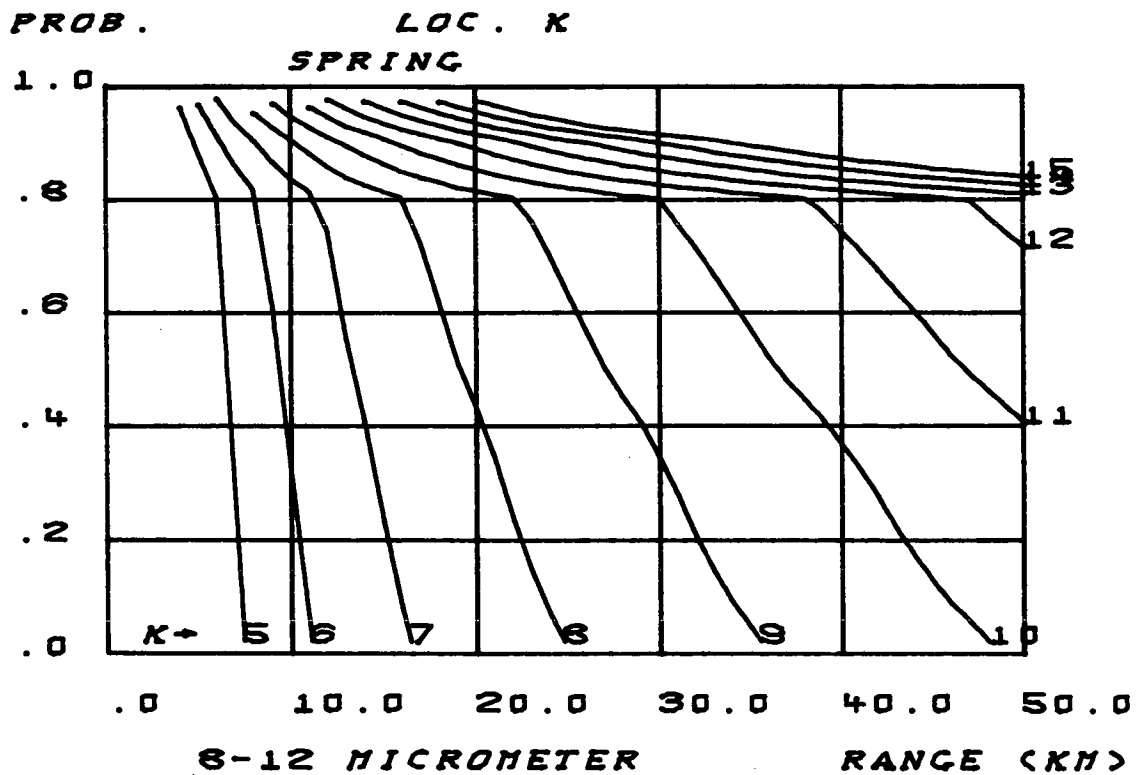
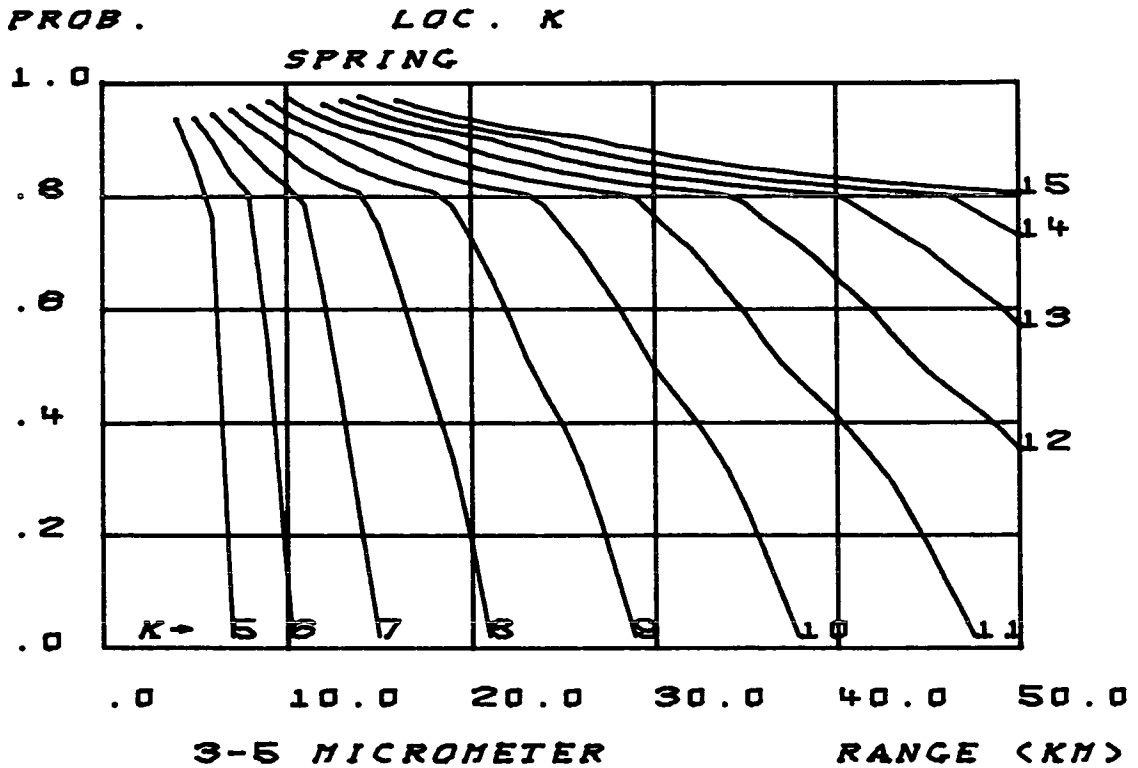


FIGURE - 29

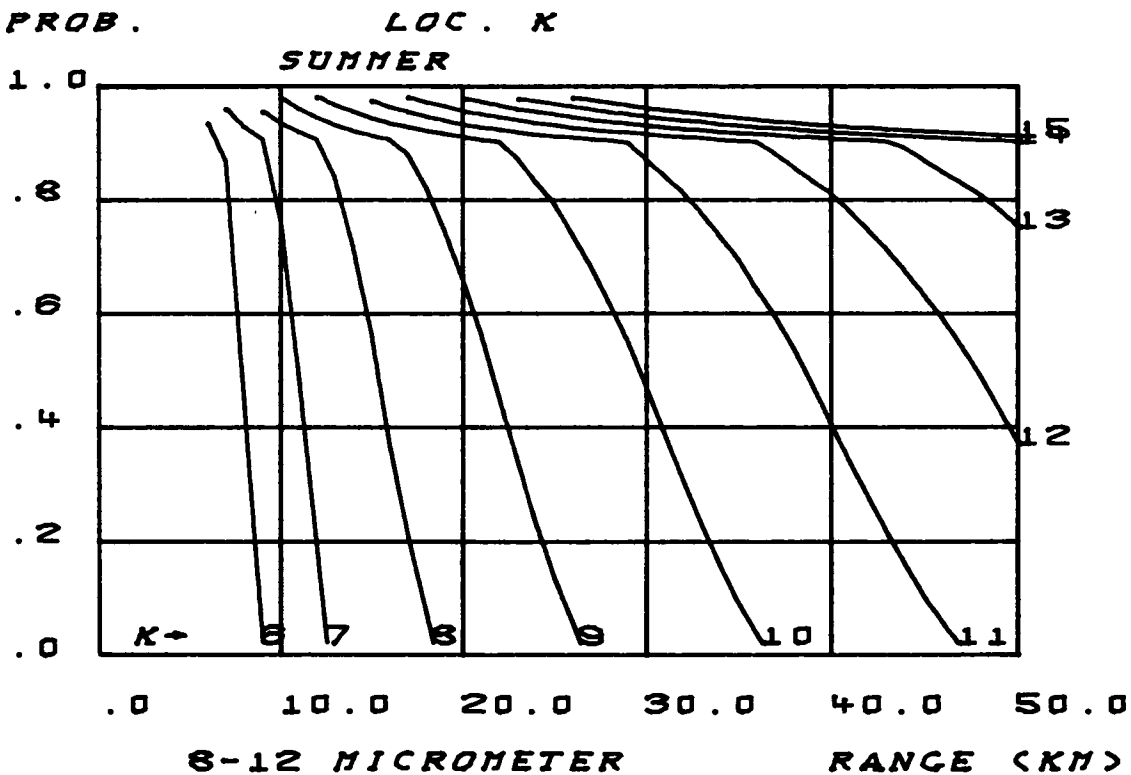
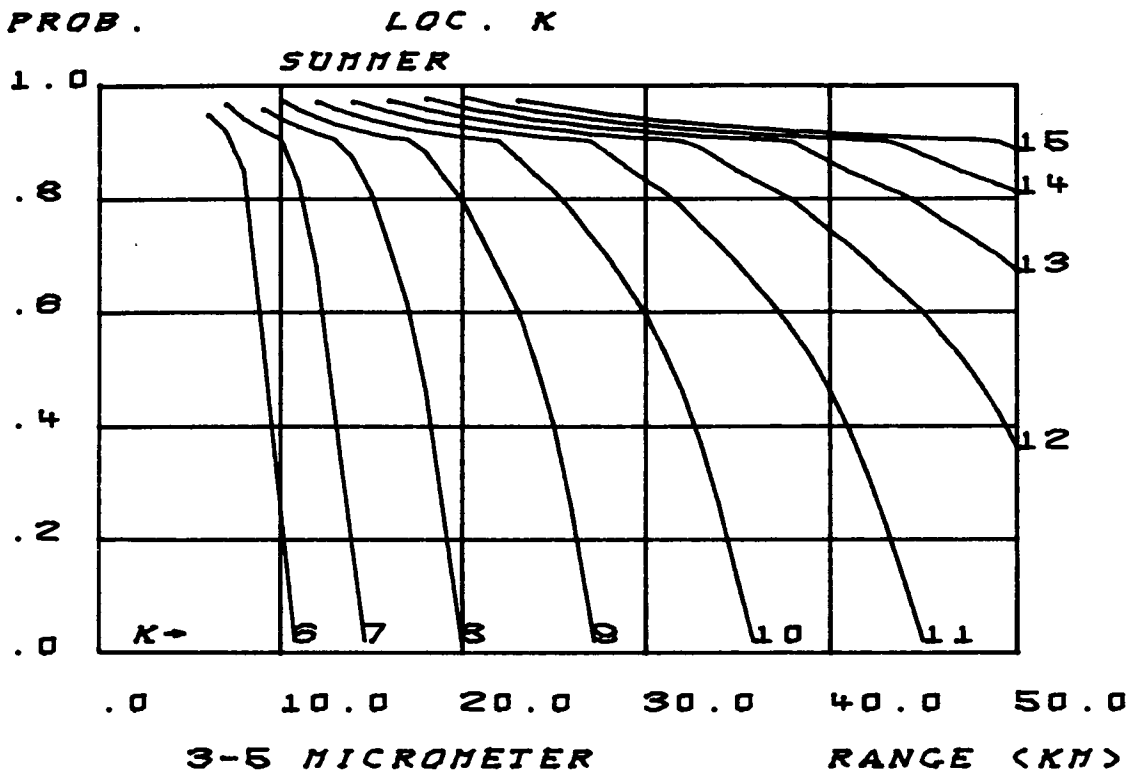


FIGURE - 30

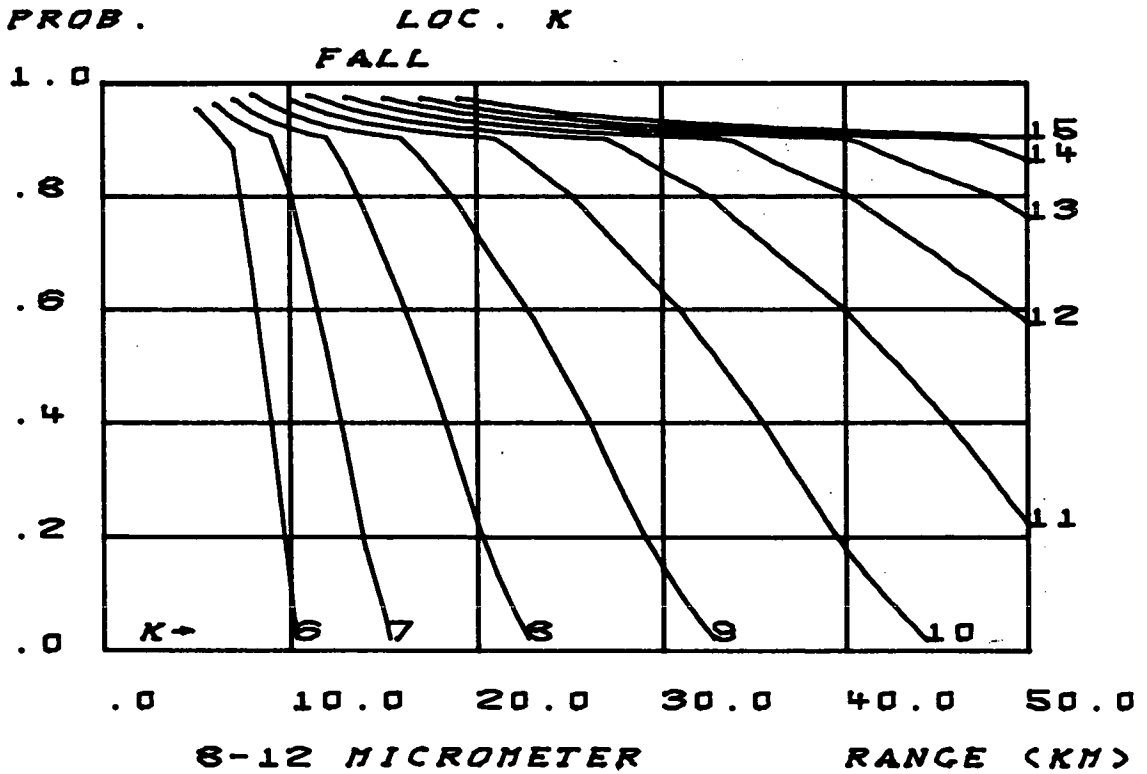
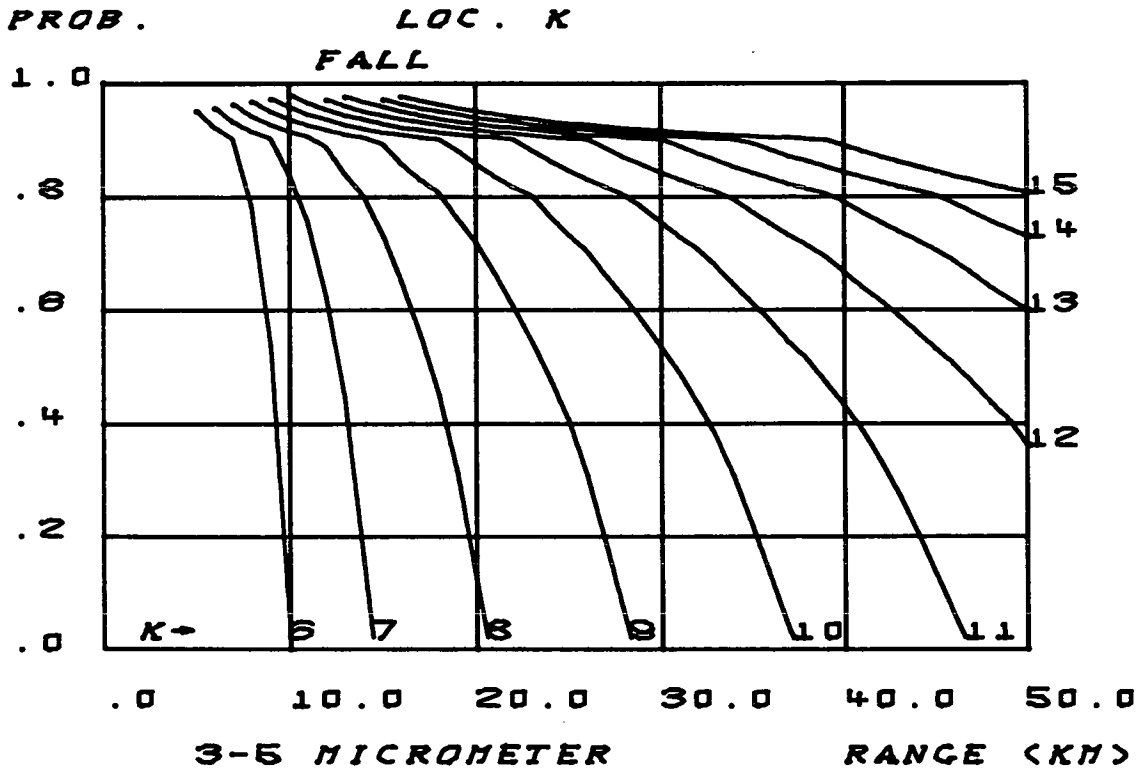


FIGURE - 31

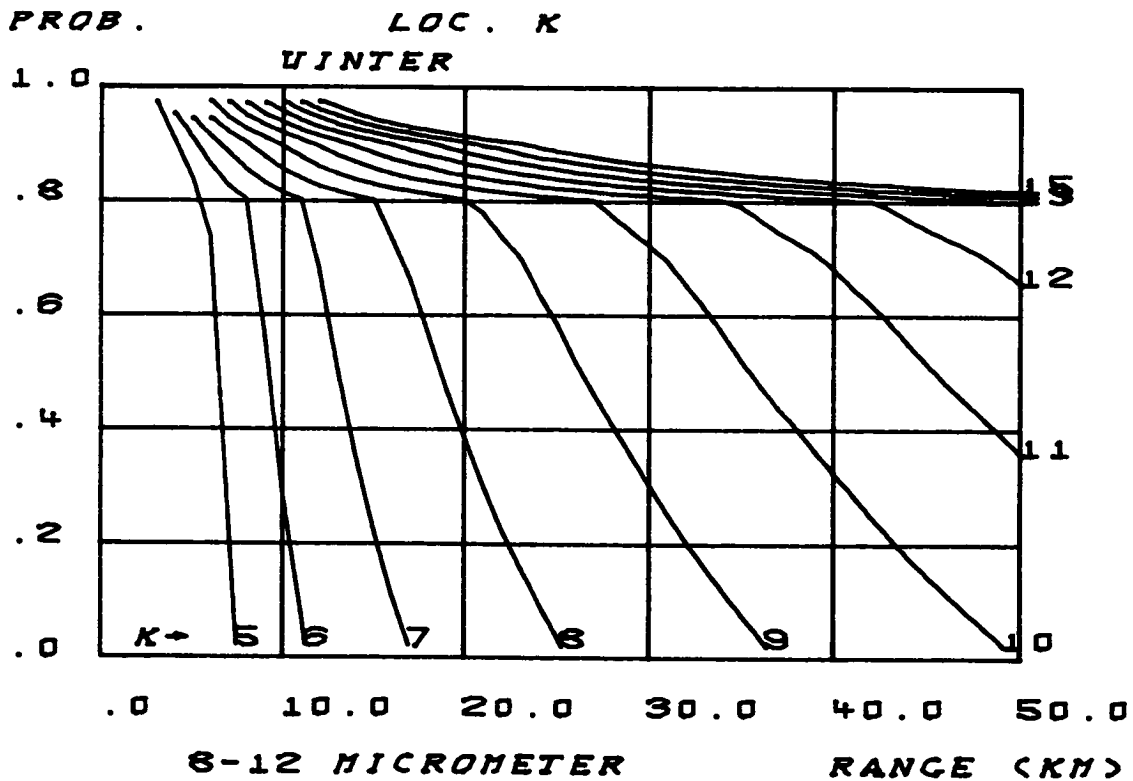
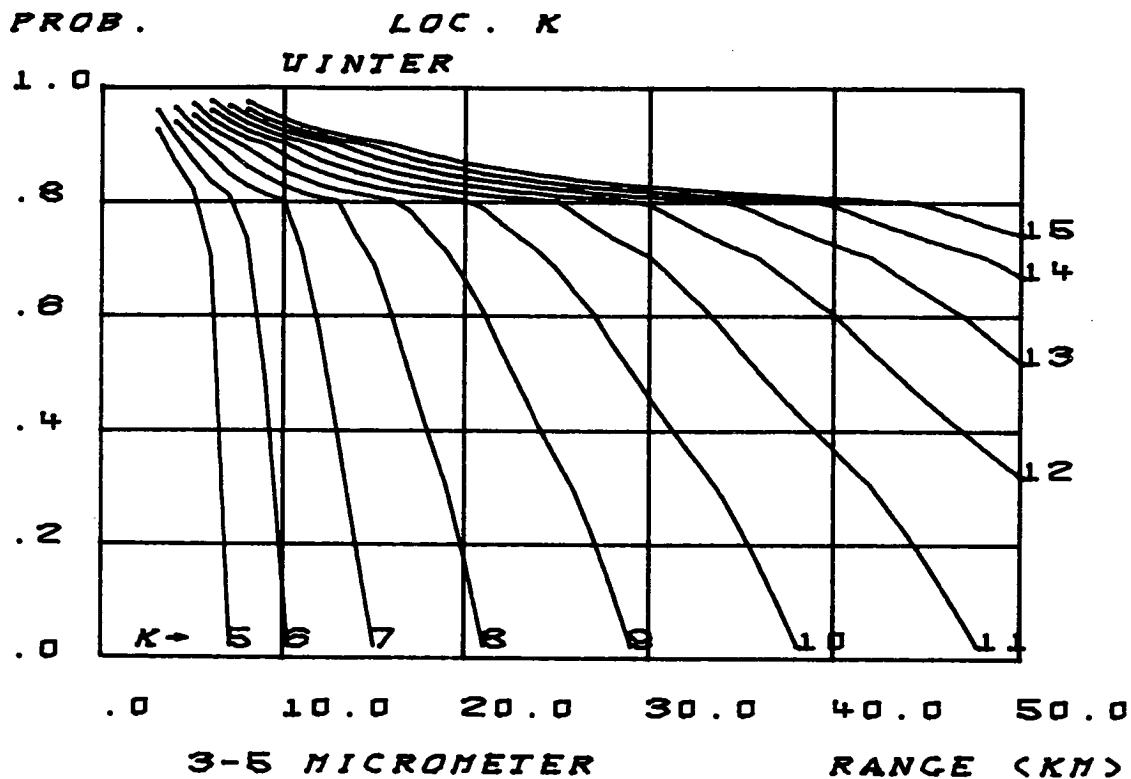


FIGURE - 32

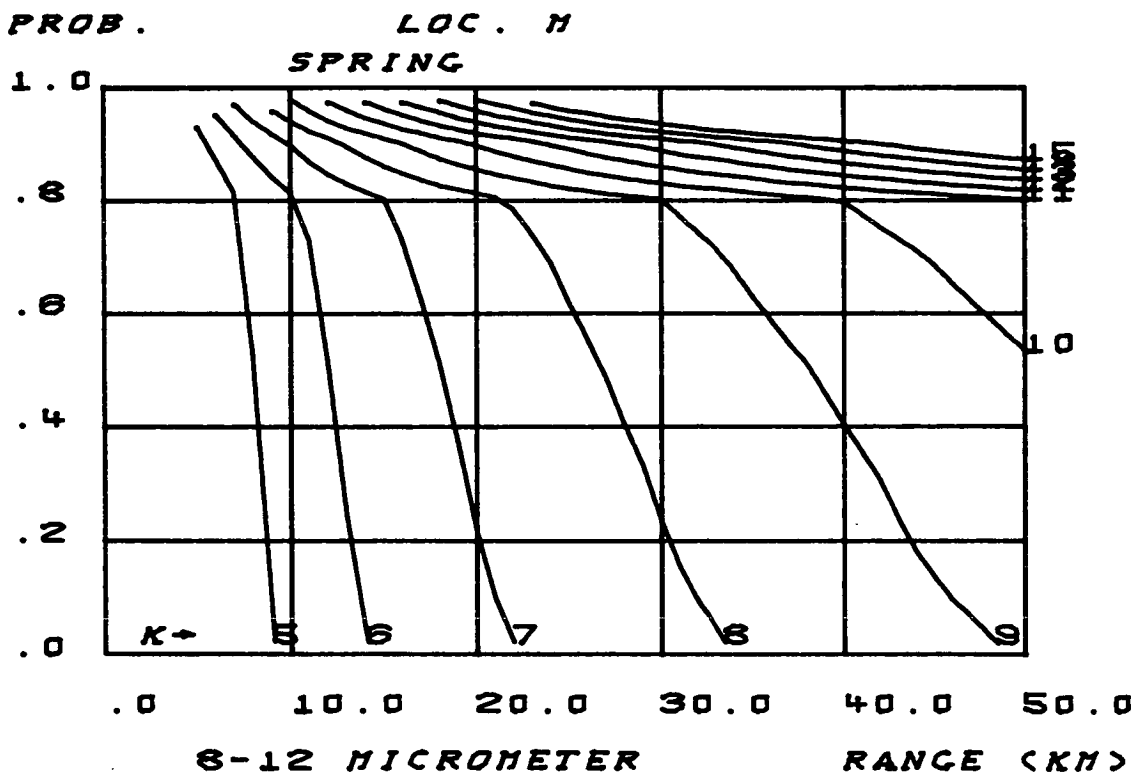
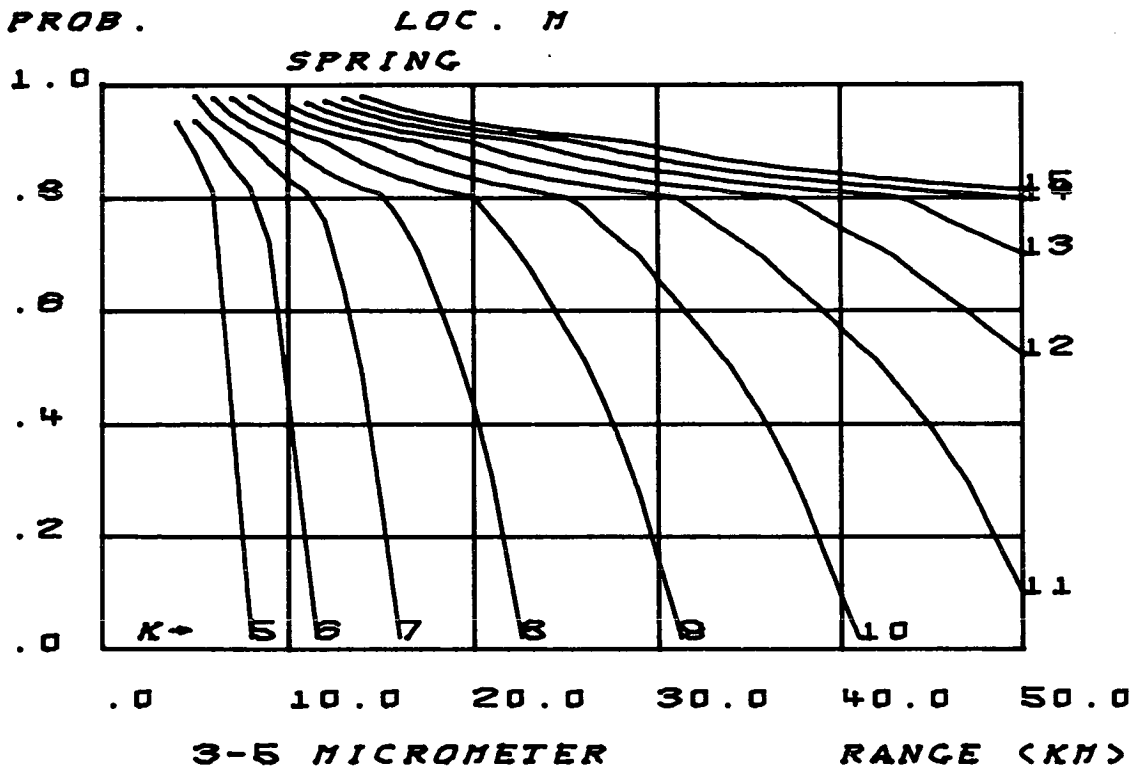


FIGURE - 33

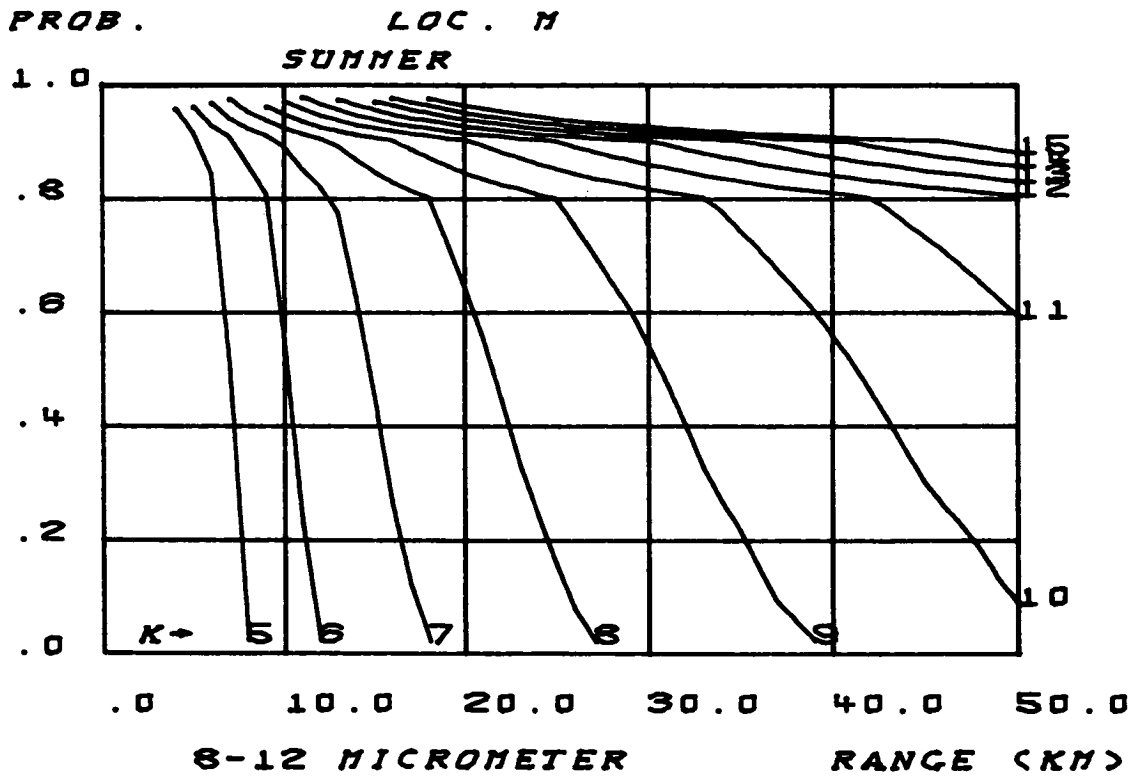
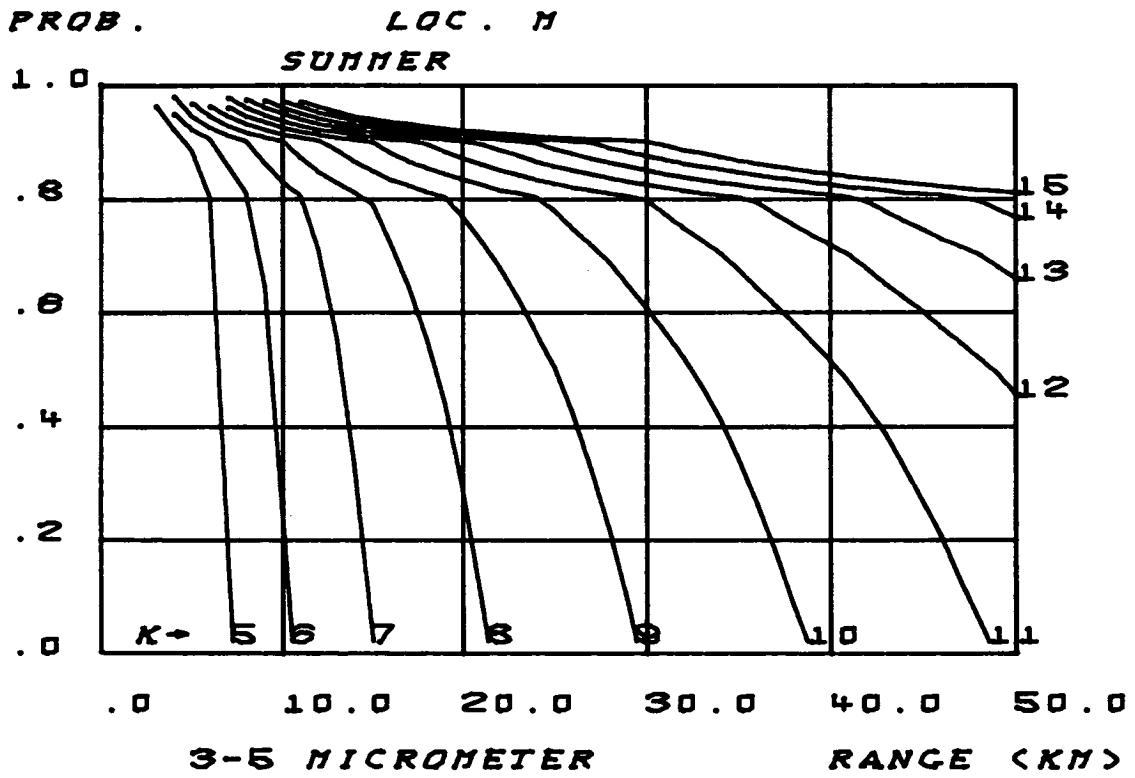


FIGURE - 34

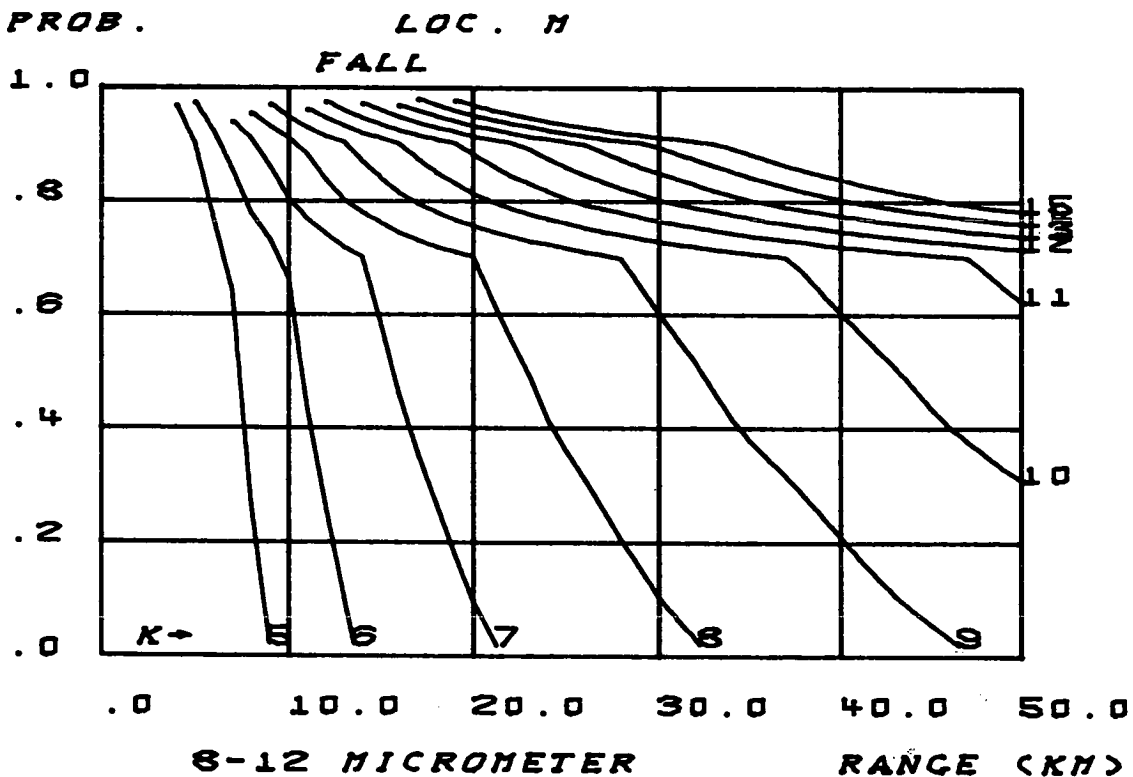
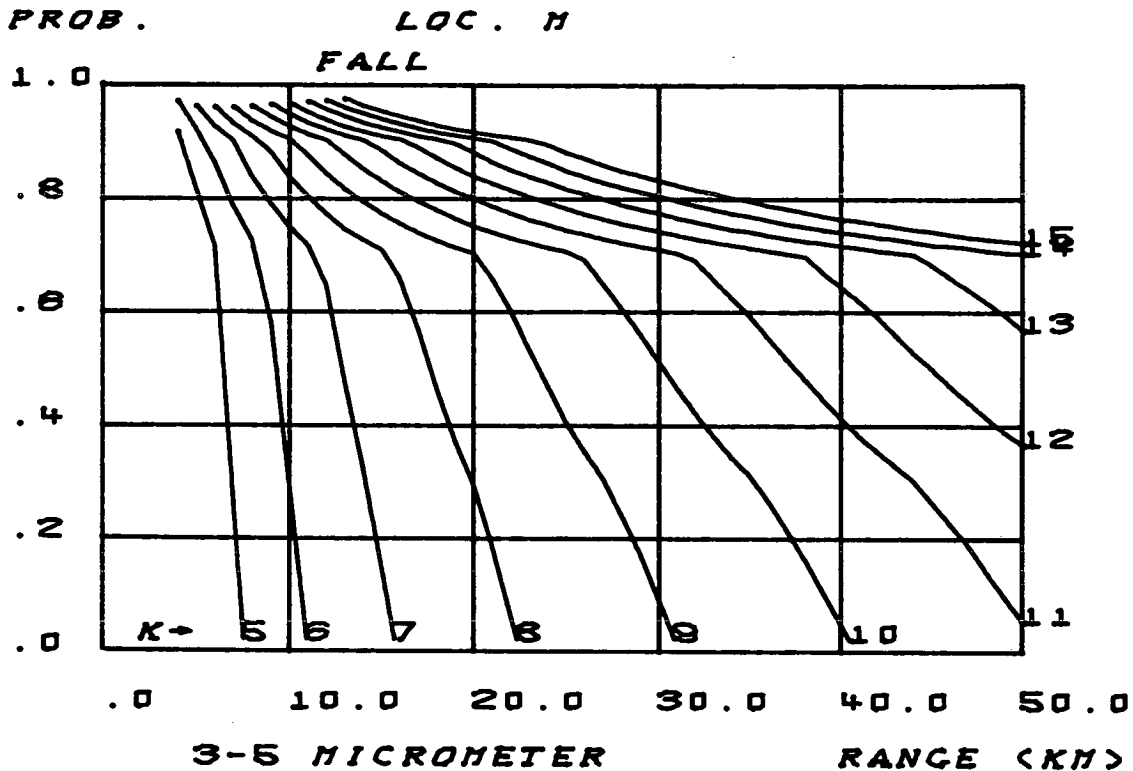


FIGURE - 35

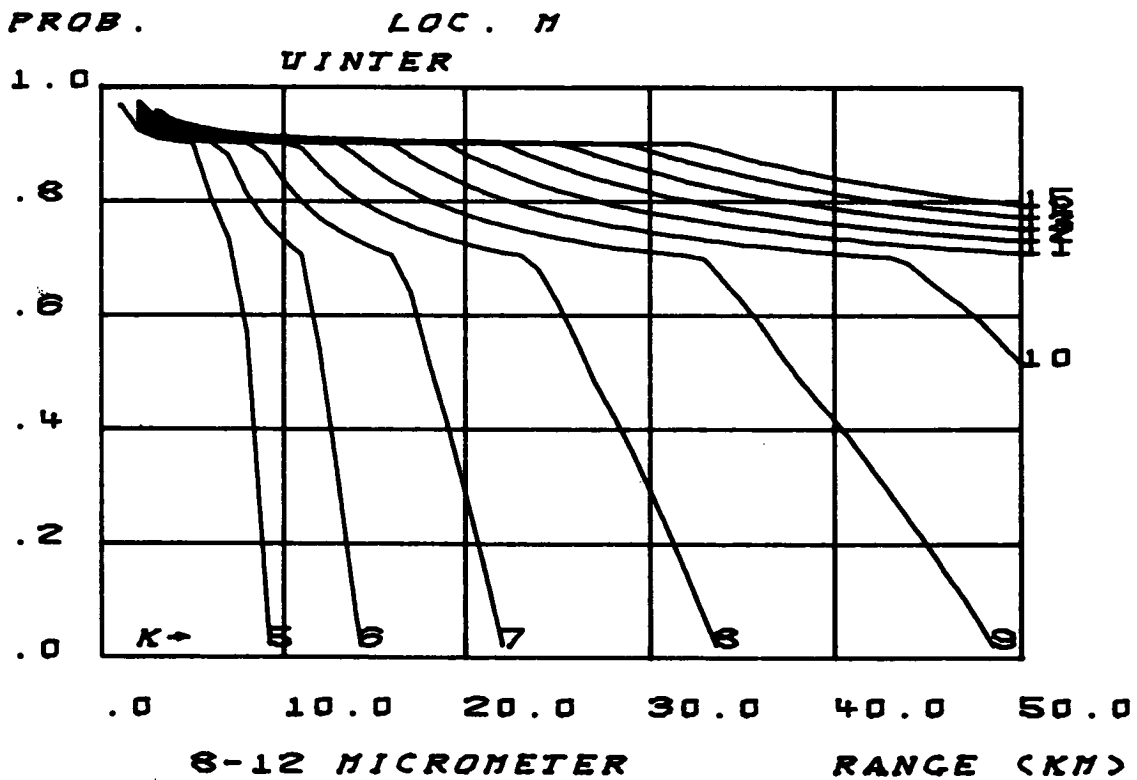
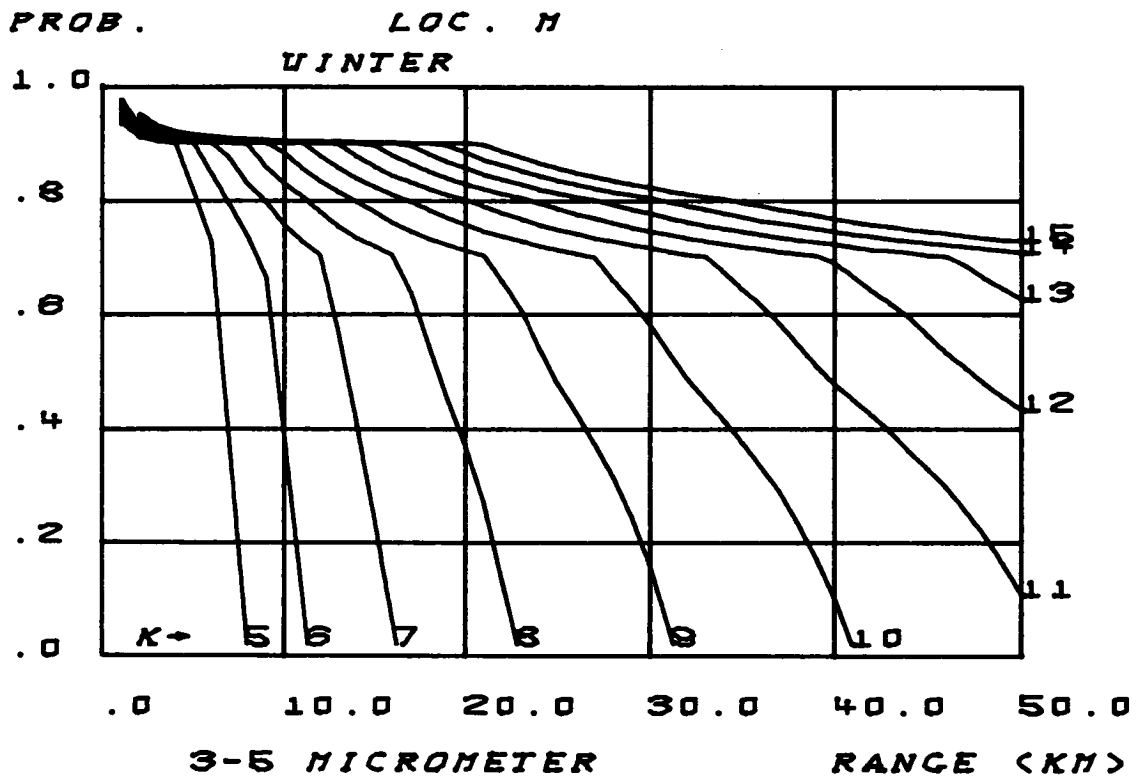


FIGURE - 36

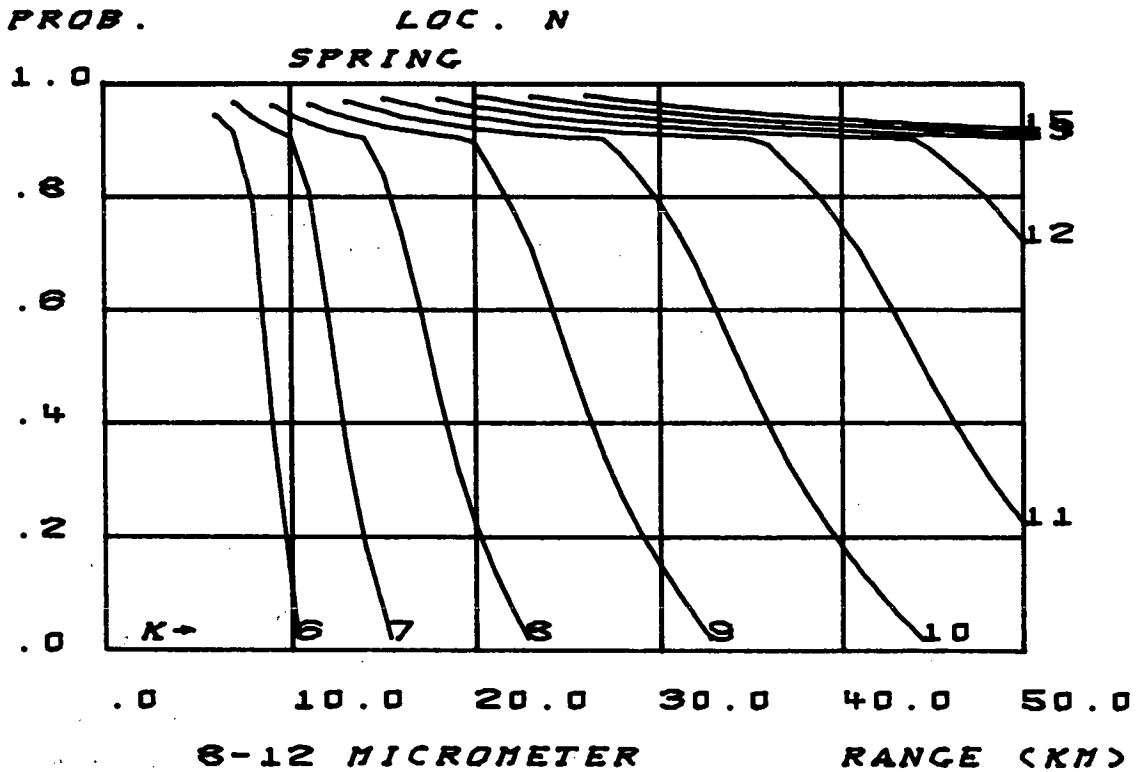
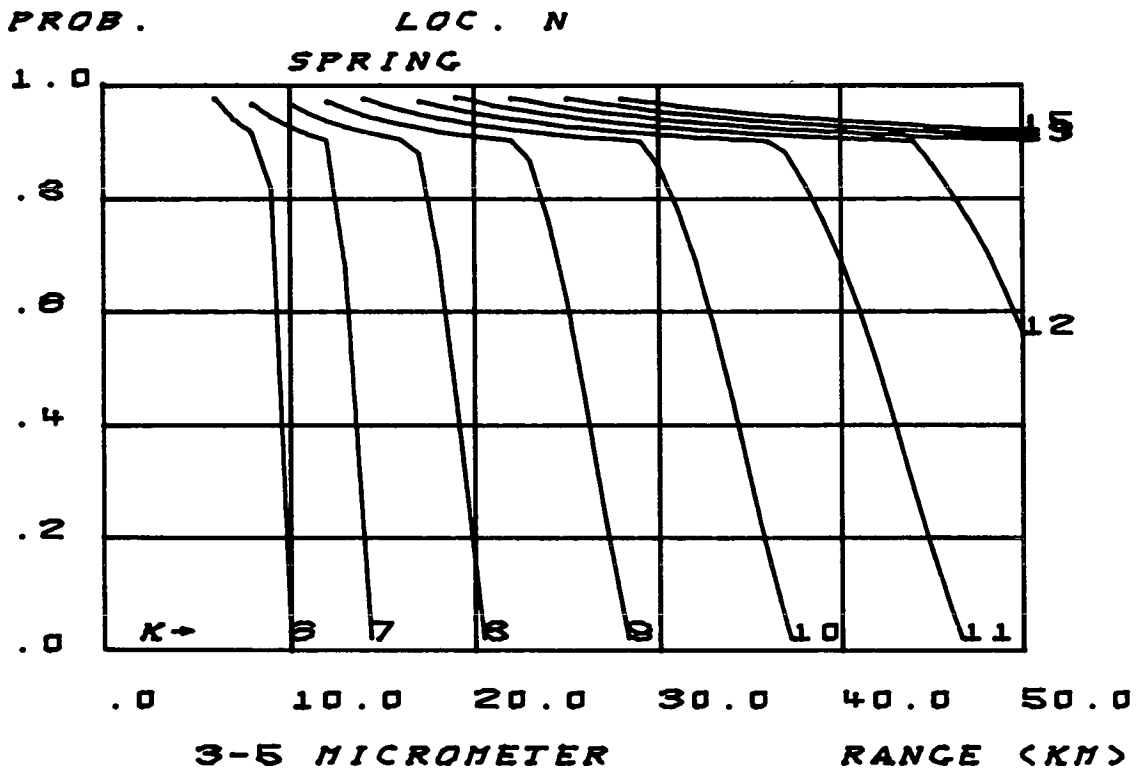


FIGURE - 37

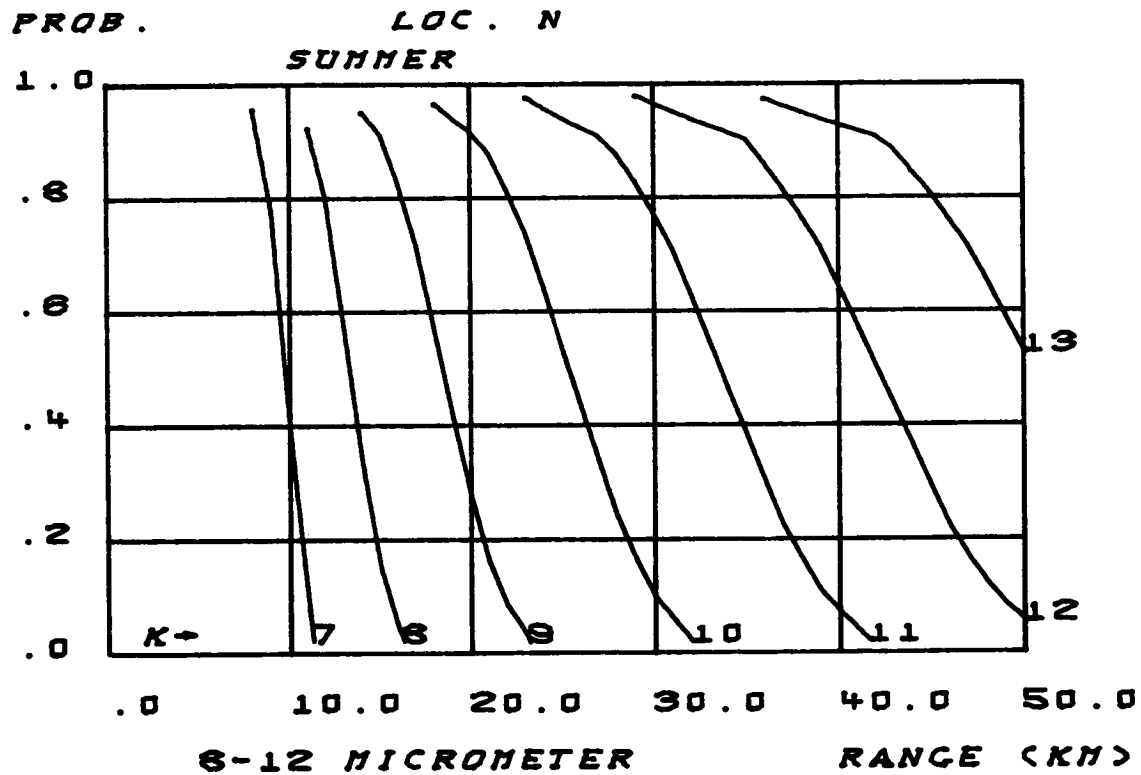
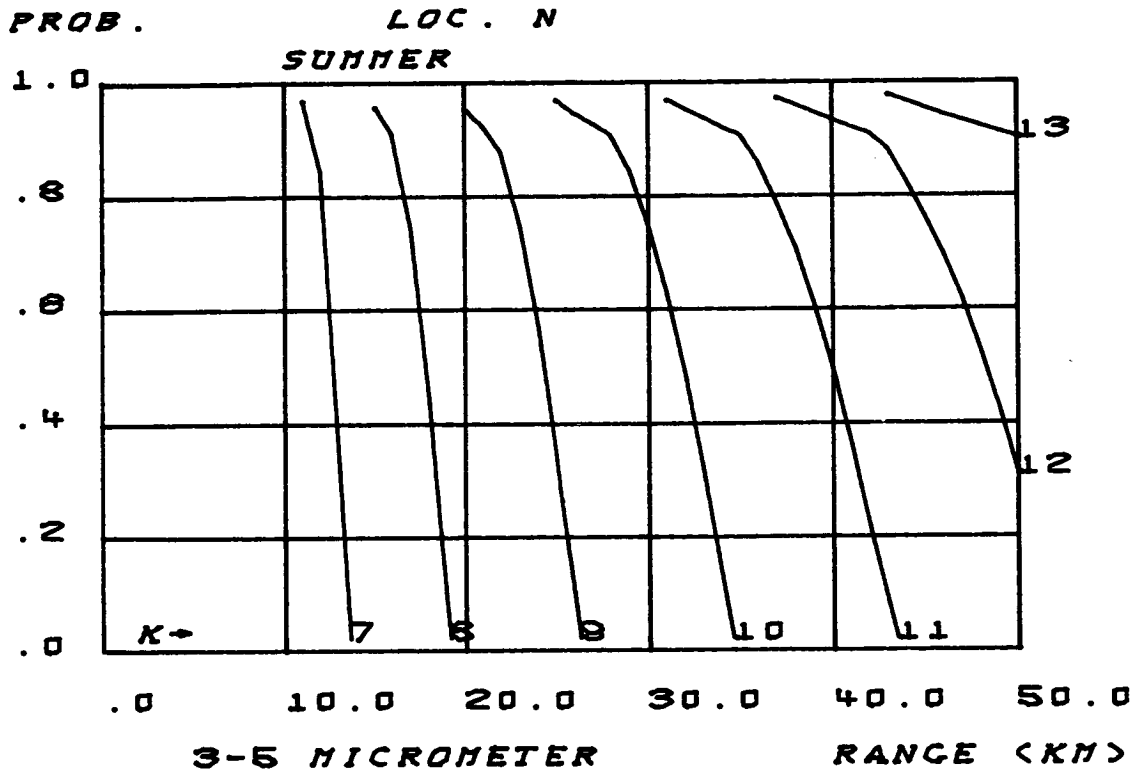


FIGURE - 38

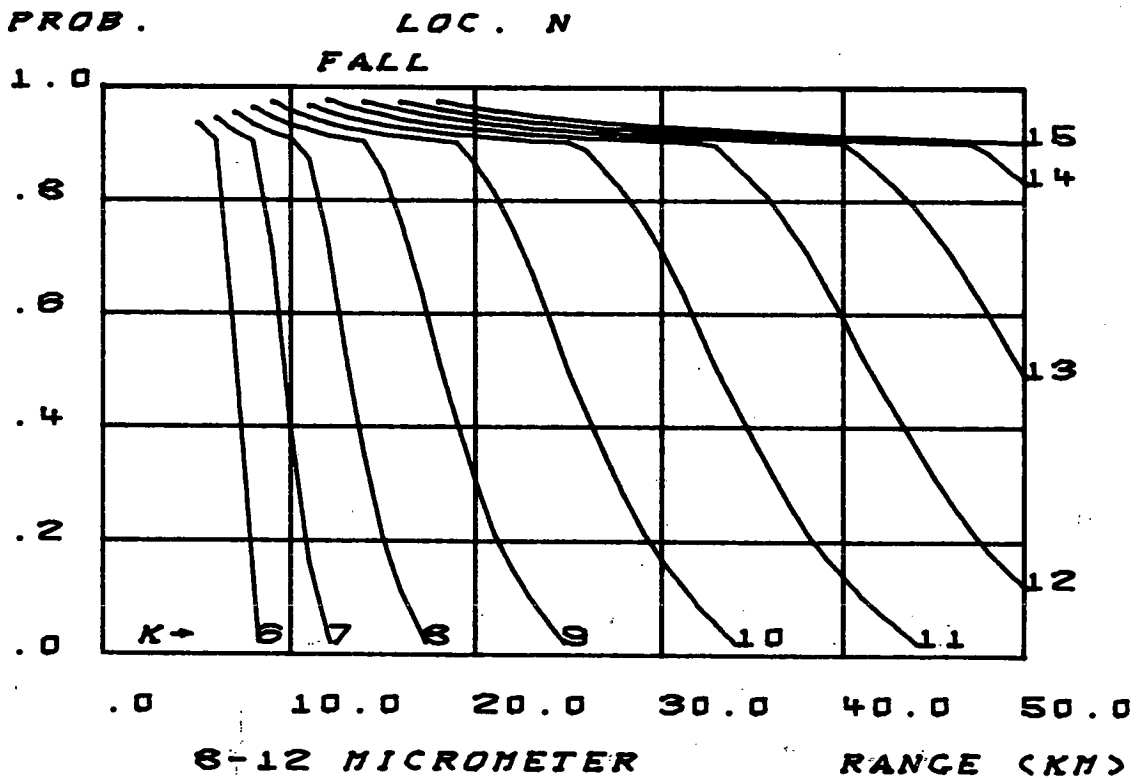
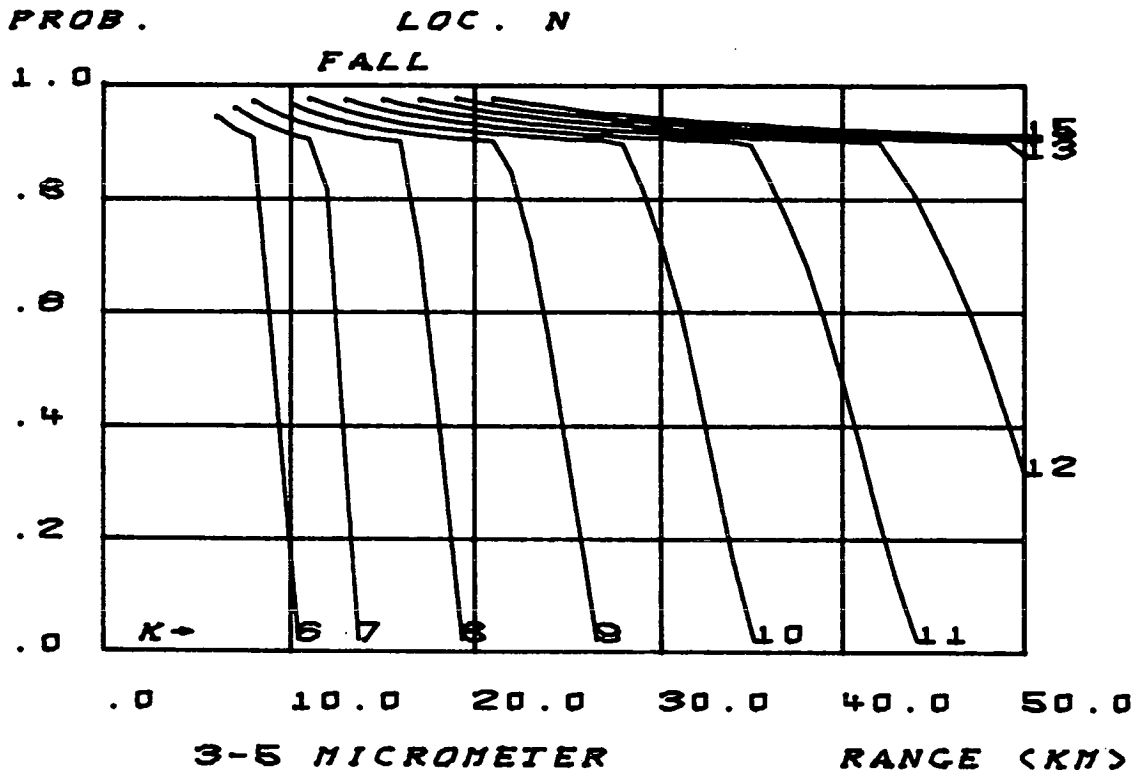


FIGURE - 39

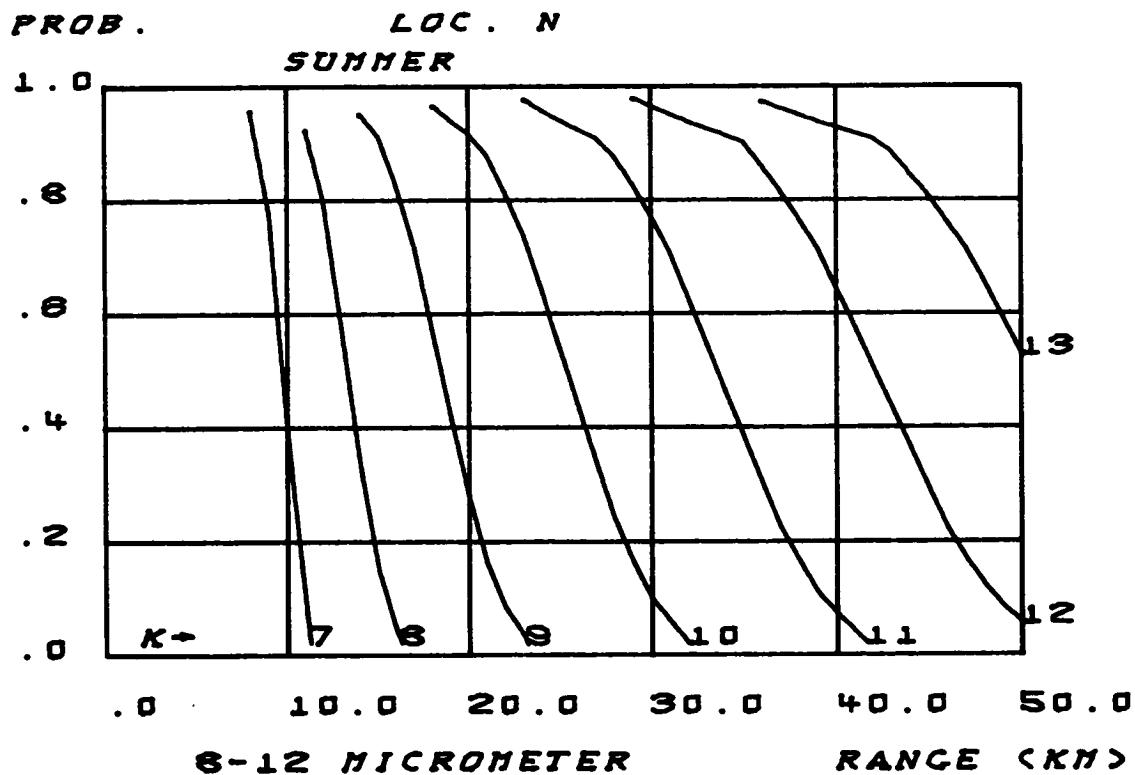
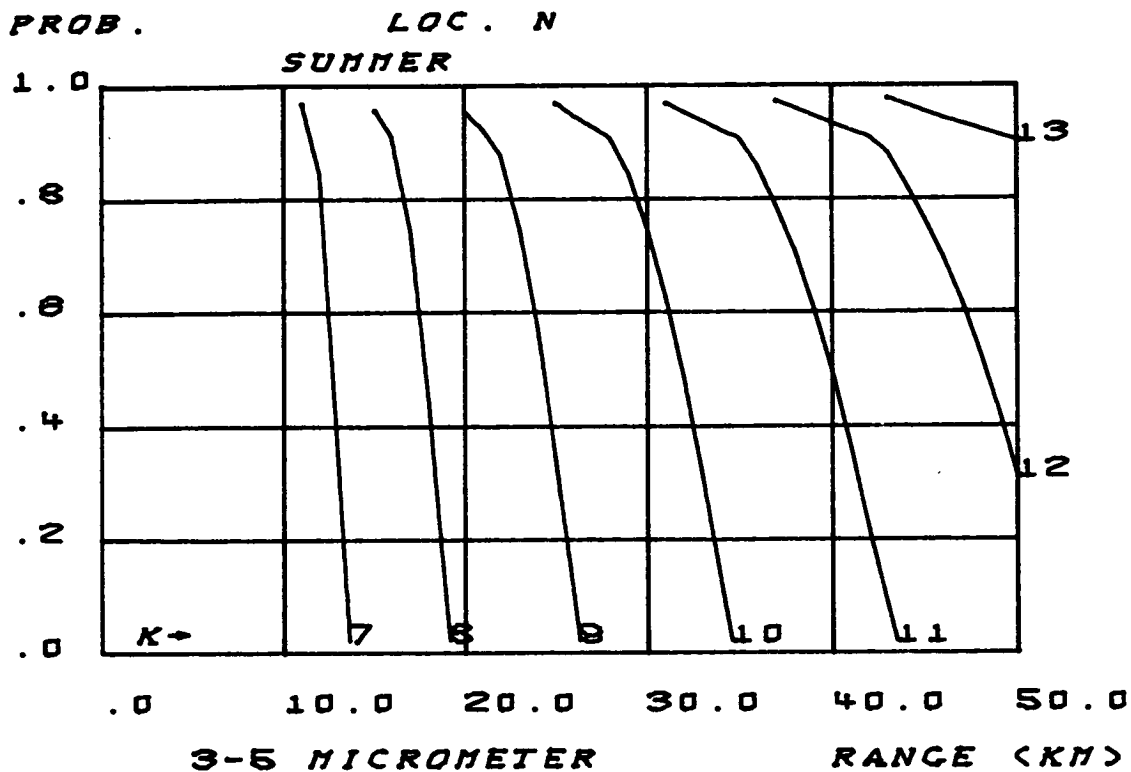


FIGURE - 38

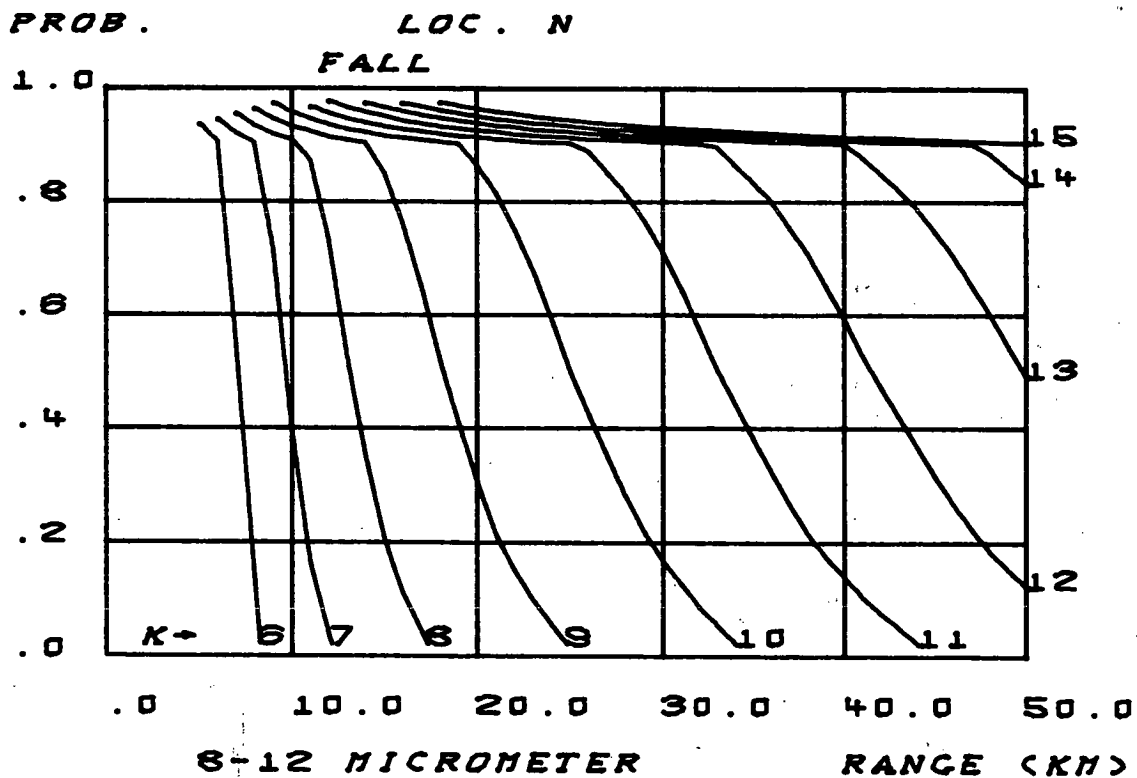
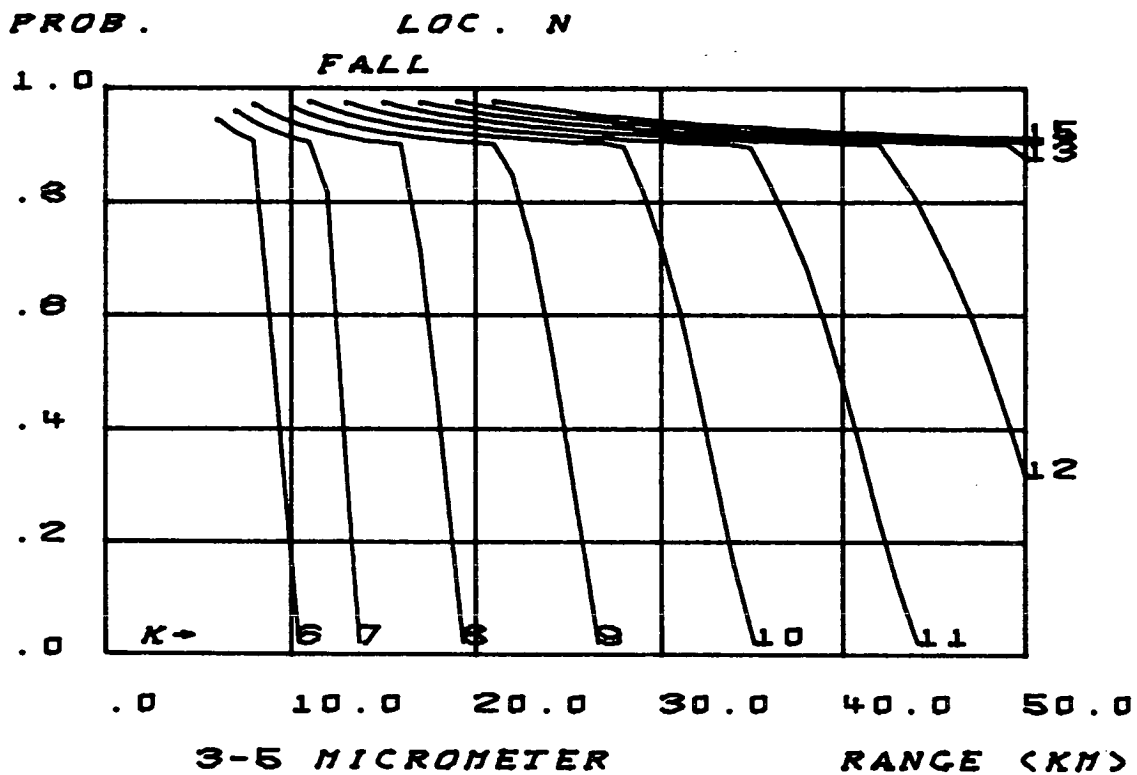


FIGURE - 39

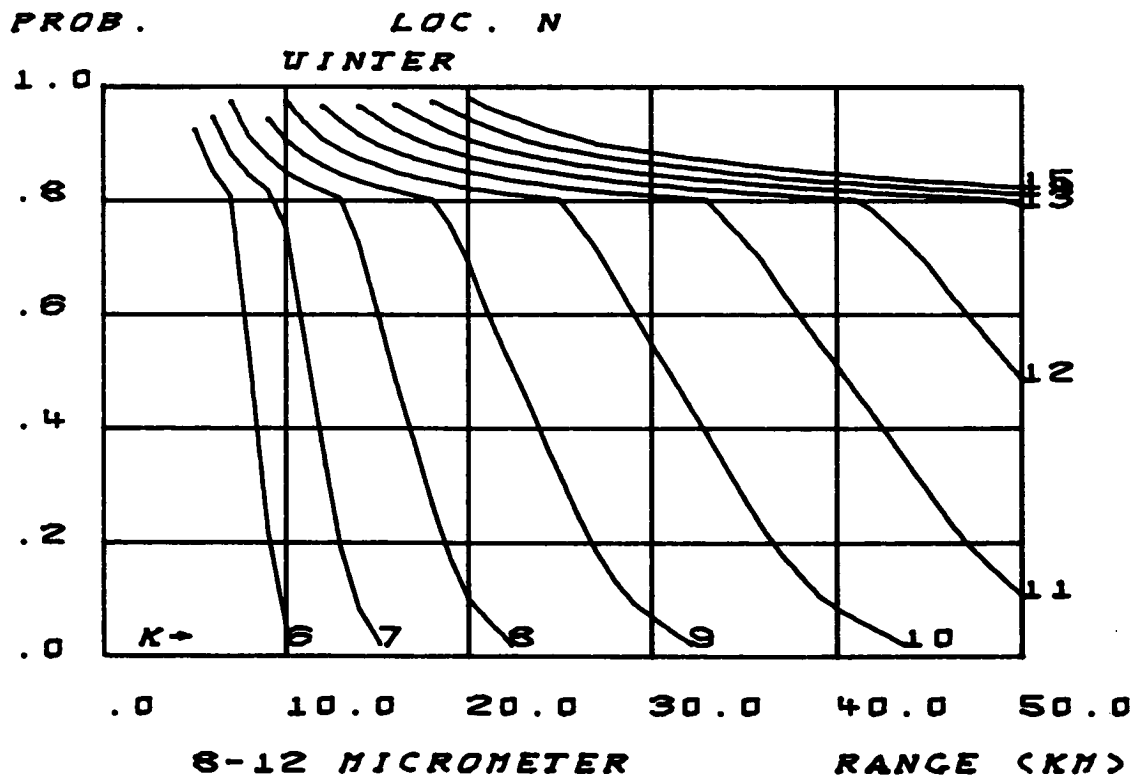
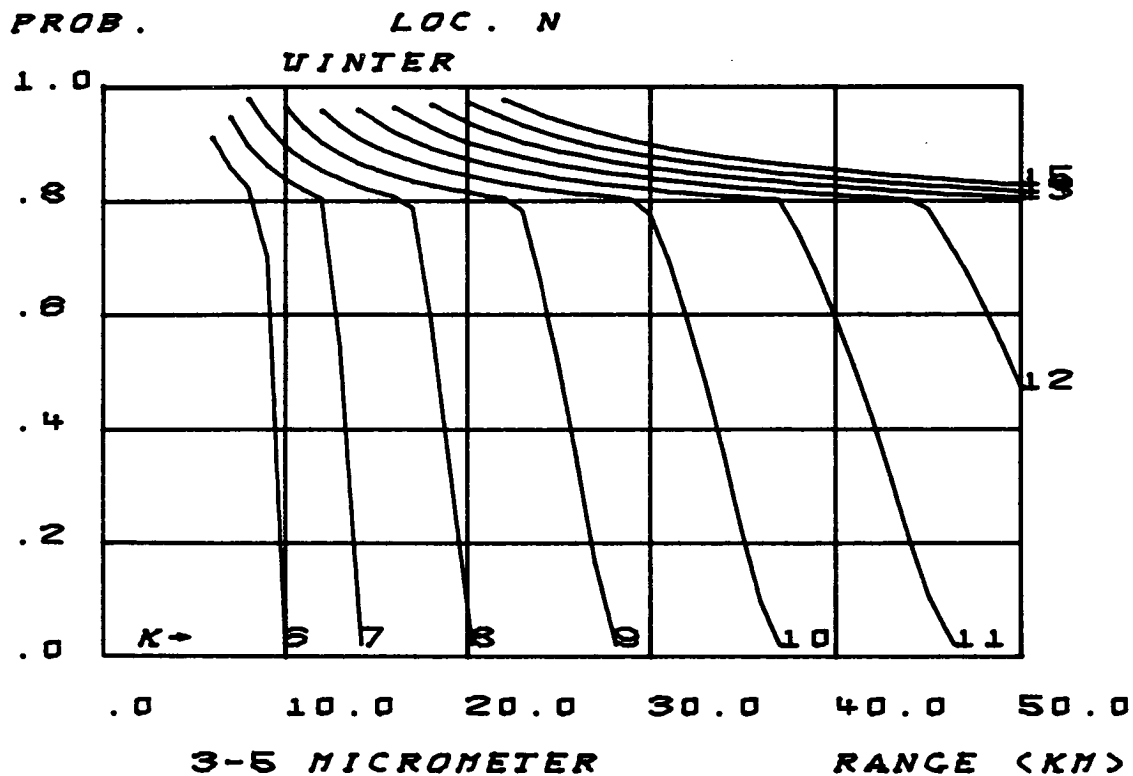


FIGURE - 40

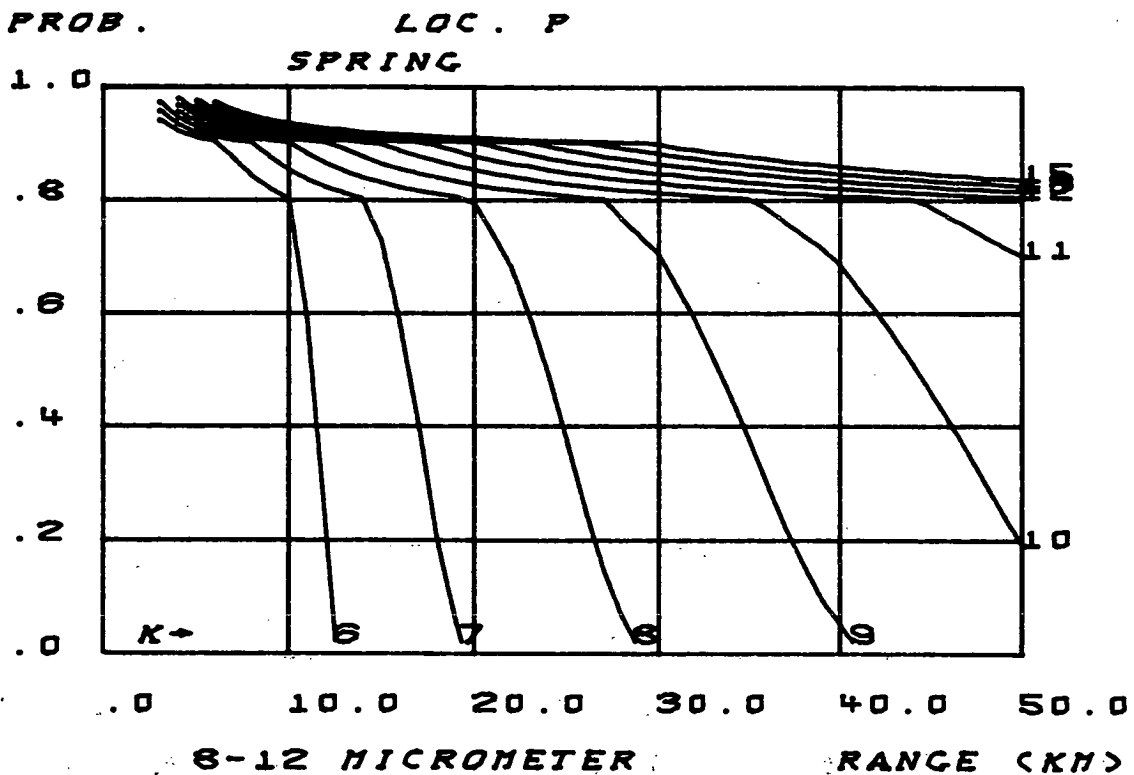
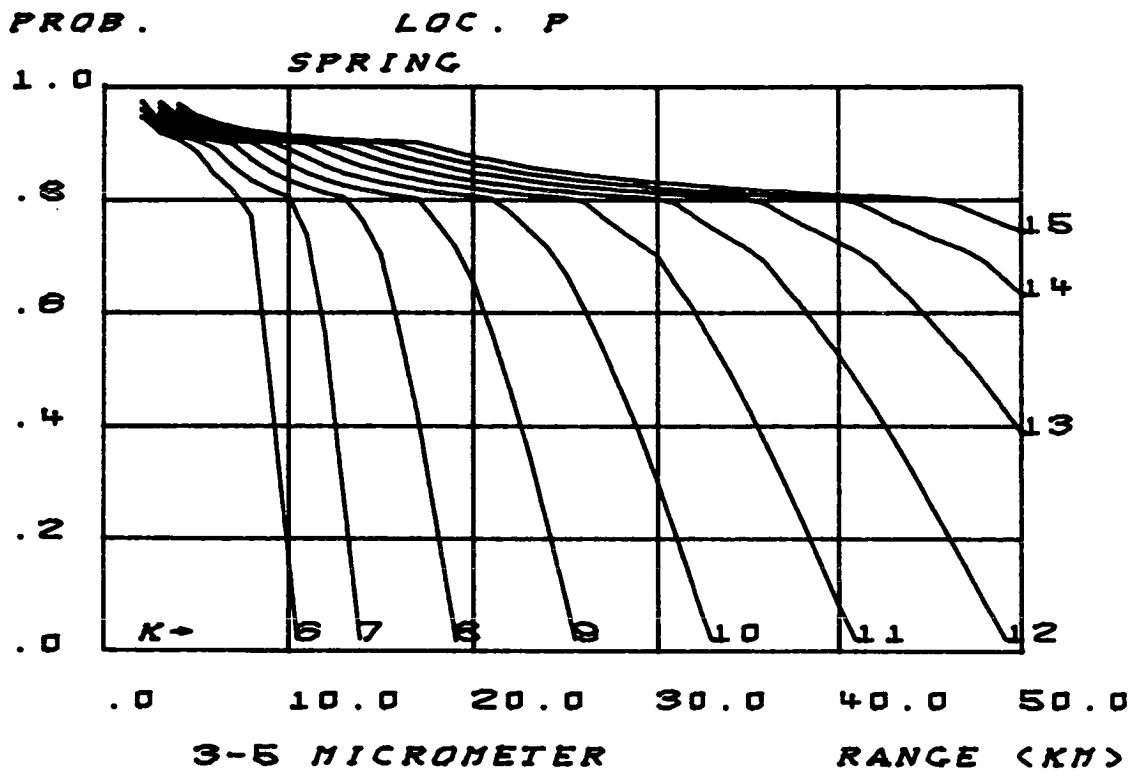


FIGURE - 41

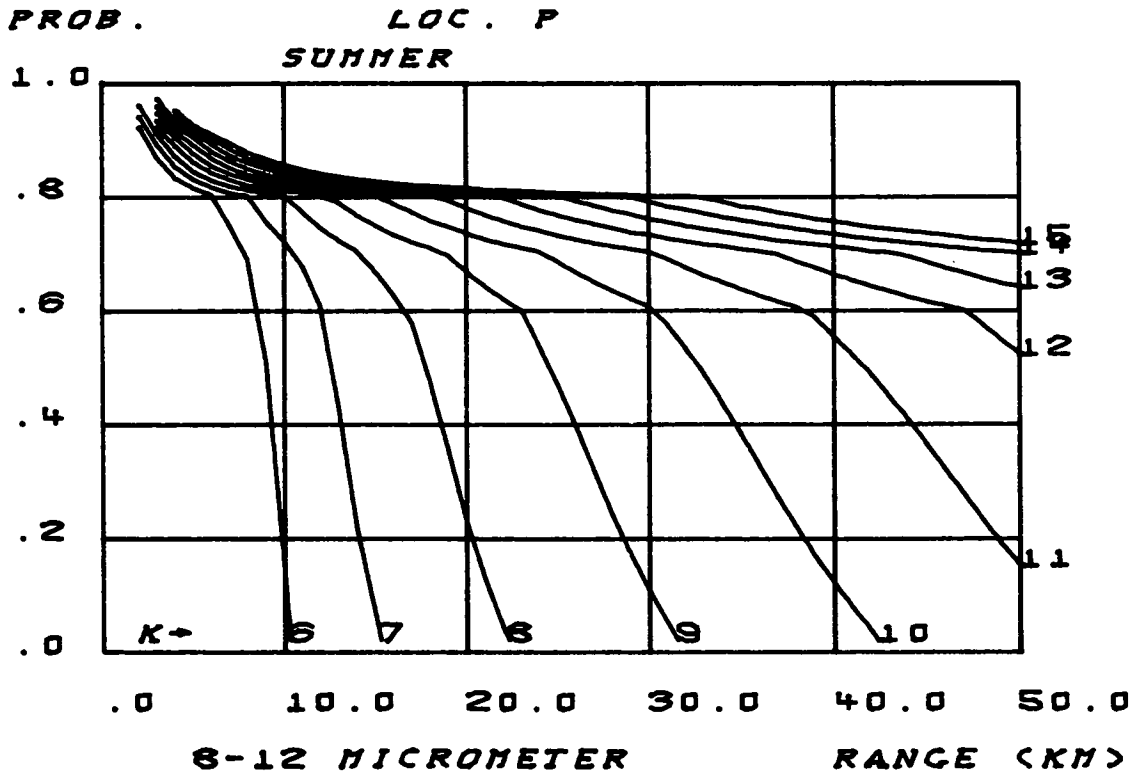
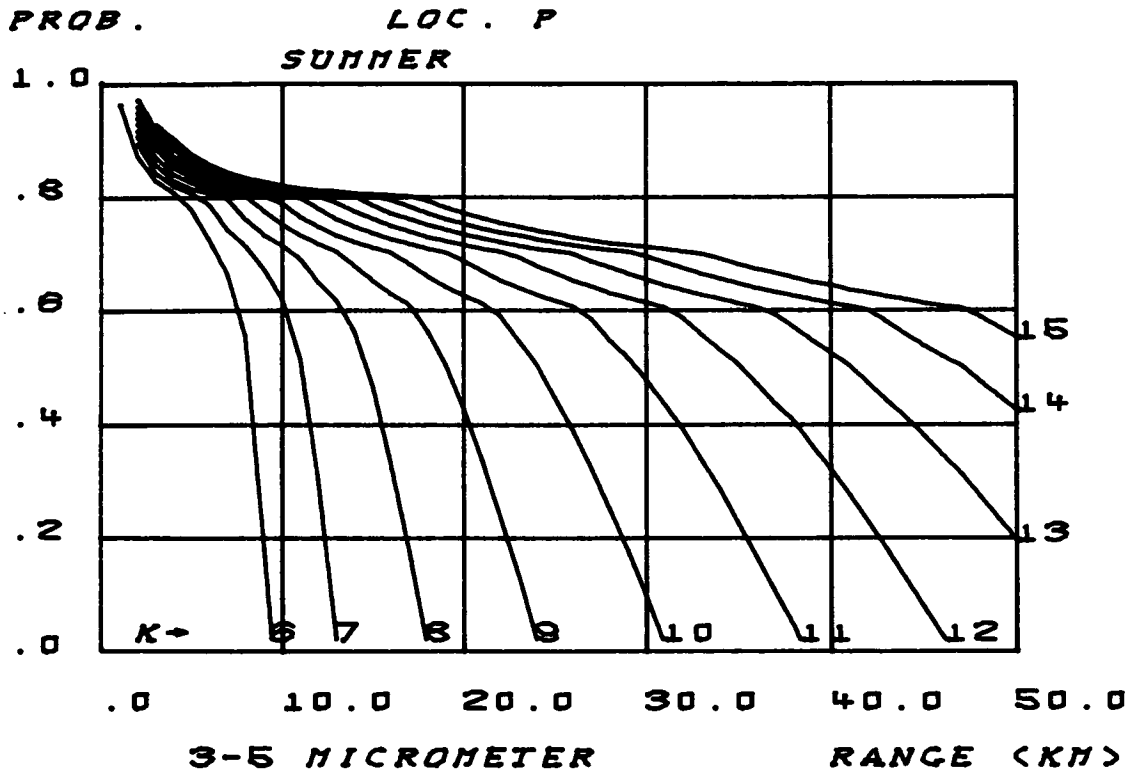


FIGURE - 42

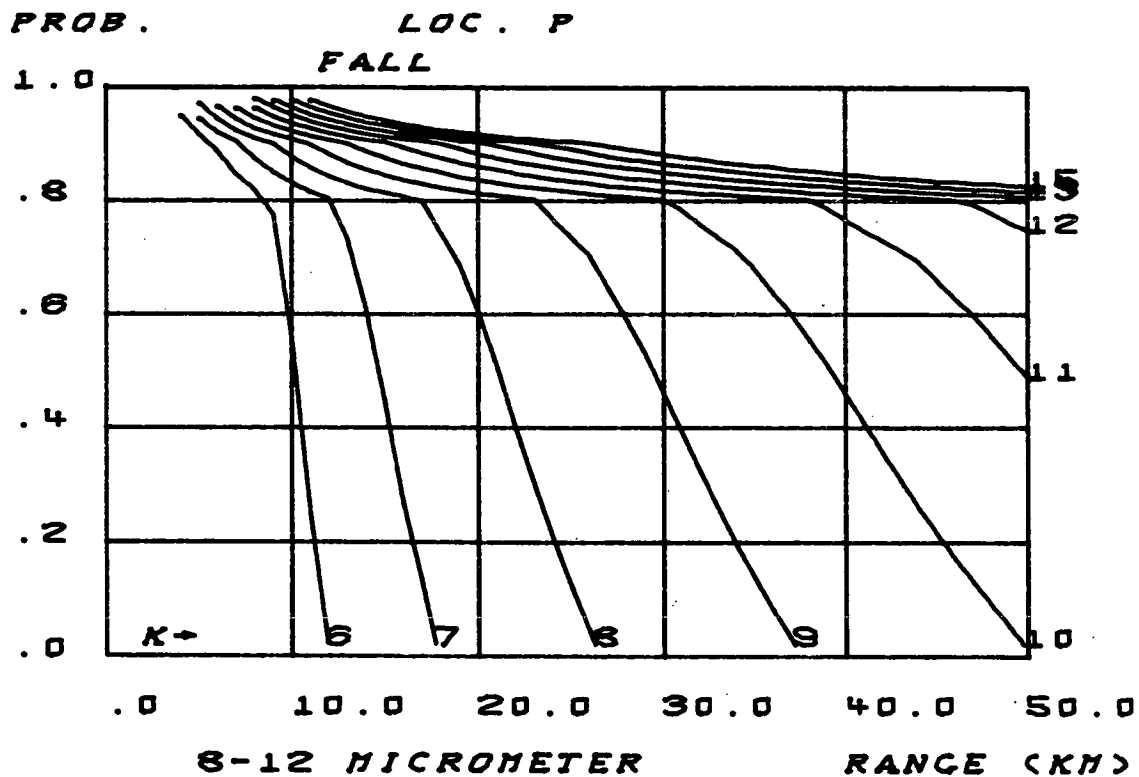
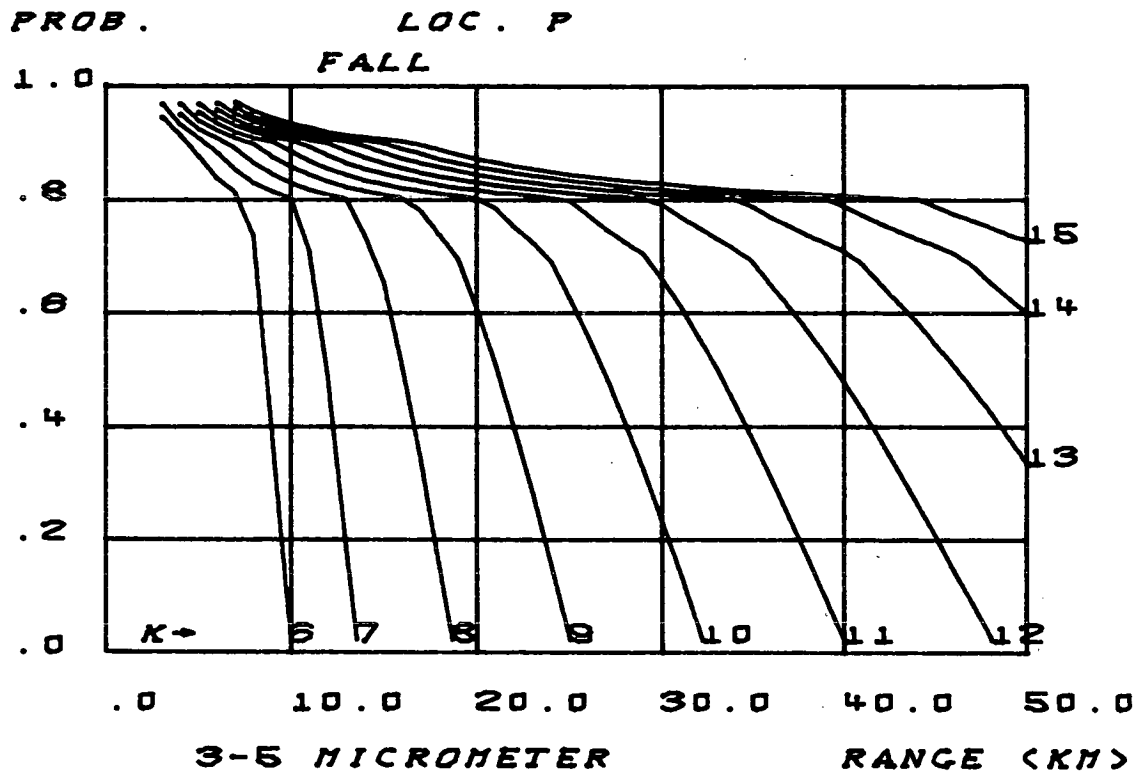


FIGURE - 43

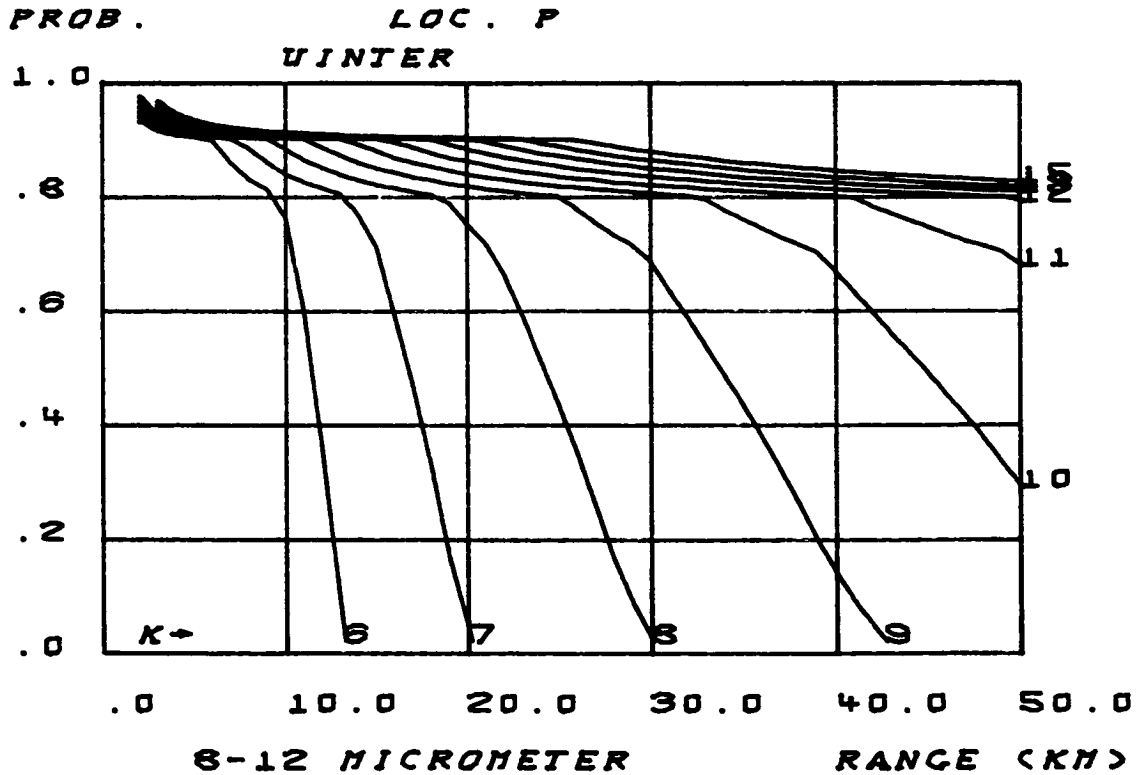
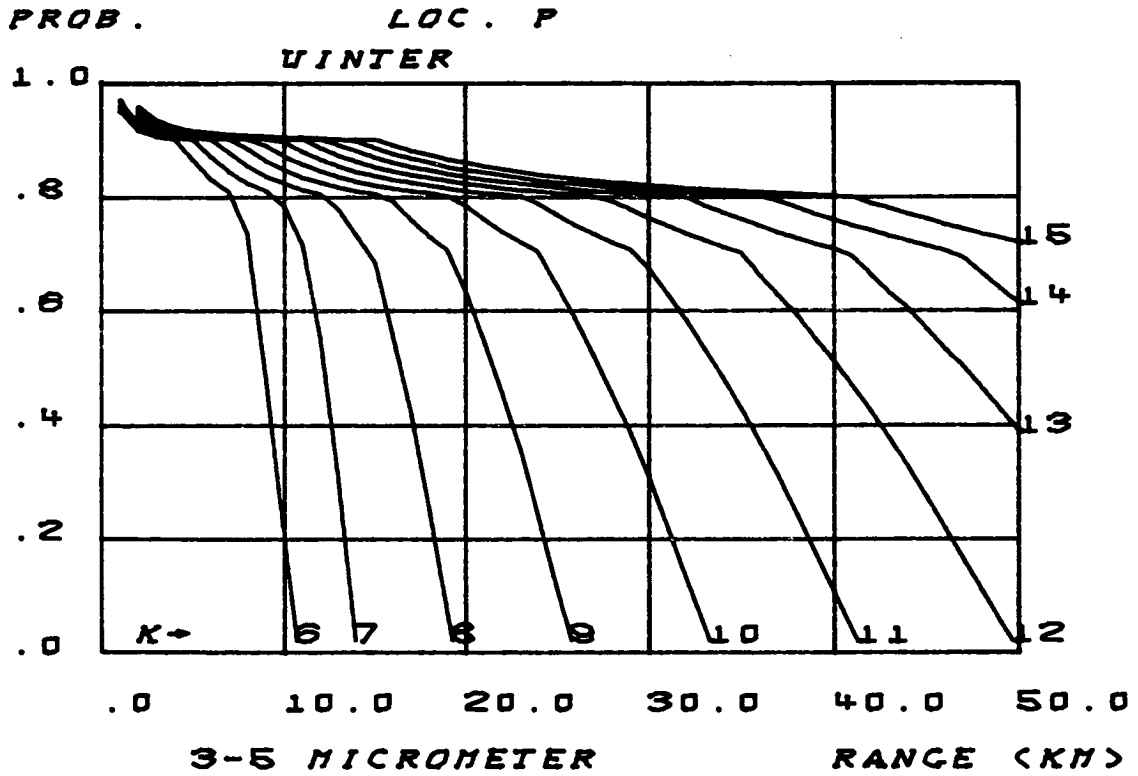


FIGURE - 44

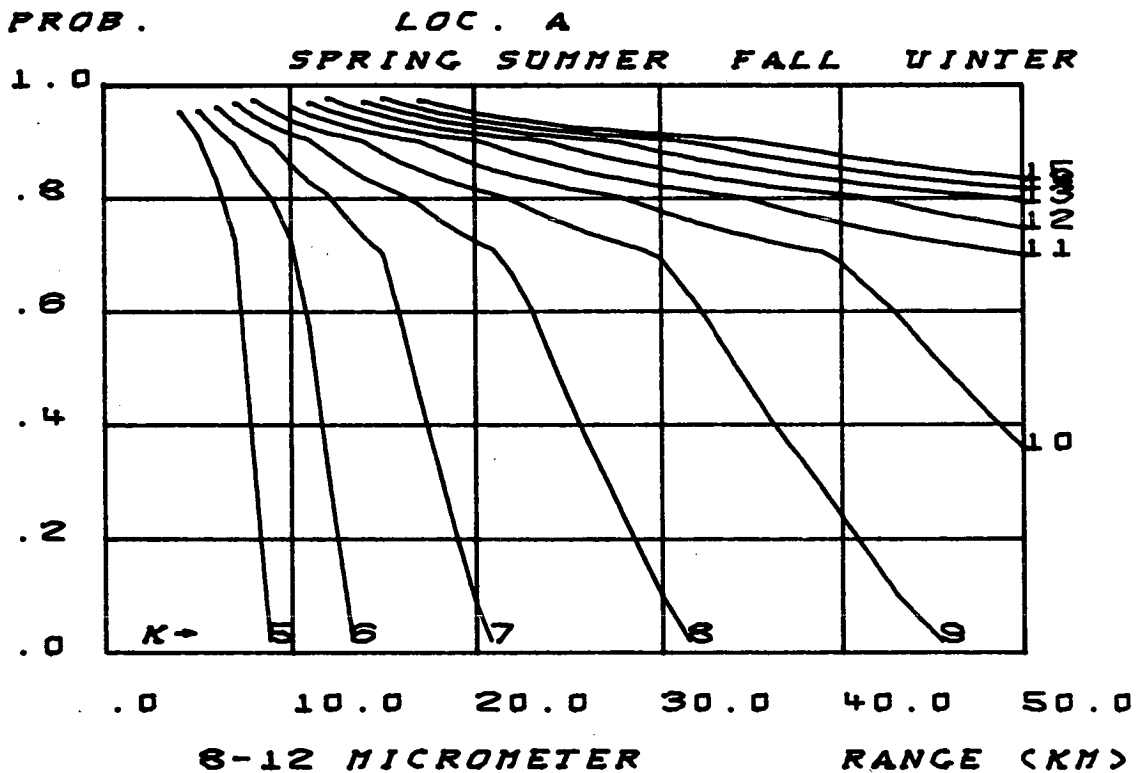
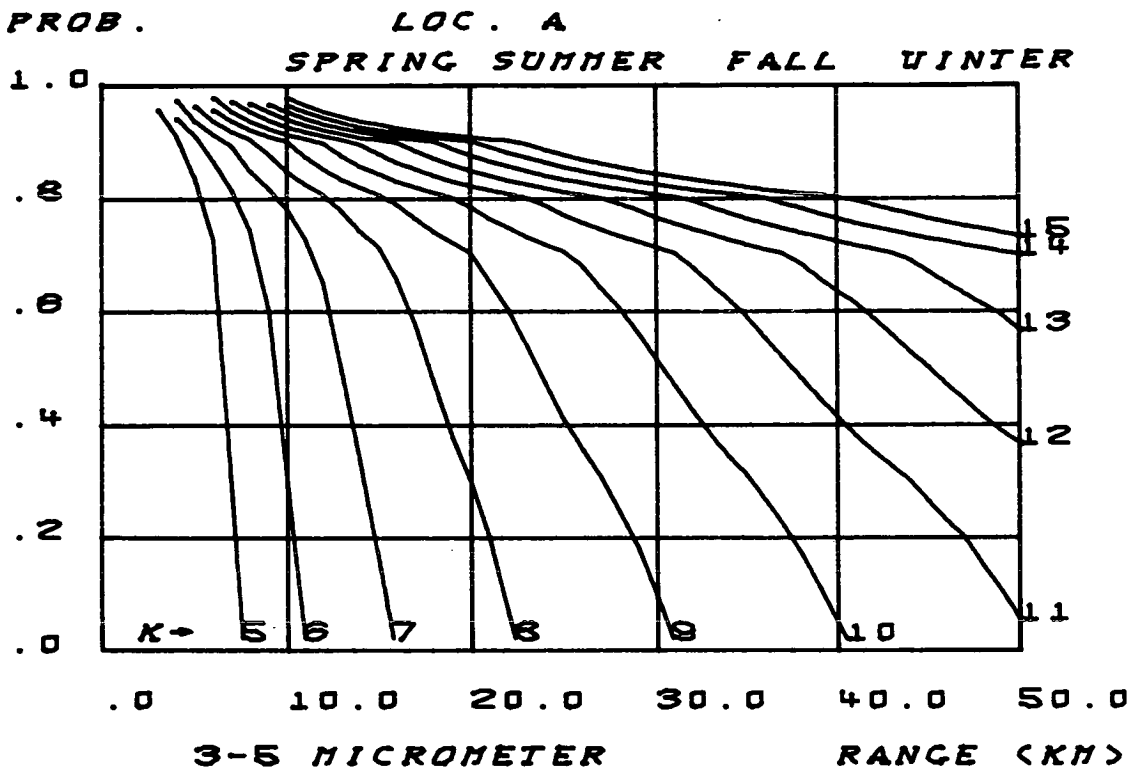


FIGURE - 45

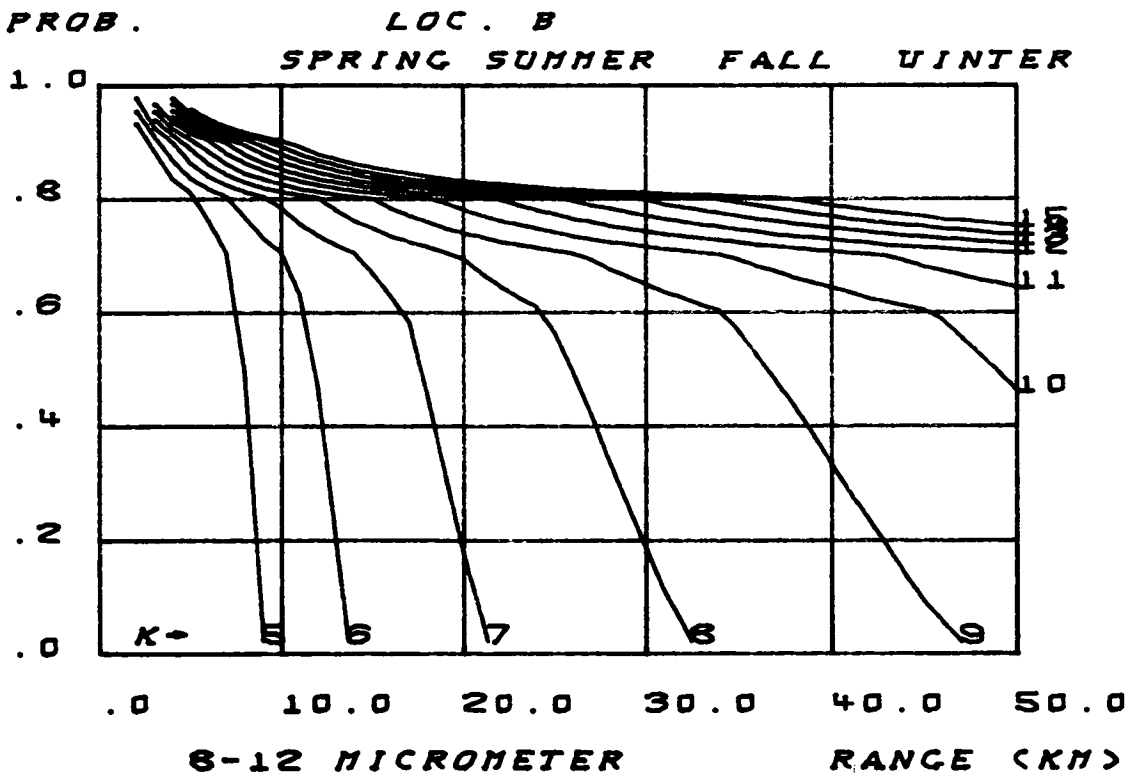
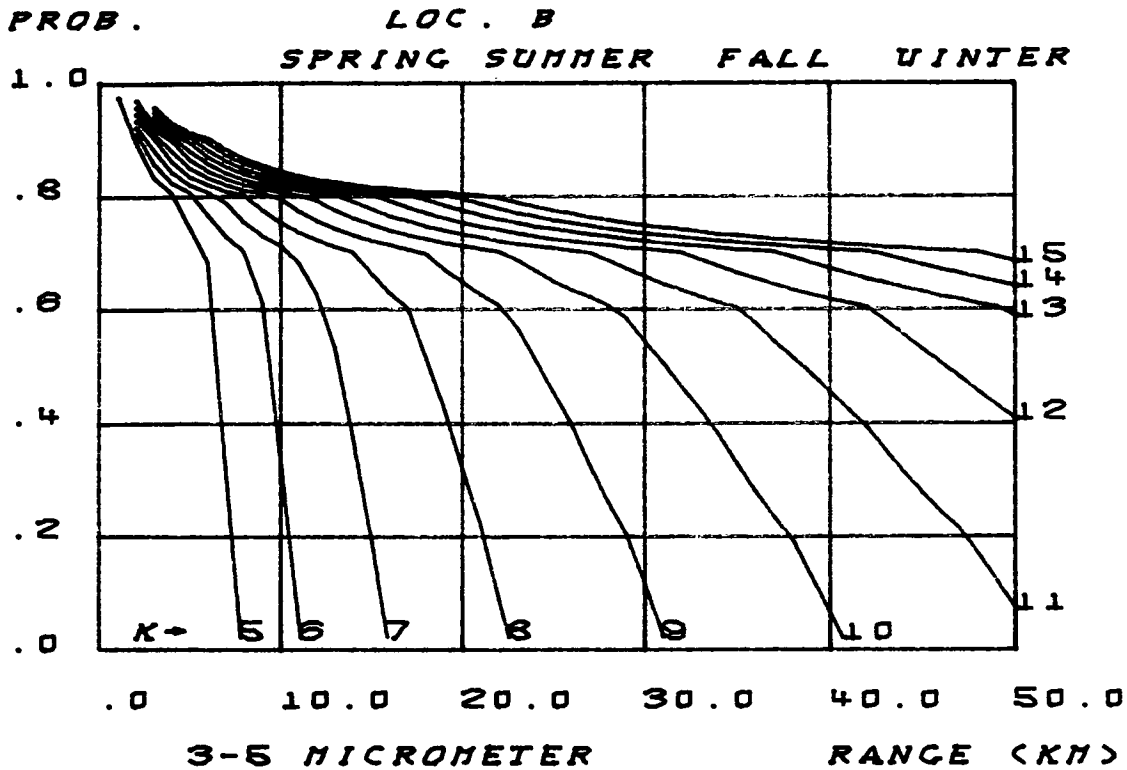


FIGURE - 46

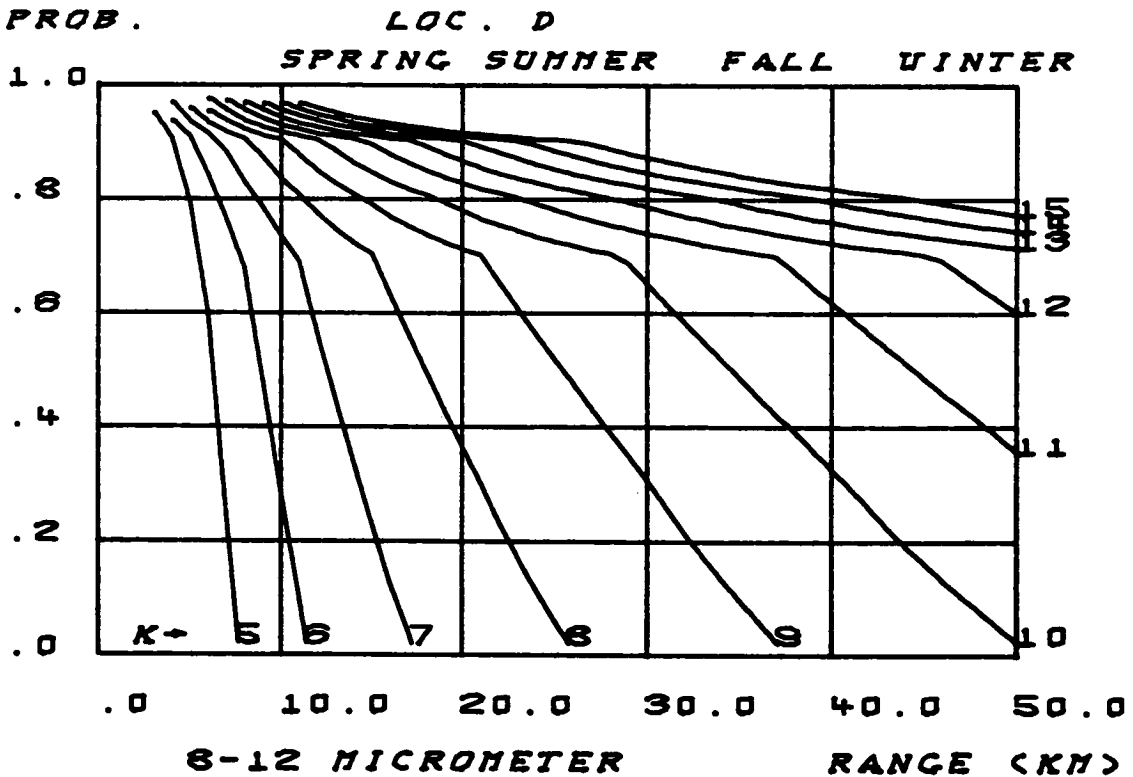
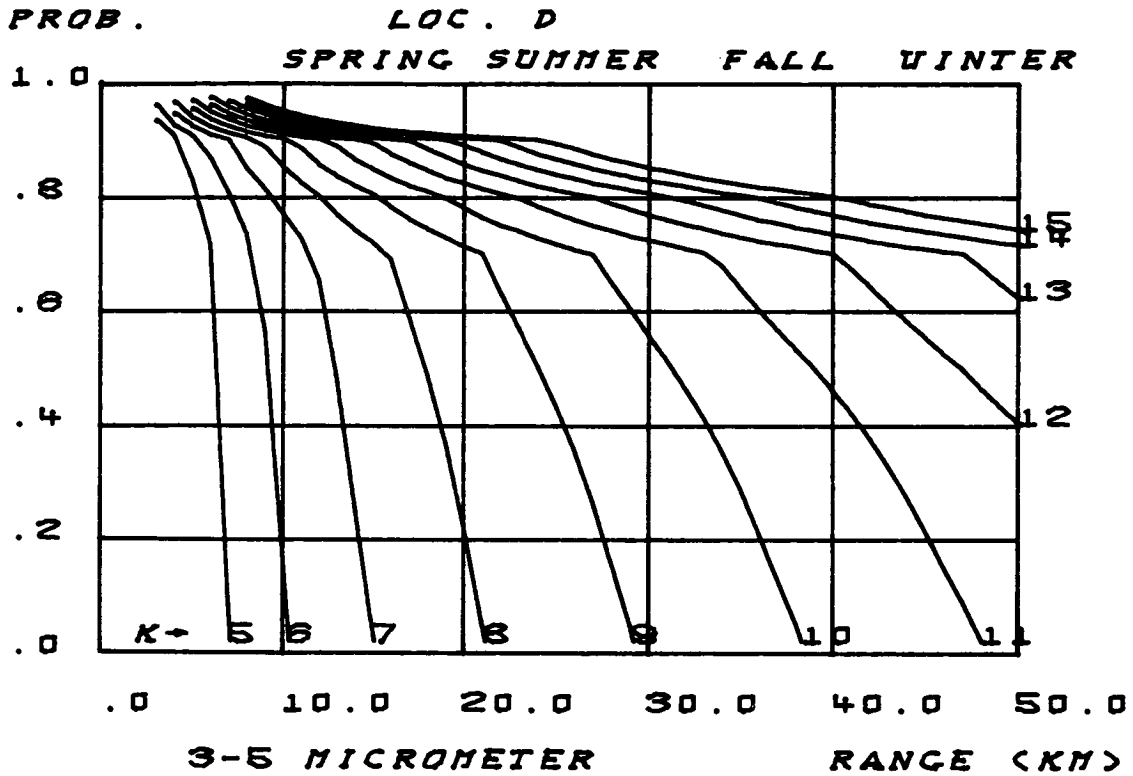


FIGURE - 48

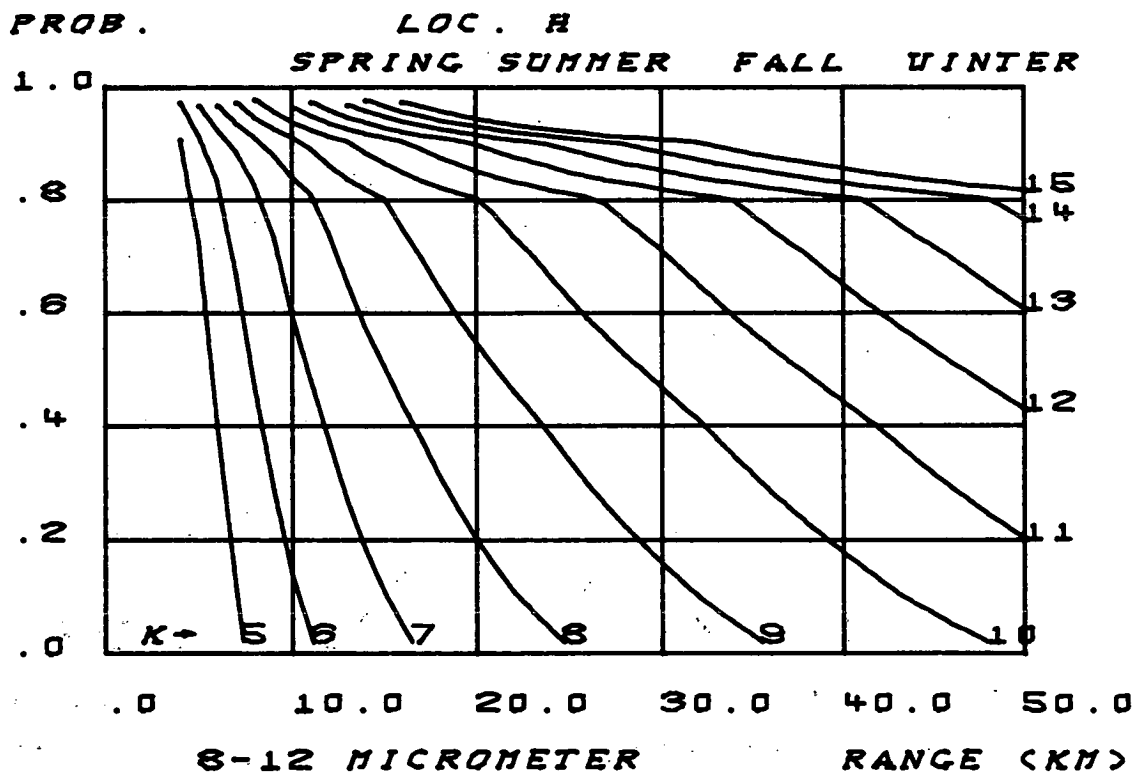
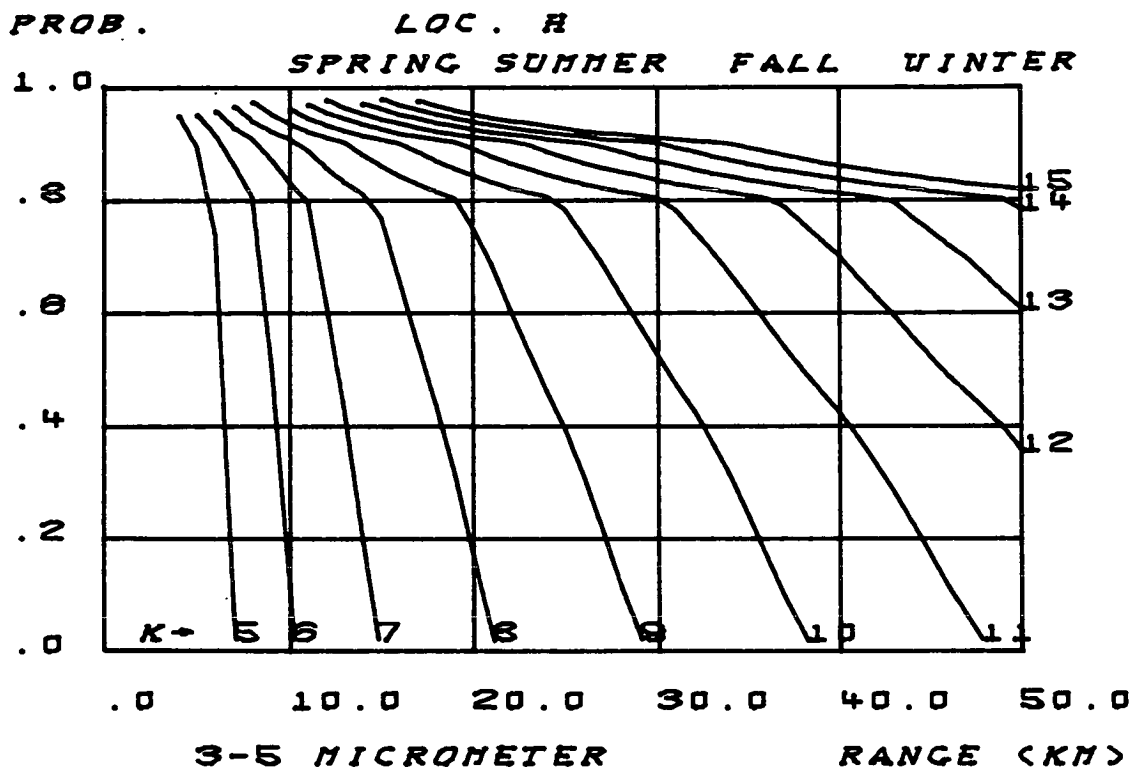


FIGURE - 49

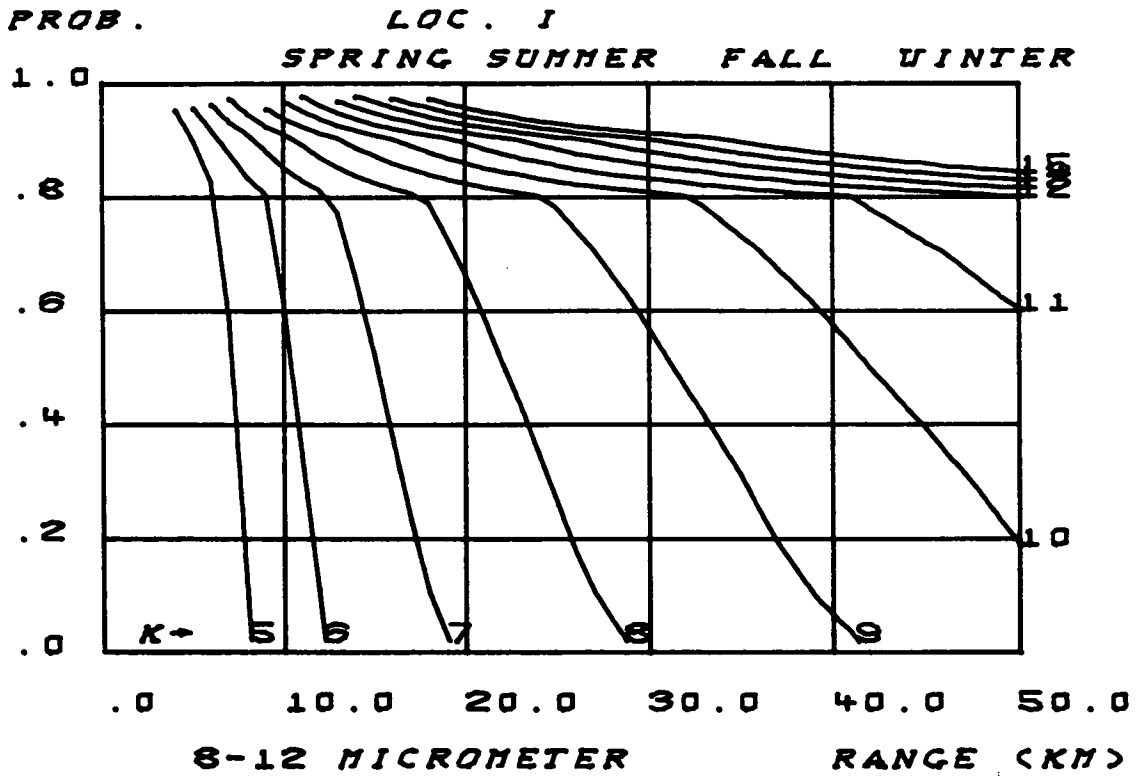
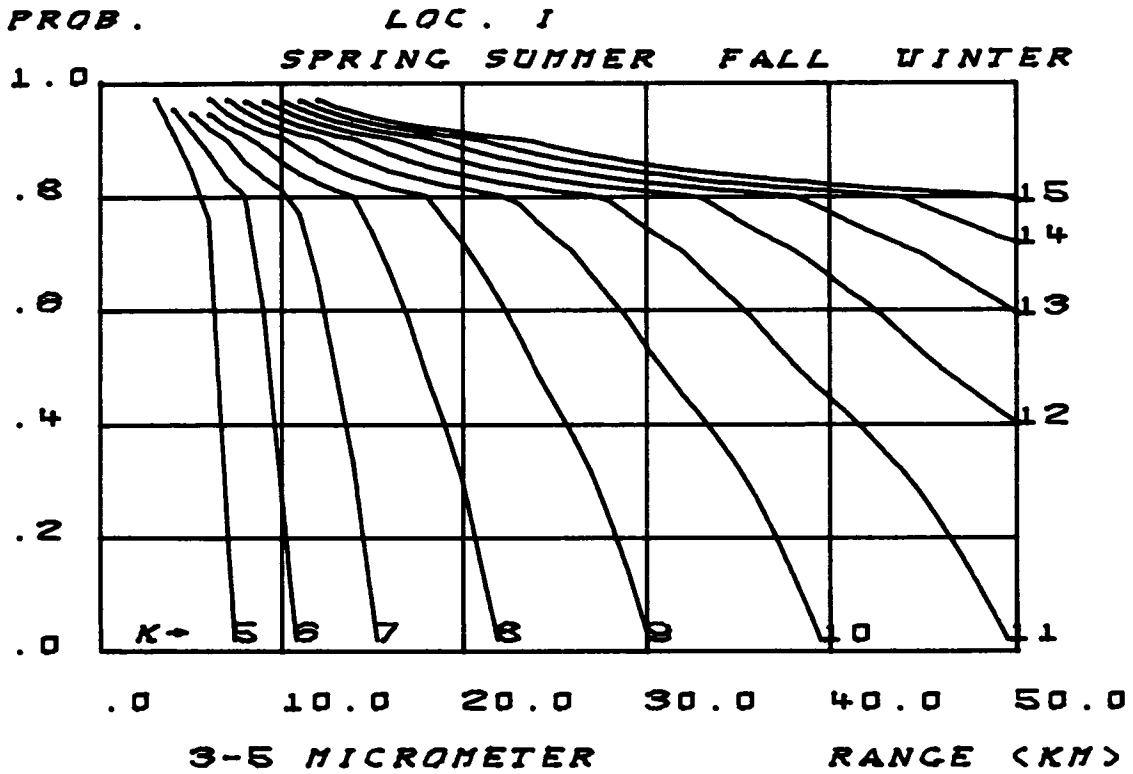


FIGURE - 50

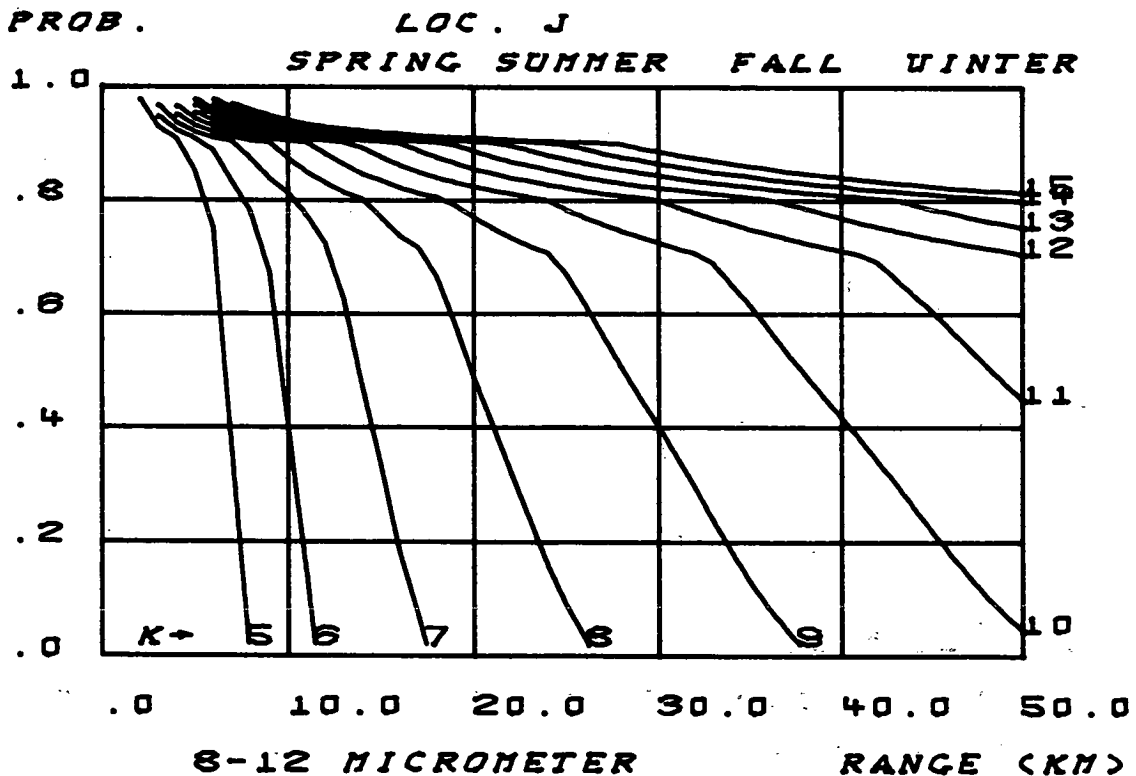
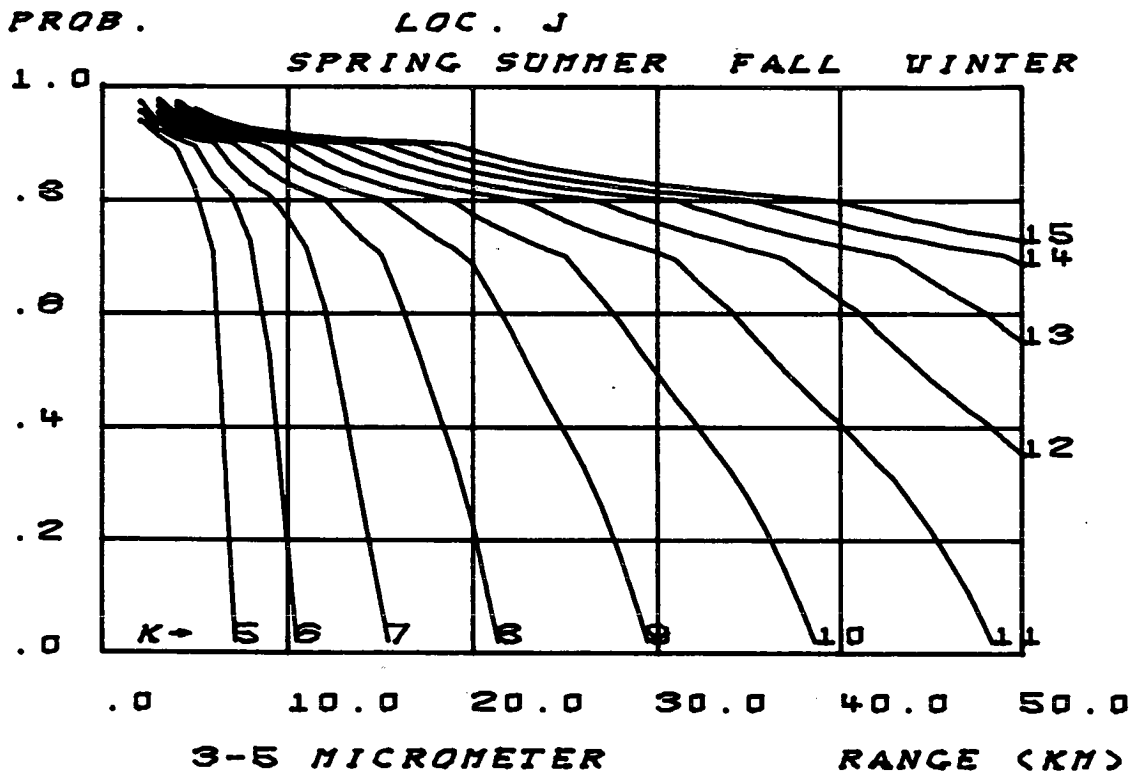


FIGURE - 51

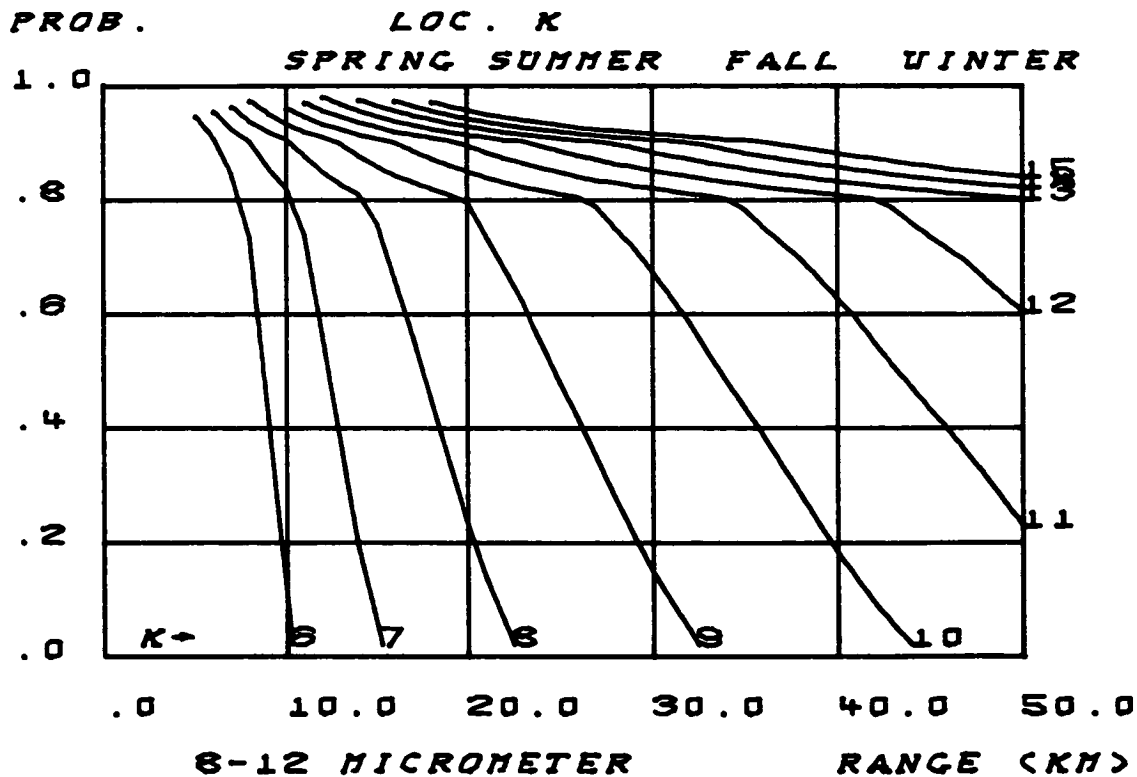
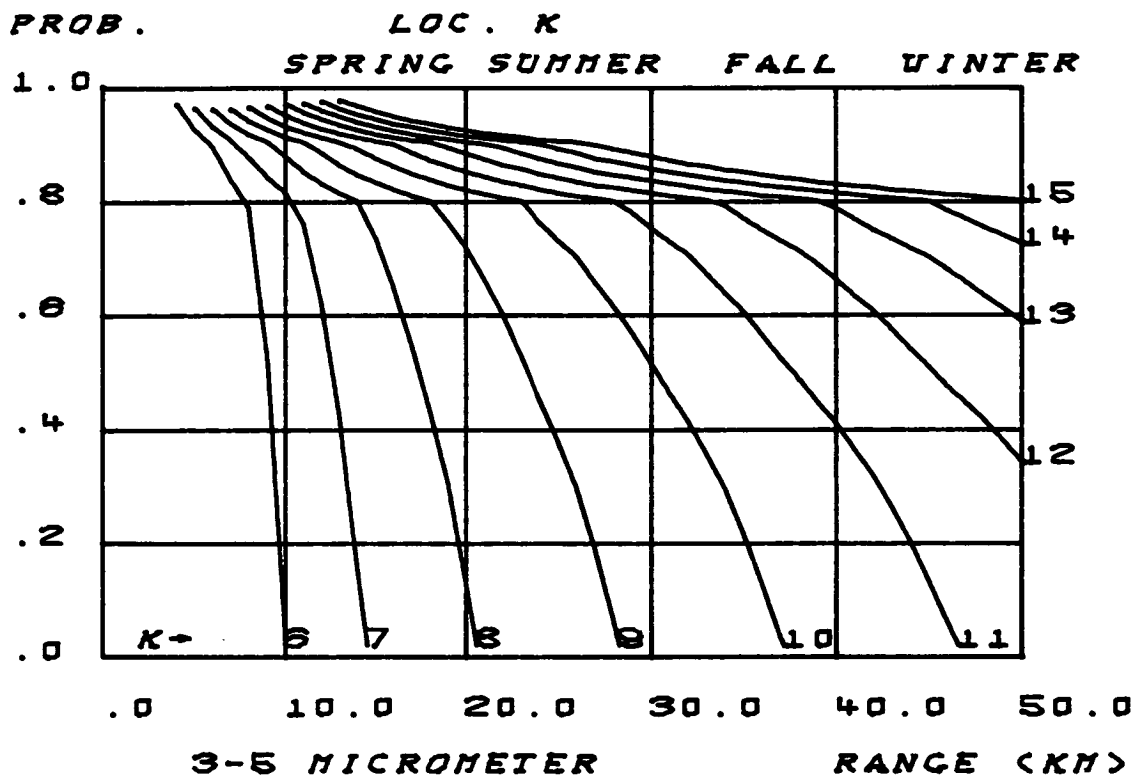


FIGURE - 52

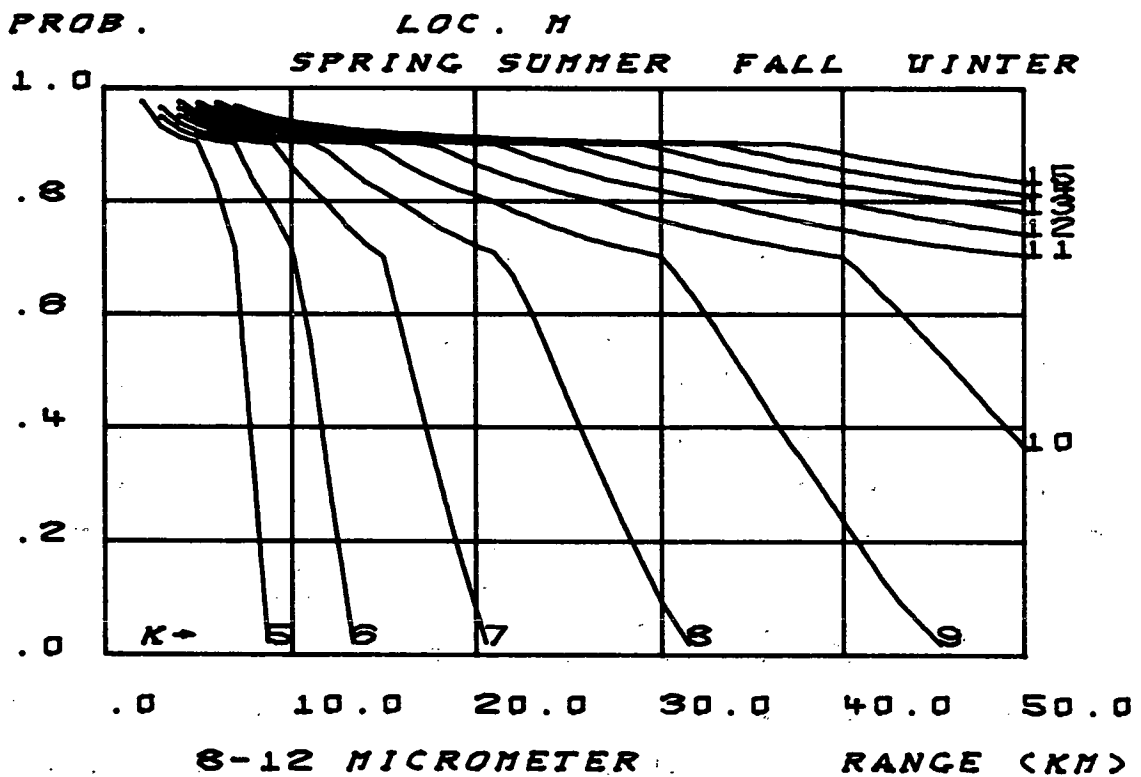
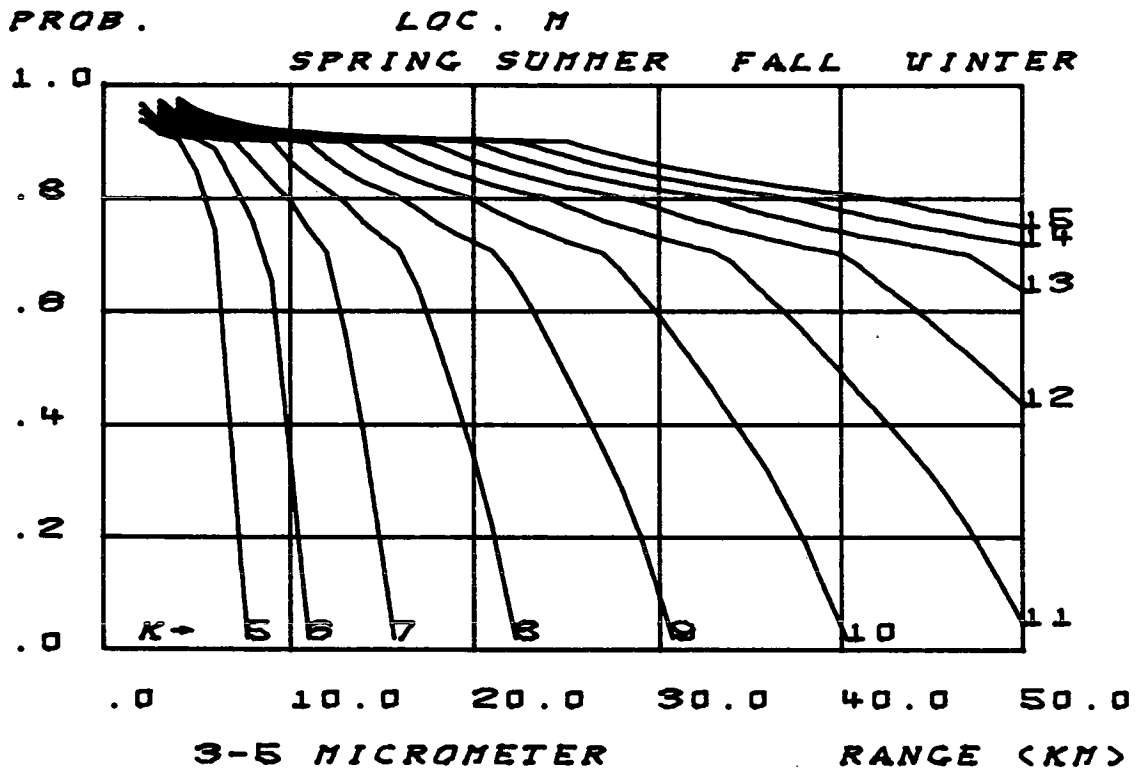


FIGURE - 53

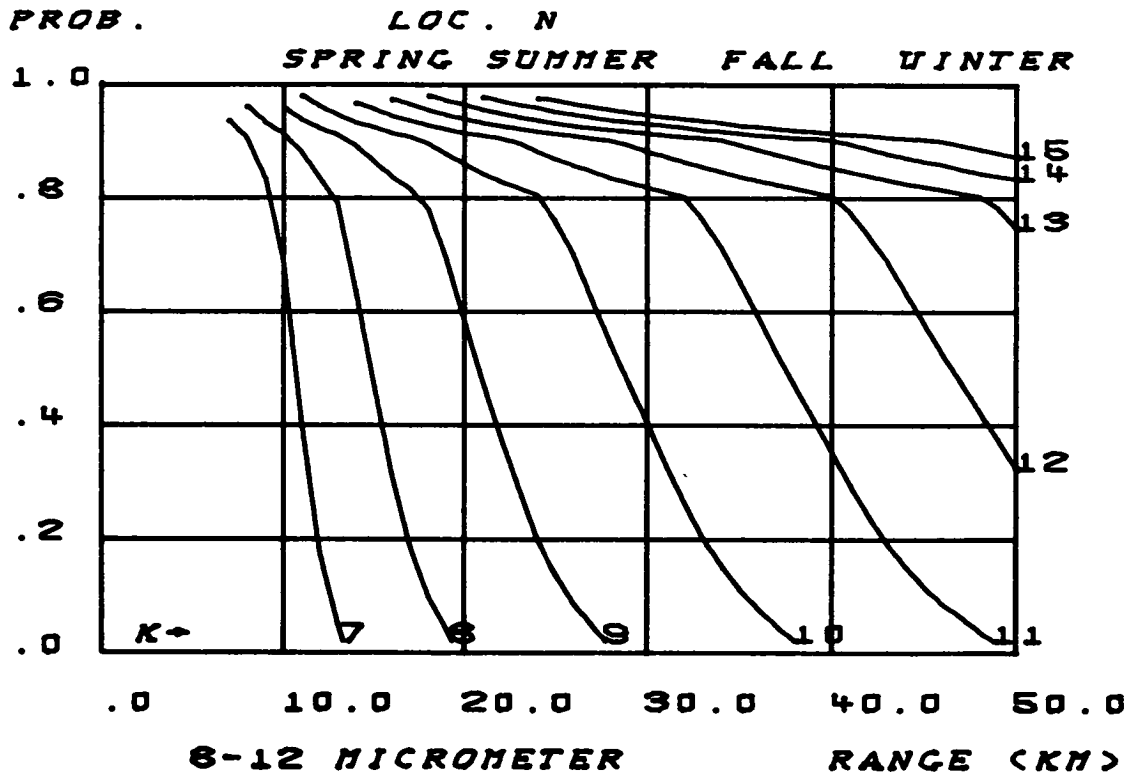
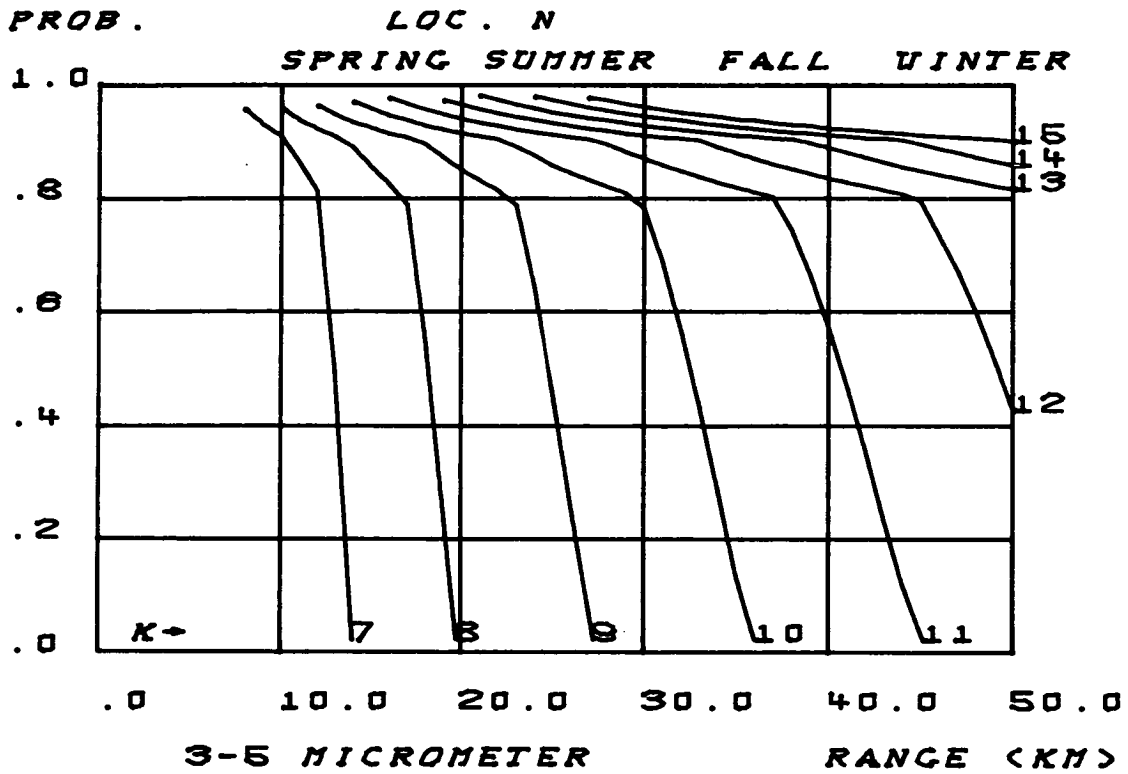


FIGURE - 54

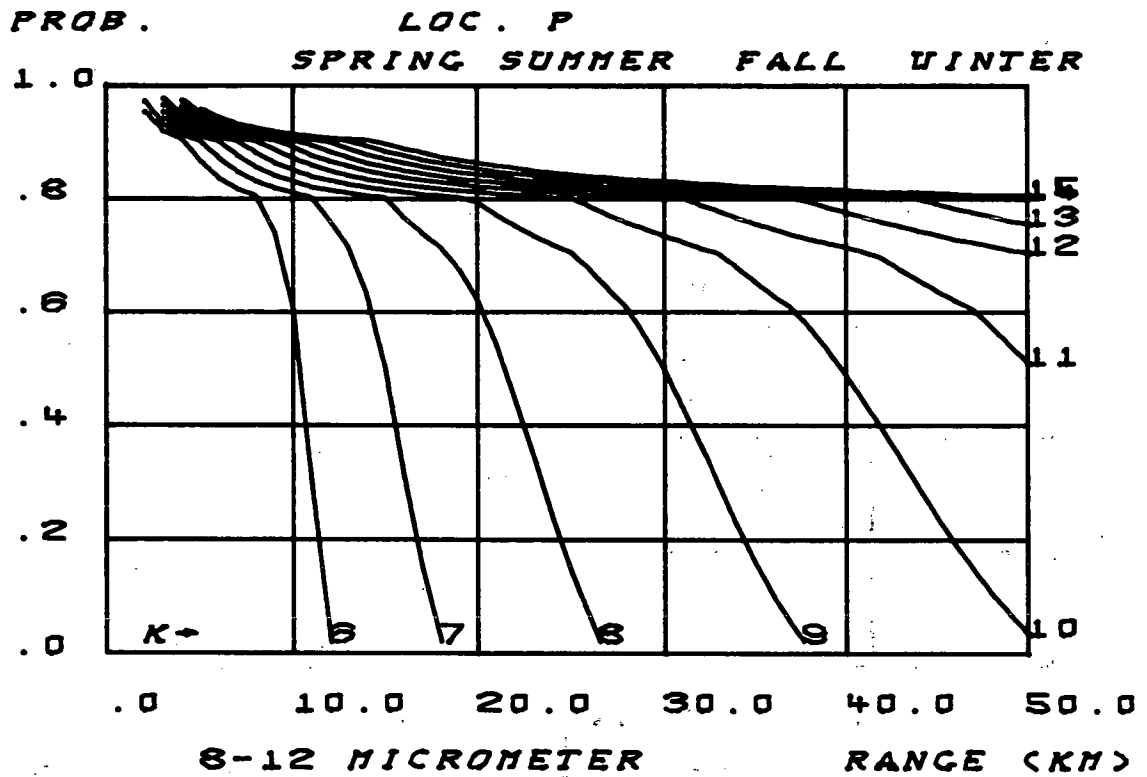
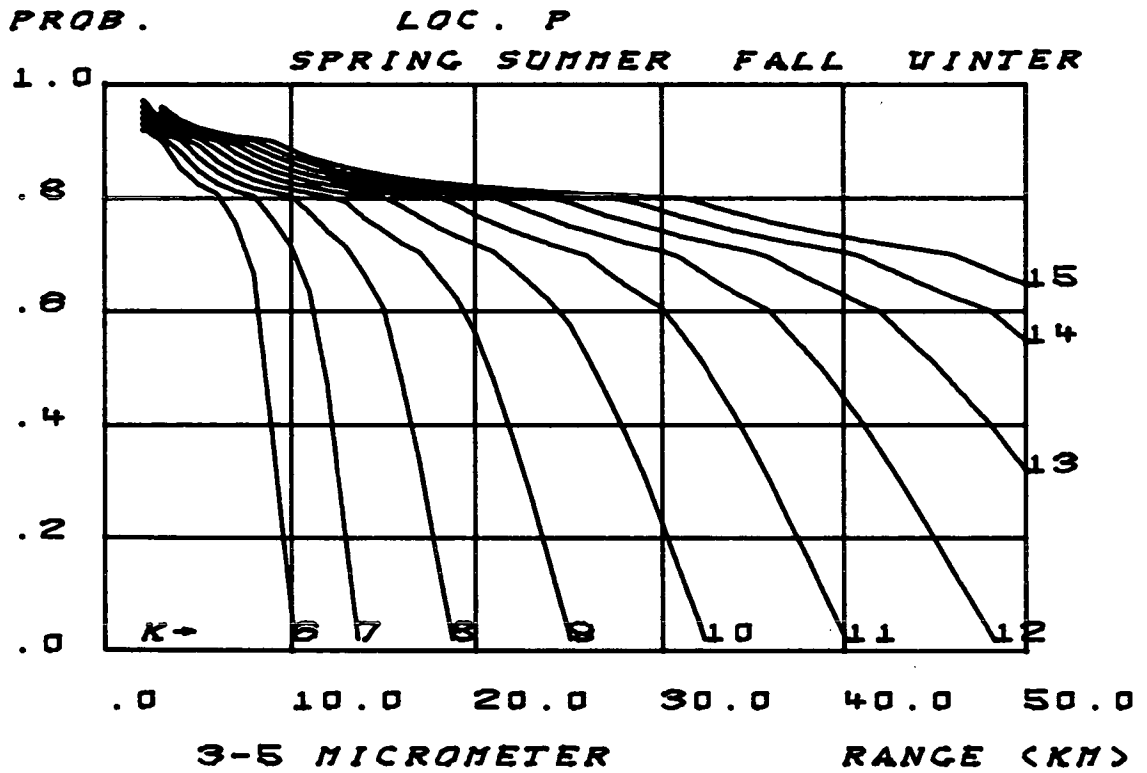


FIGURE - 55

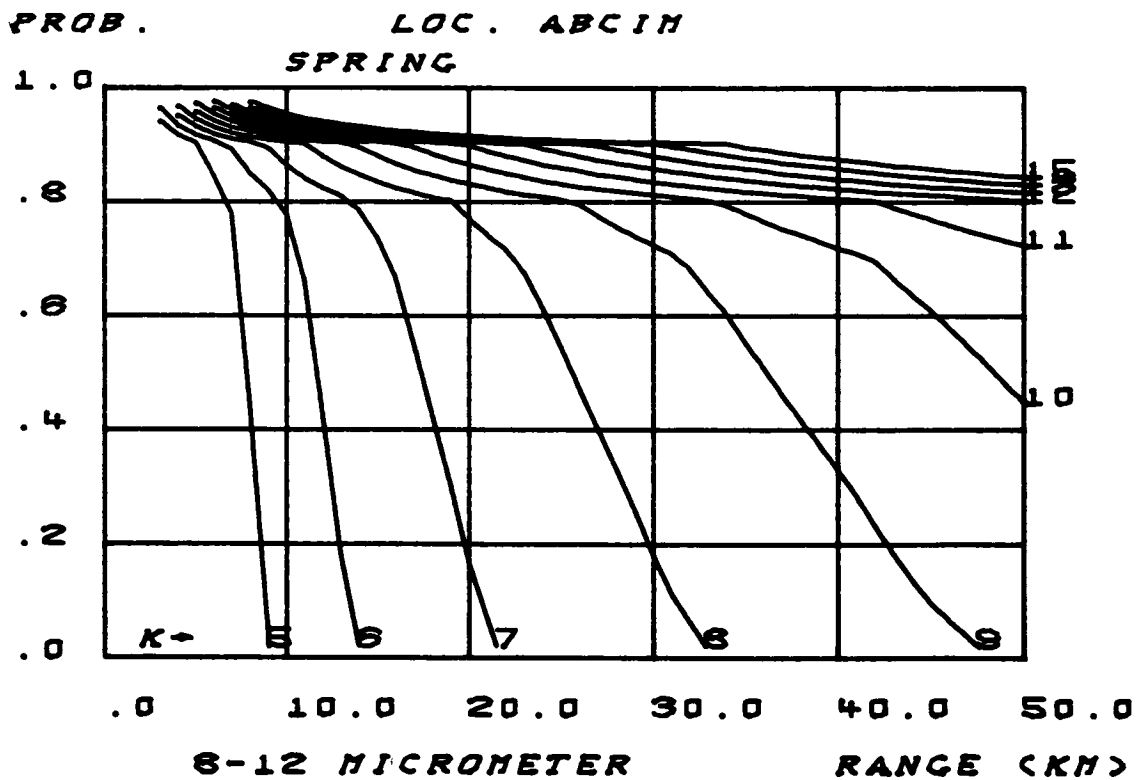
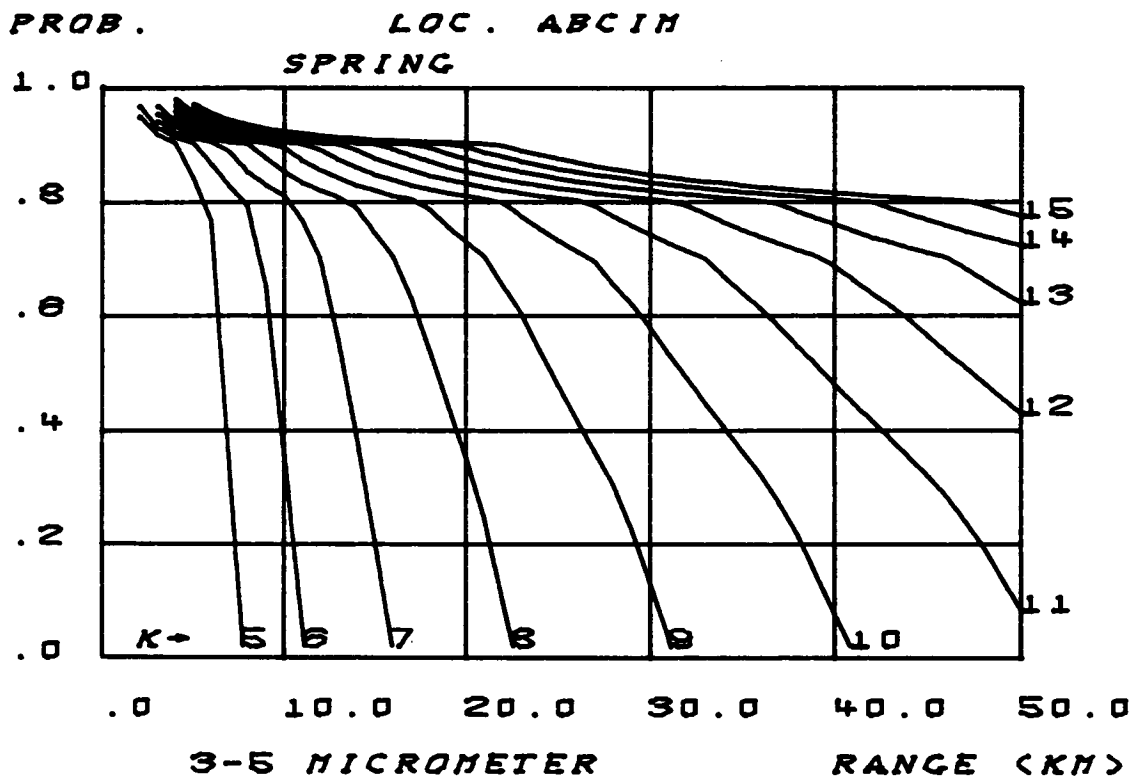


FIGURE - 56

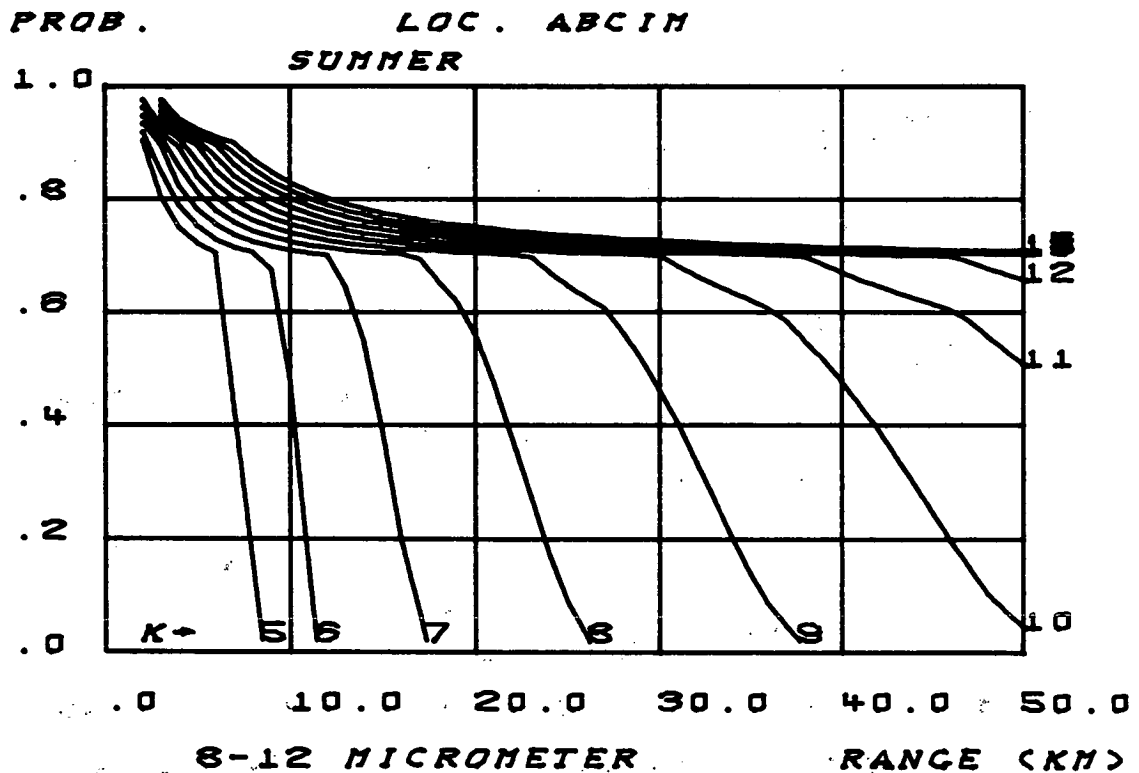
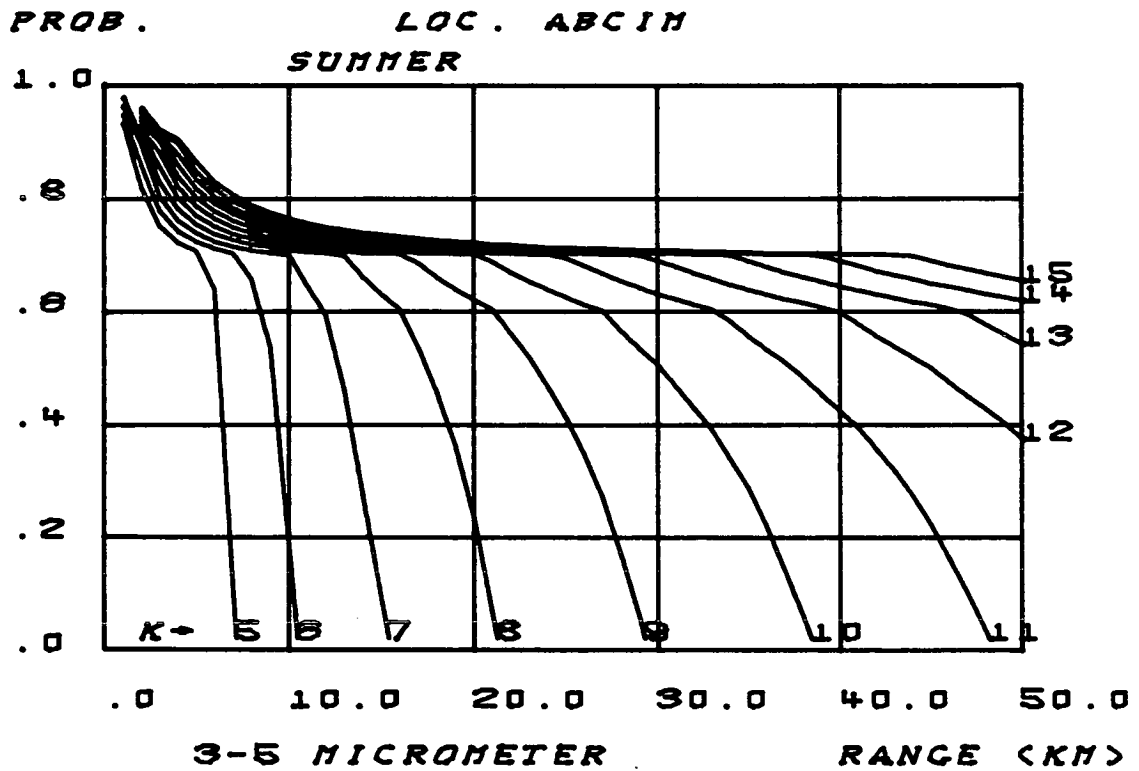


FIGURE - 57

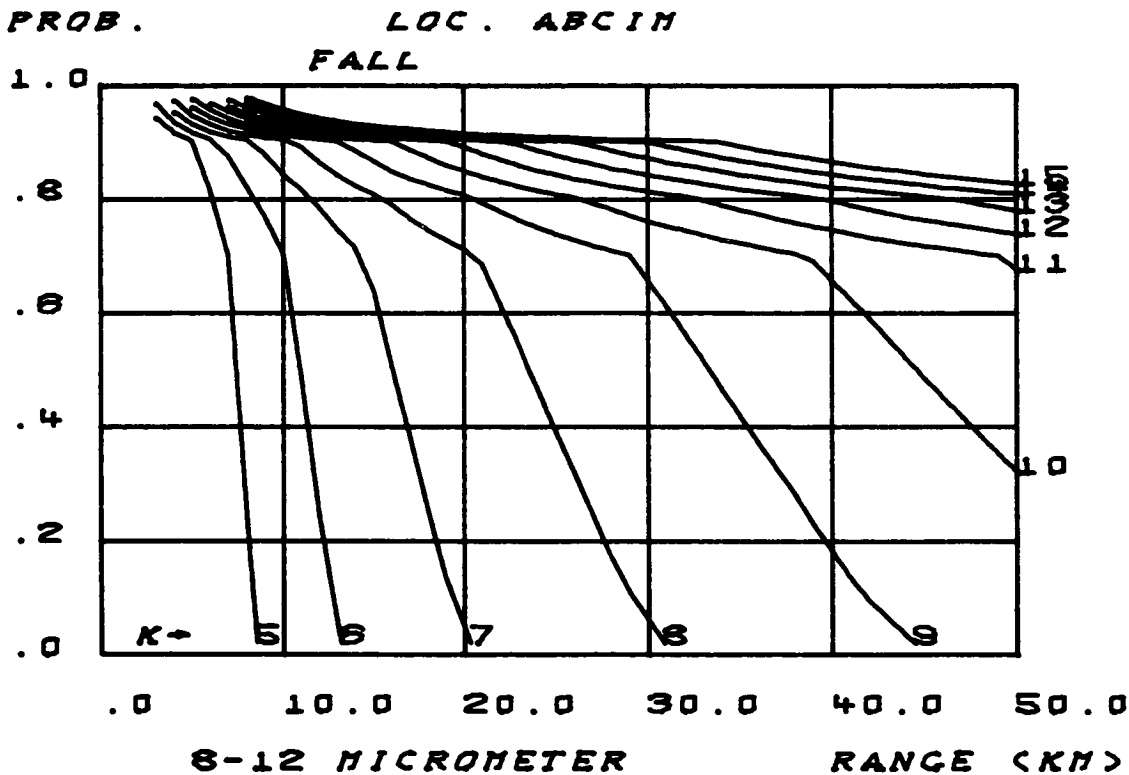
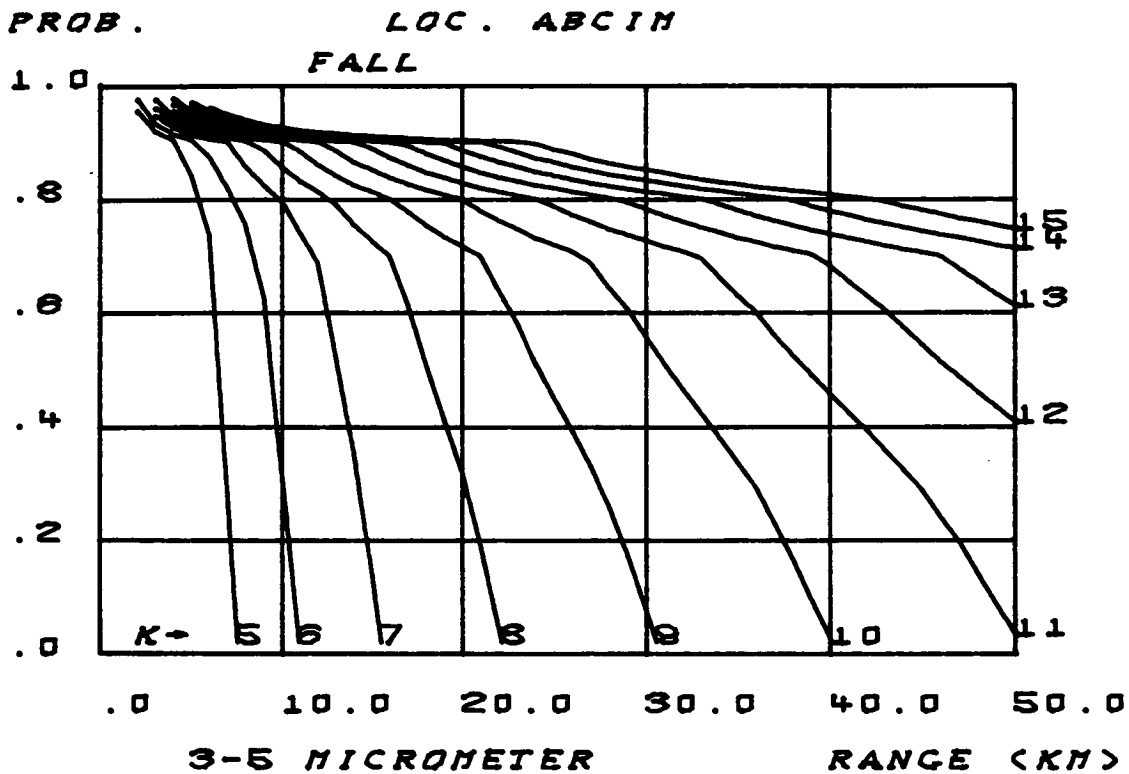


FIGURE - 58

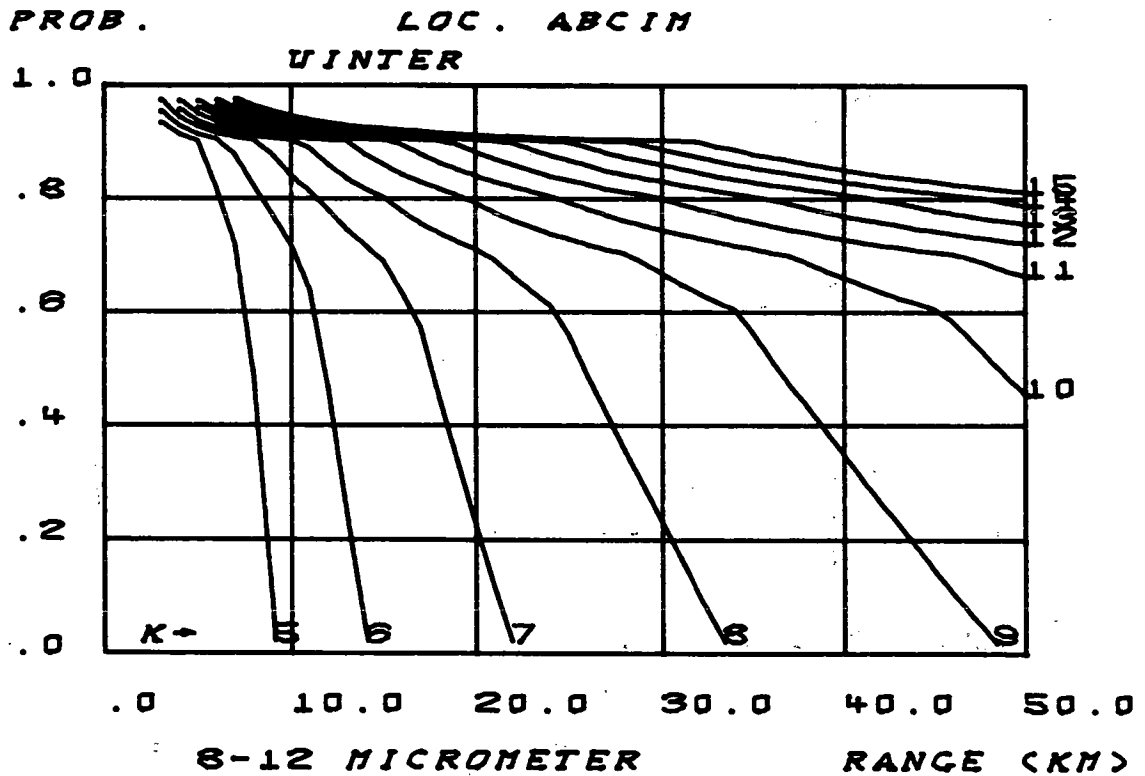
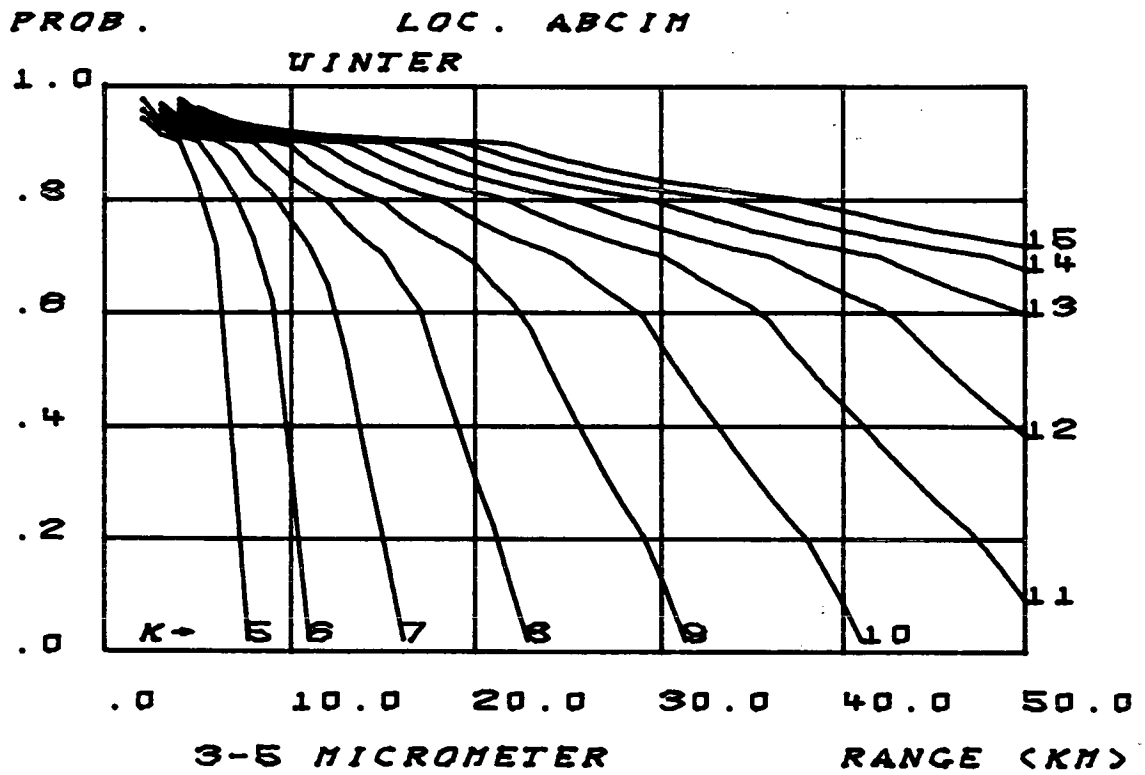


FIGURE - 59

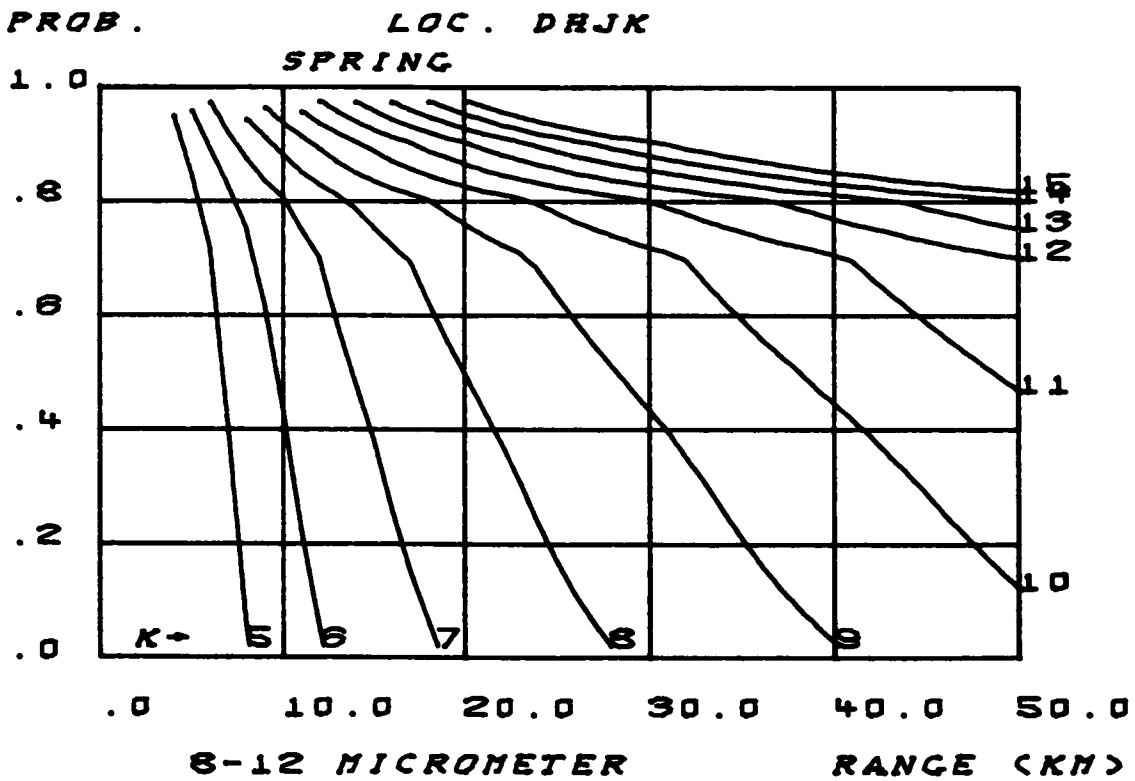
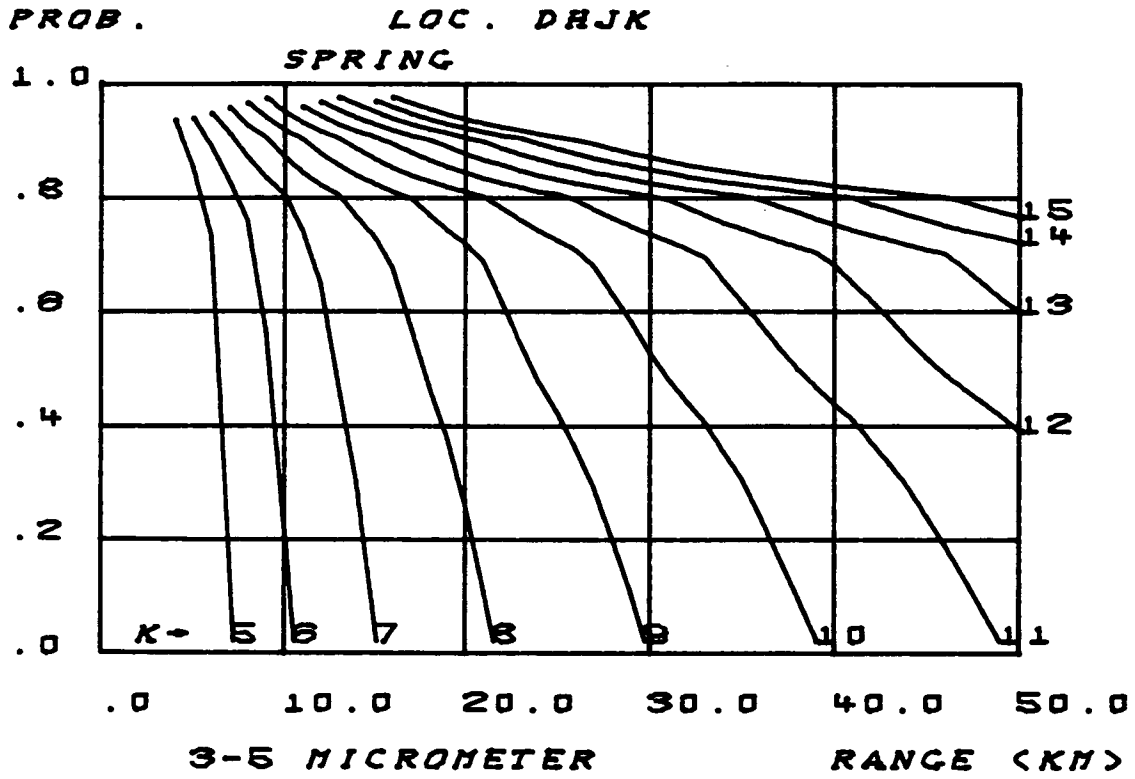


FIGURE - 60

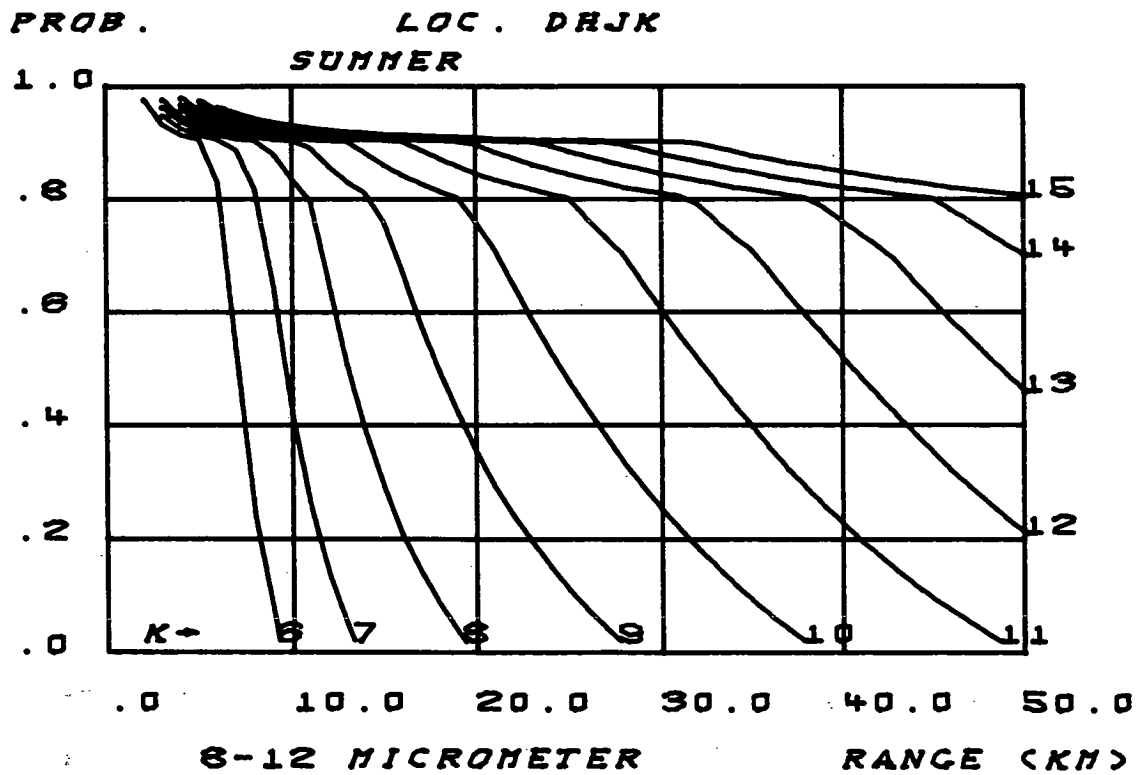
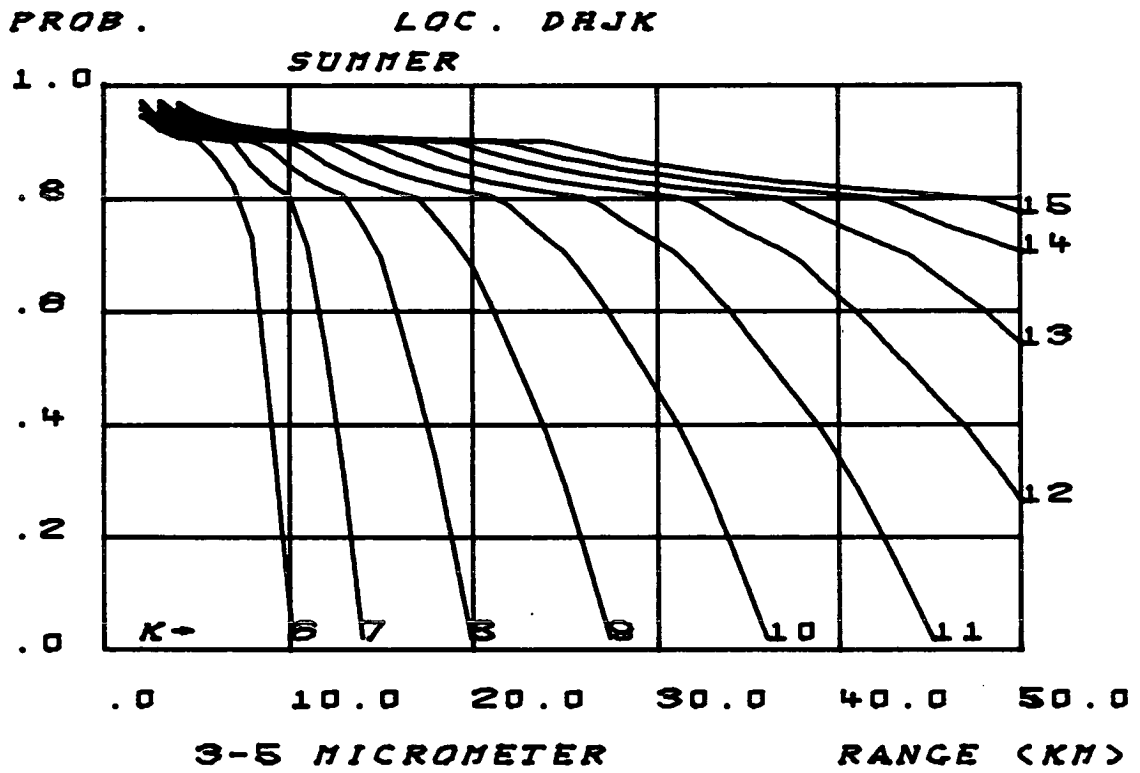


FIGURE - 61

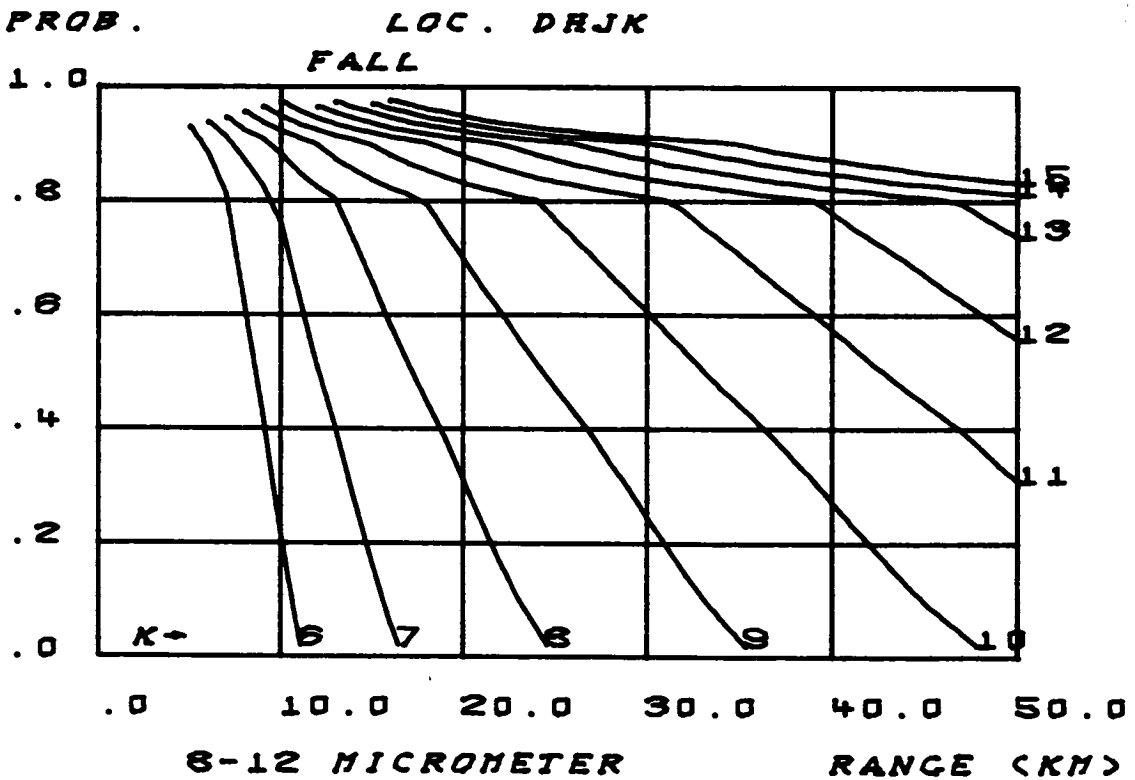
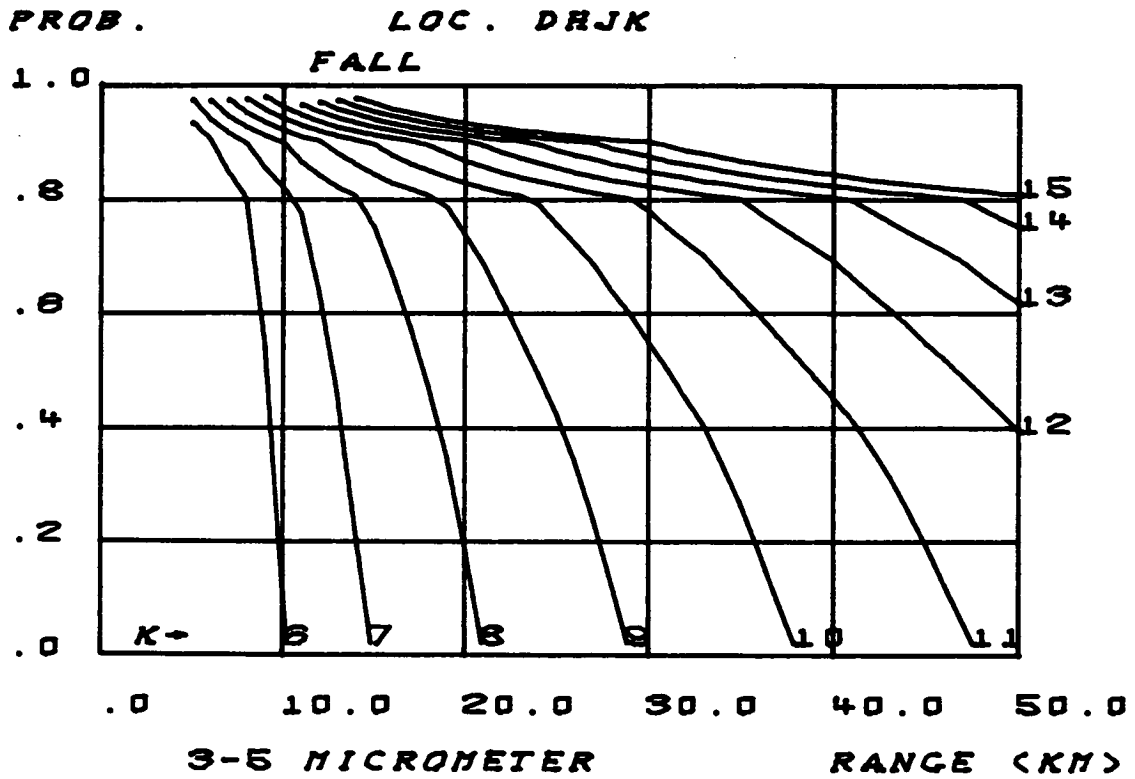


FIGURE - 62

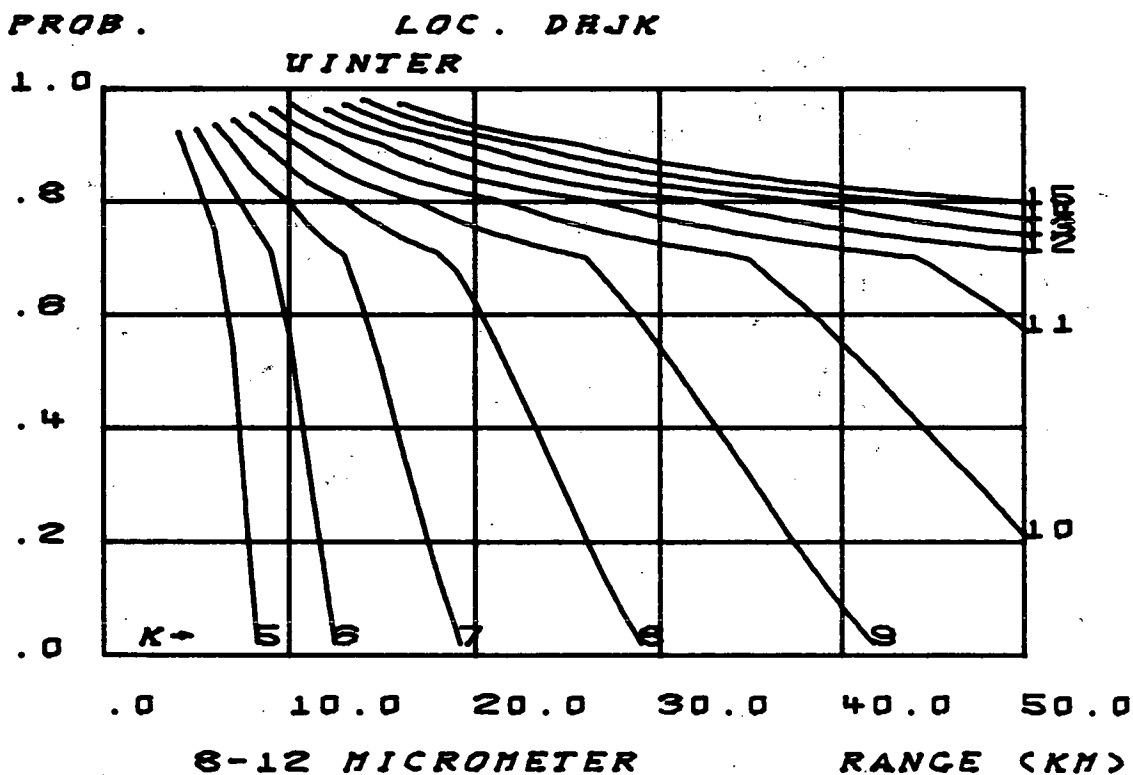
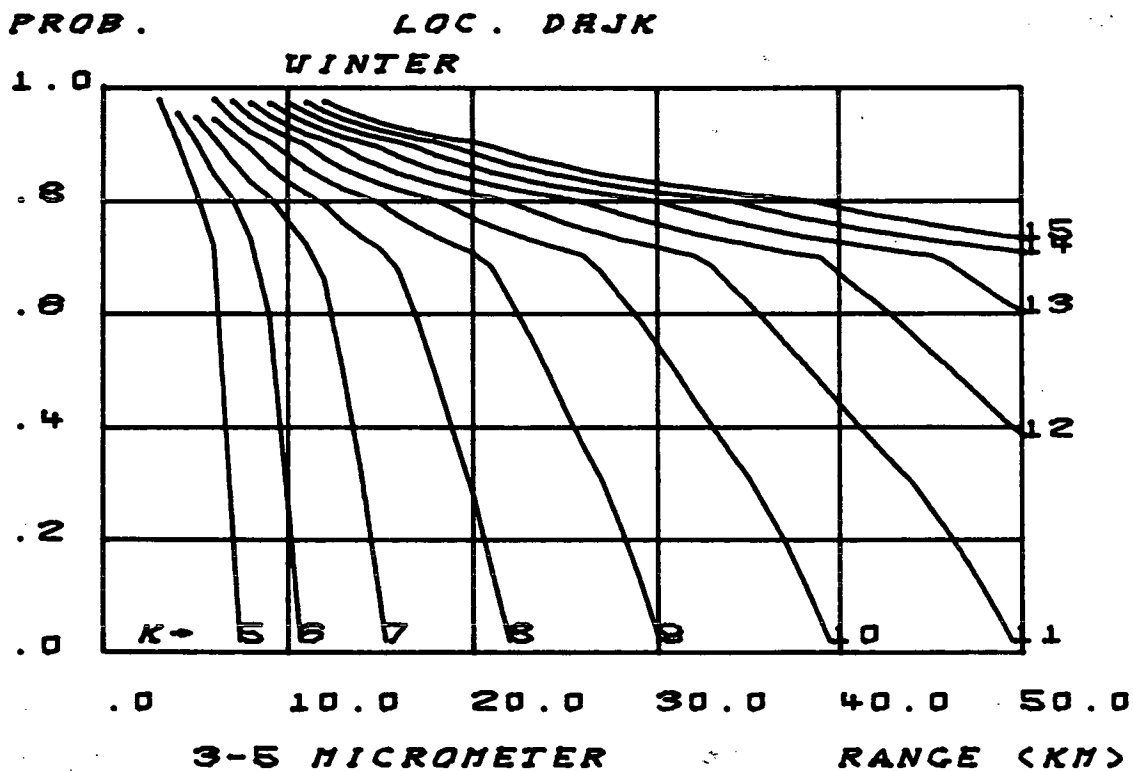


FIGURE - 63

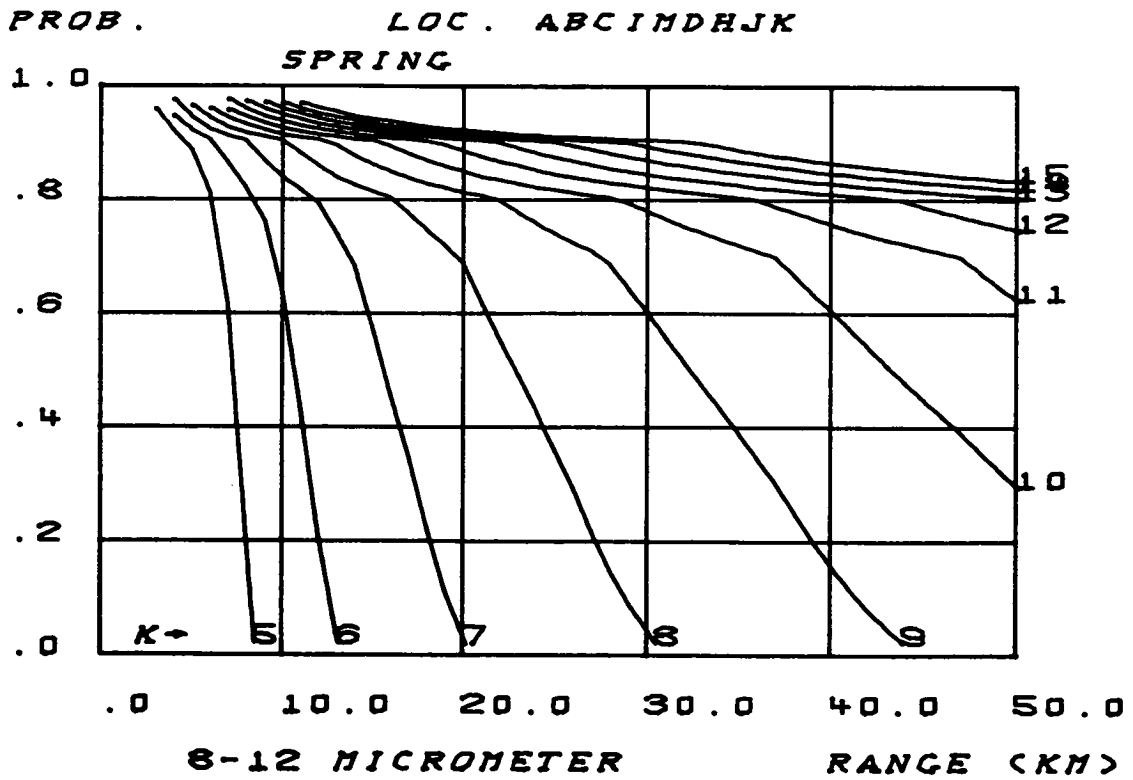
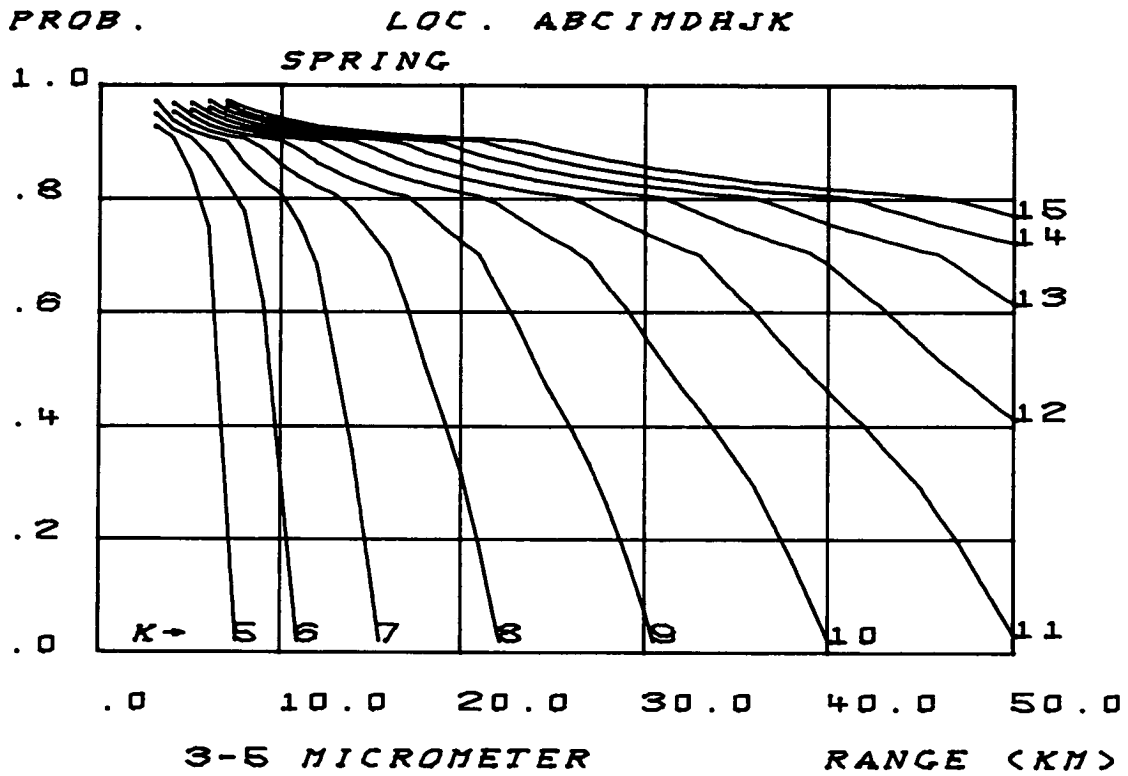


FIGURE - 64

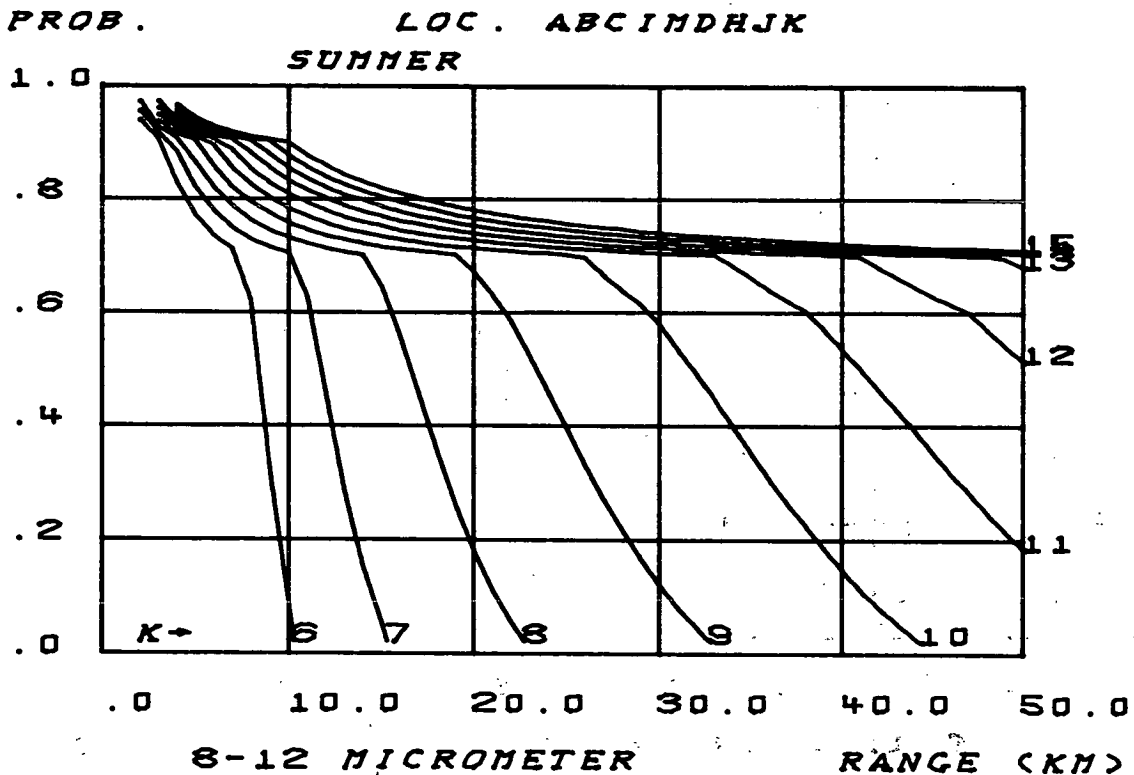
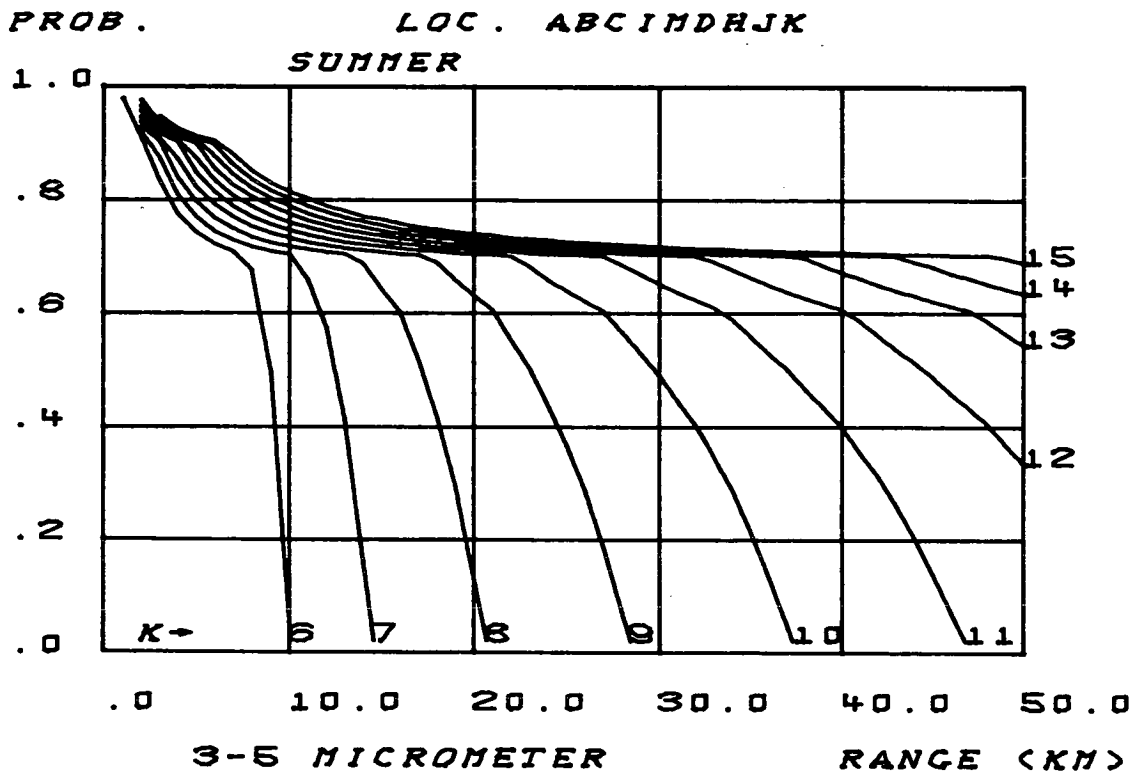


FIGURE - 65

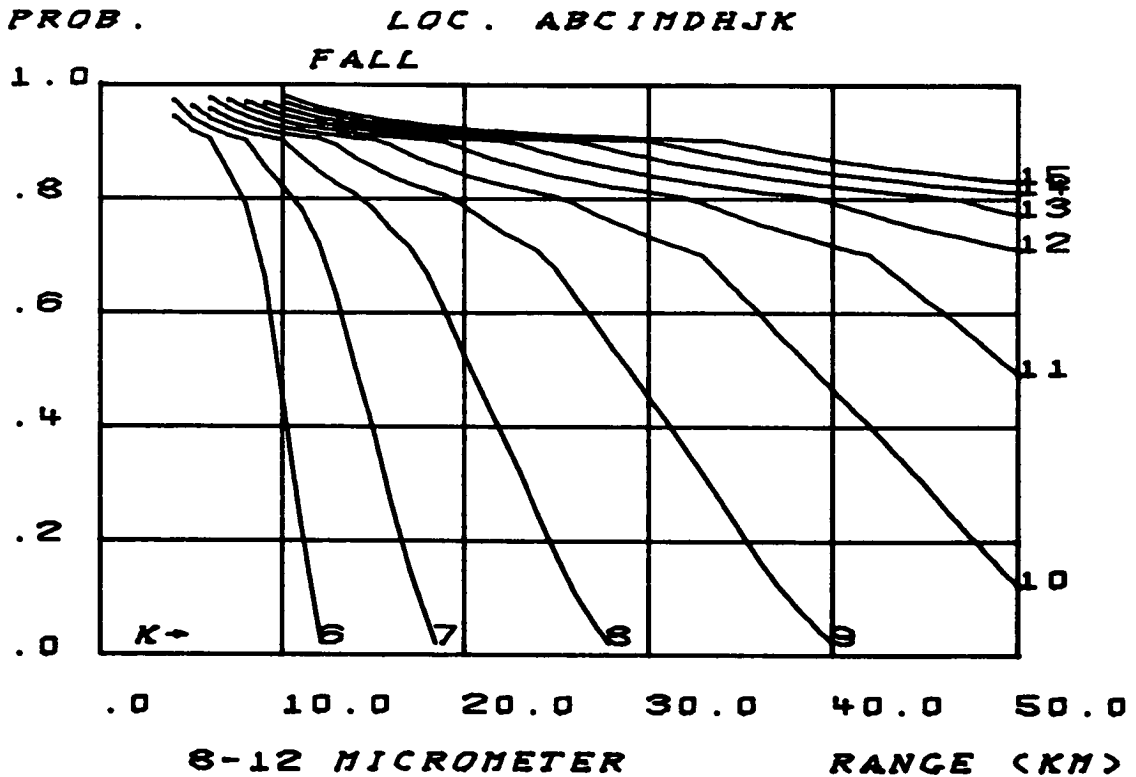
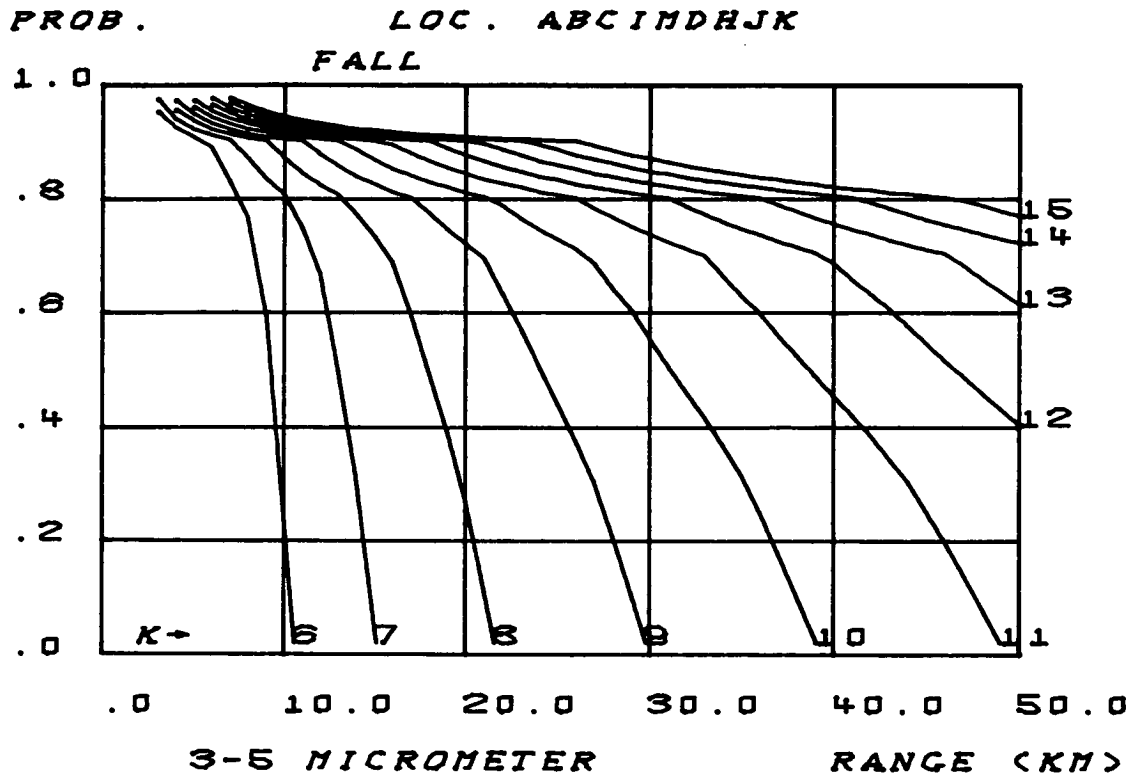


FIGURE - 66

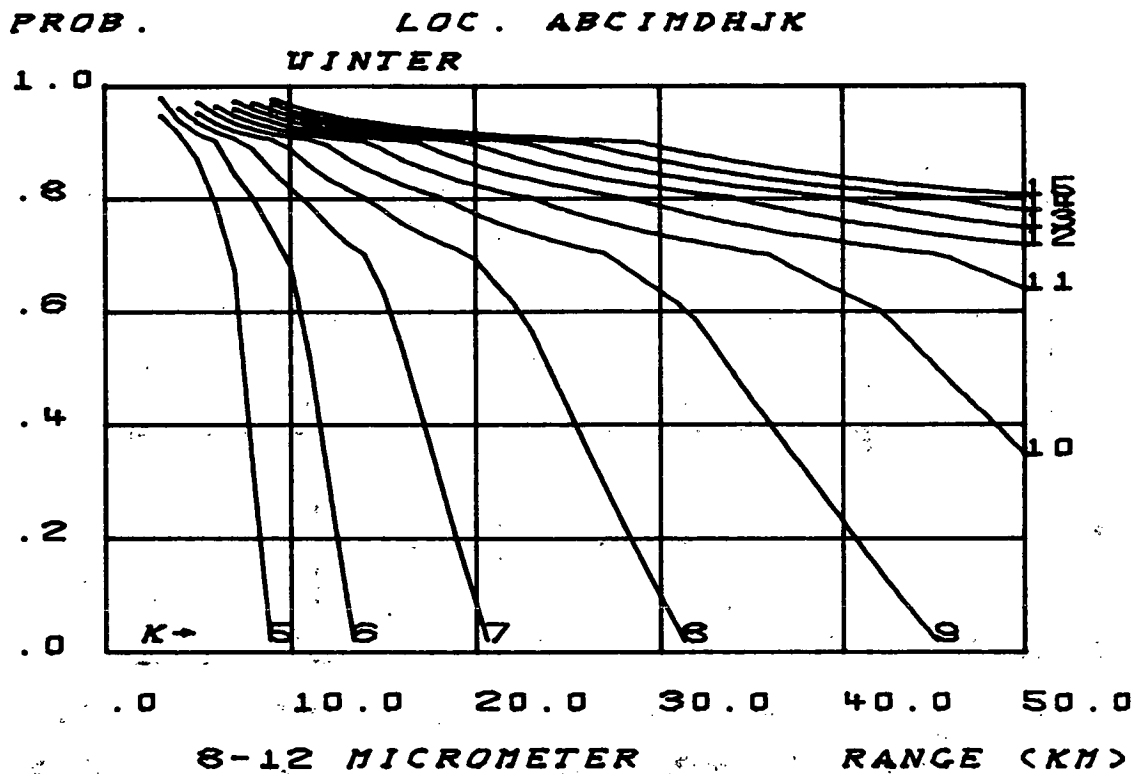
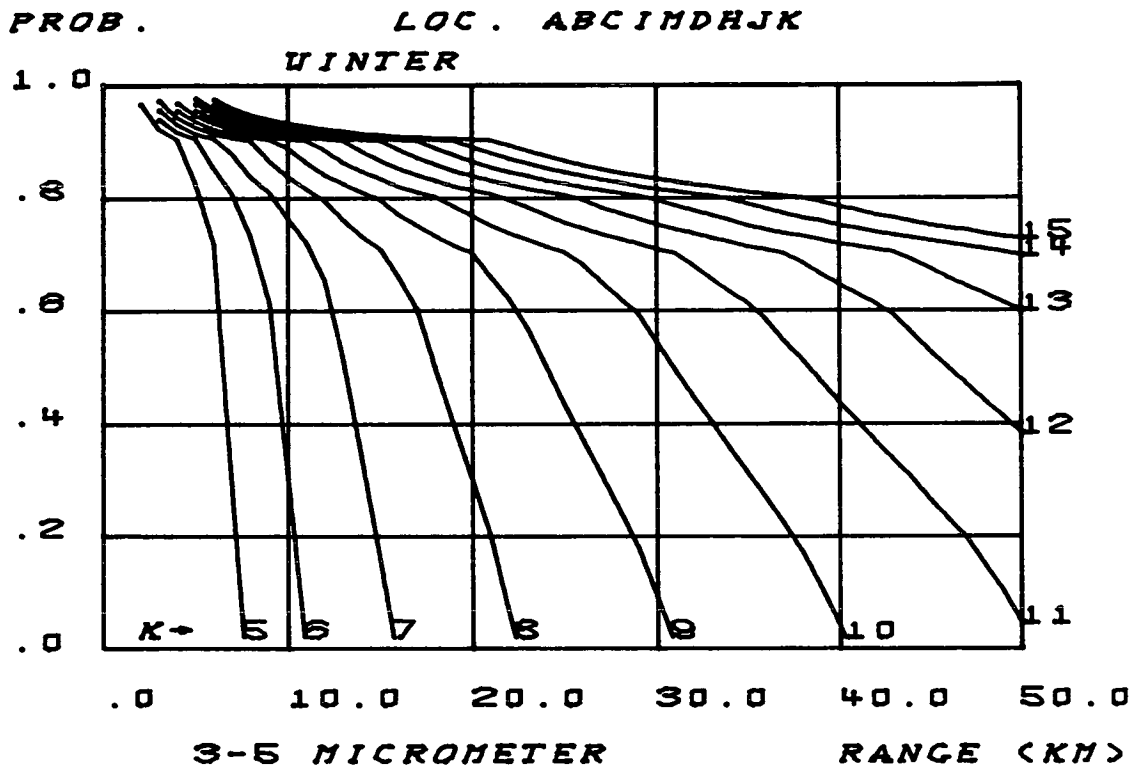


FIGURE - 67

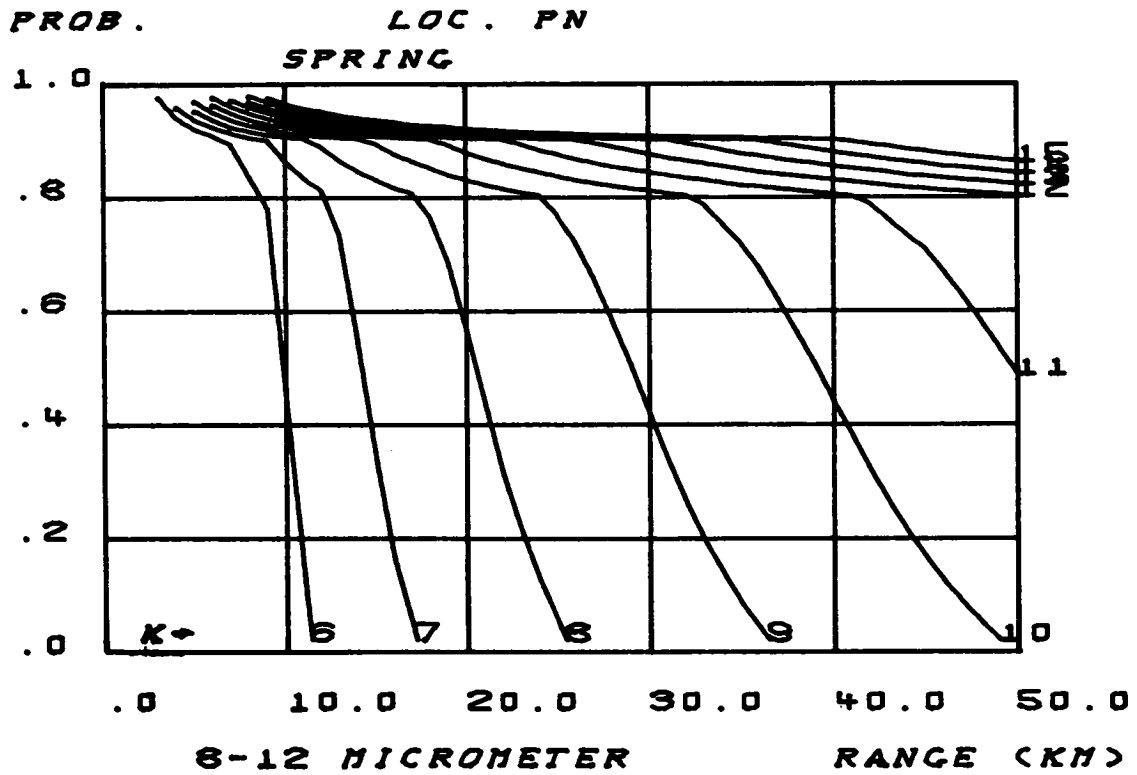
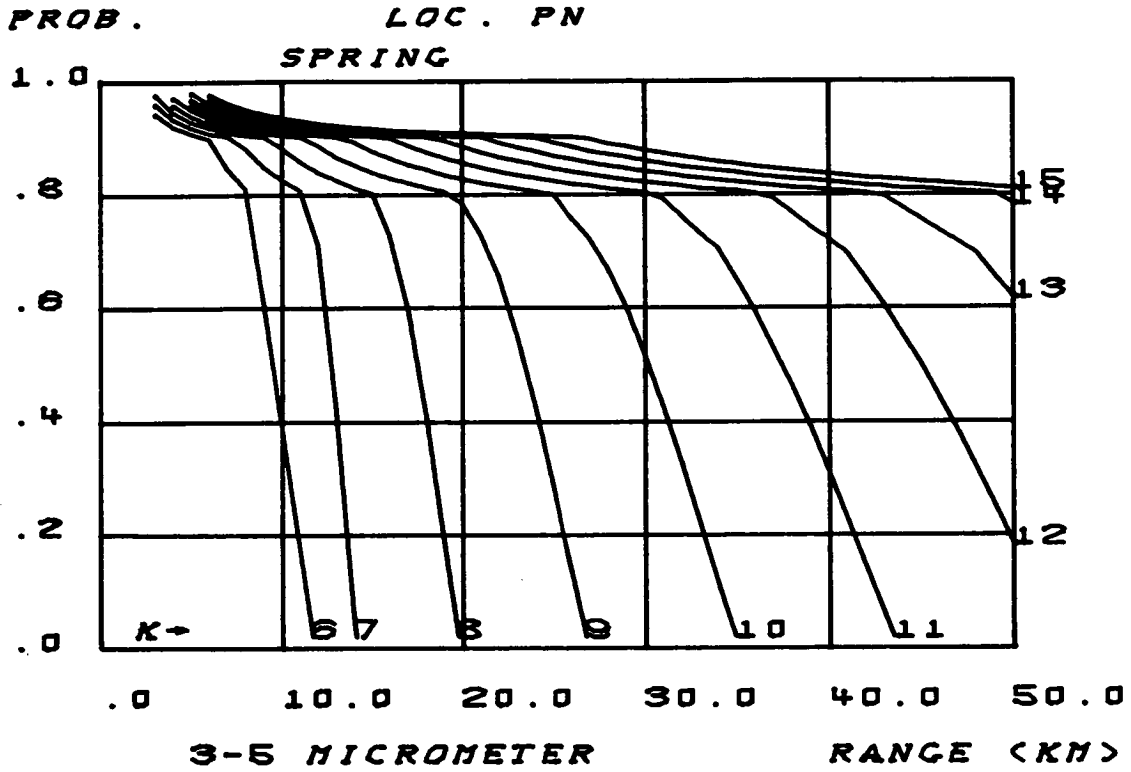


FIGURE - 68

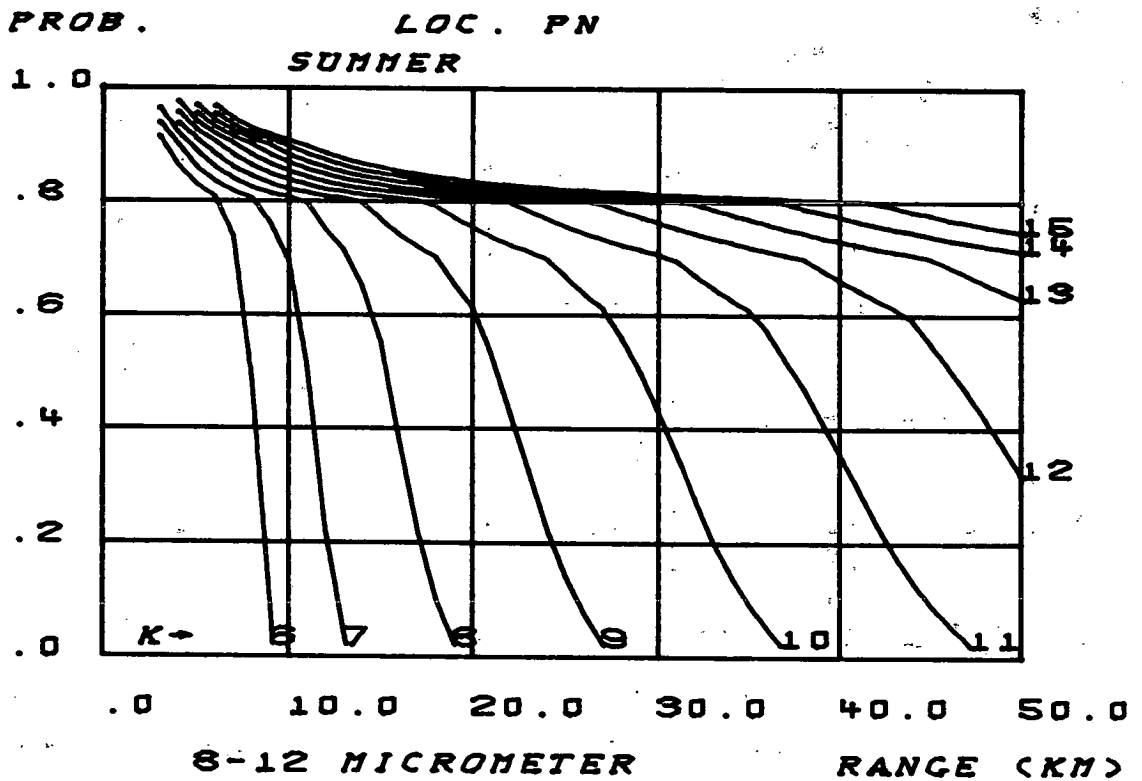
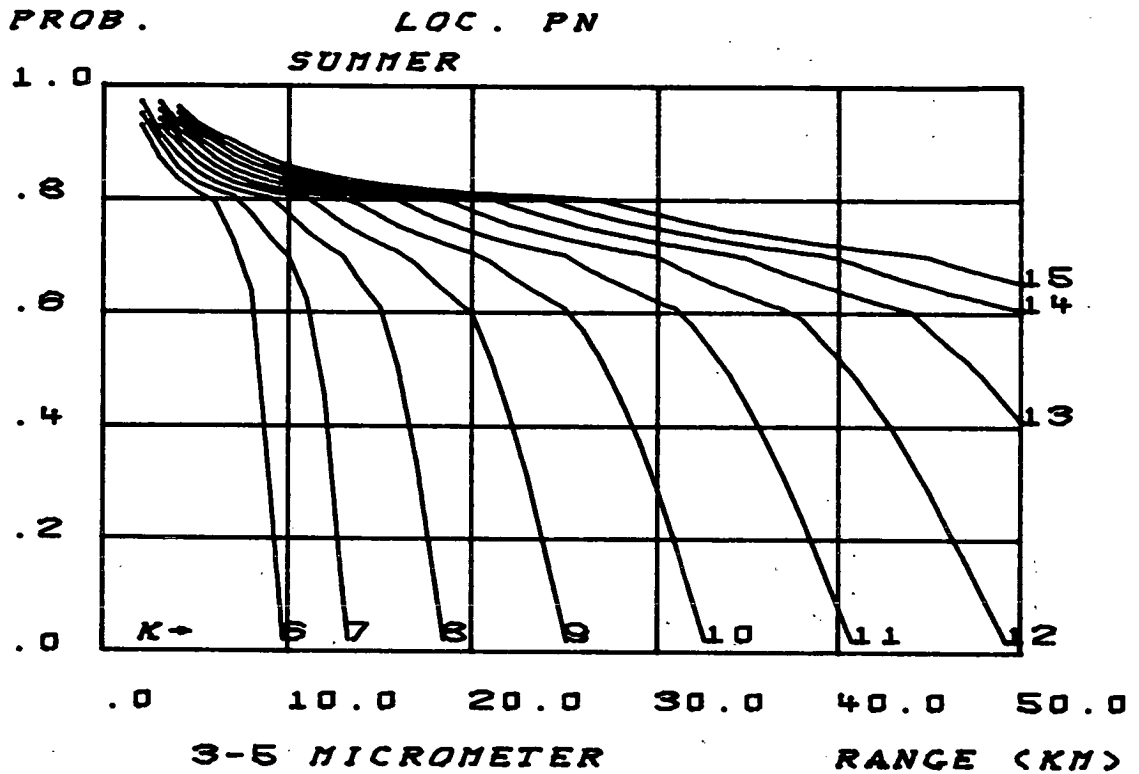


FIGURE - 69

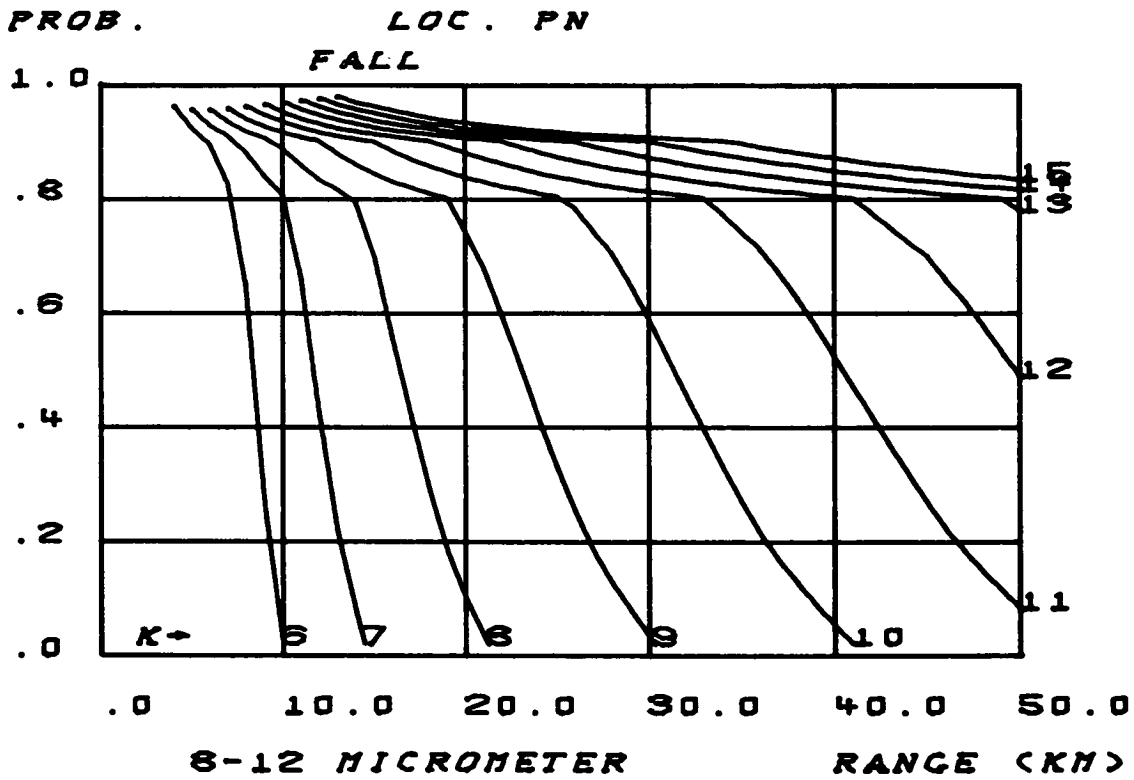
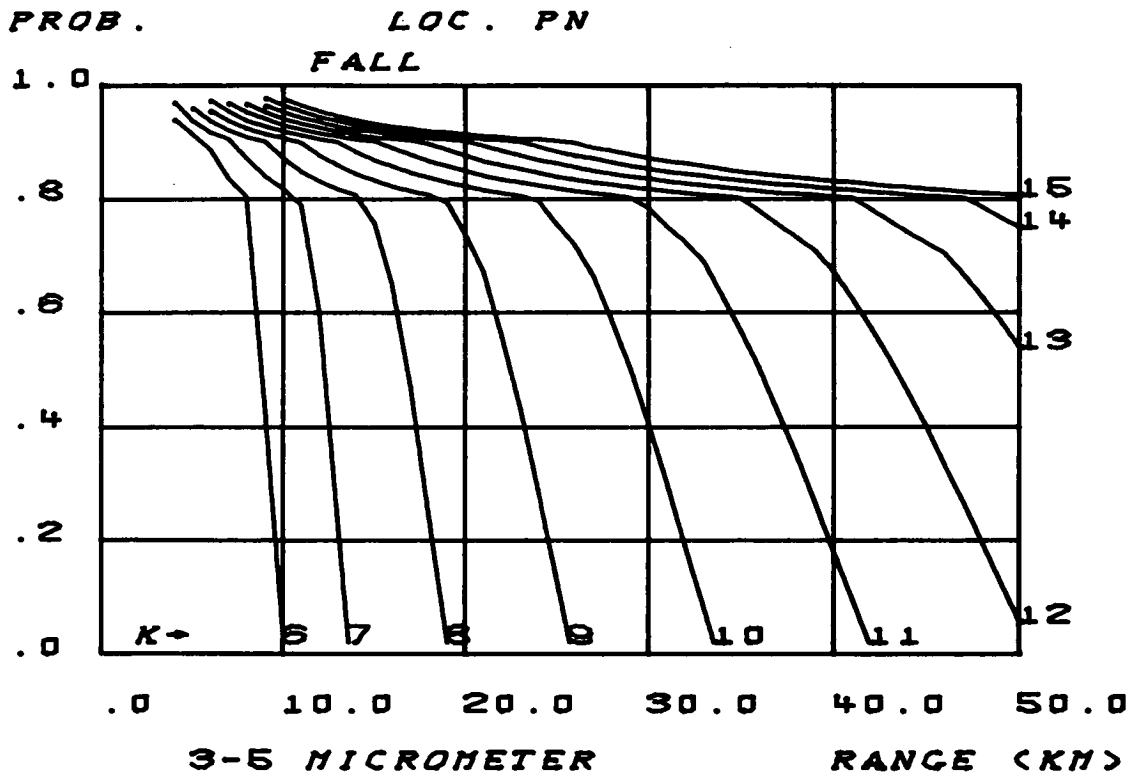


FIGURE - 70

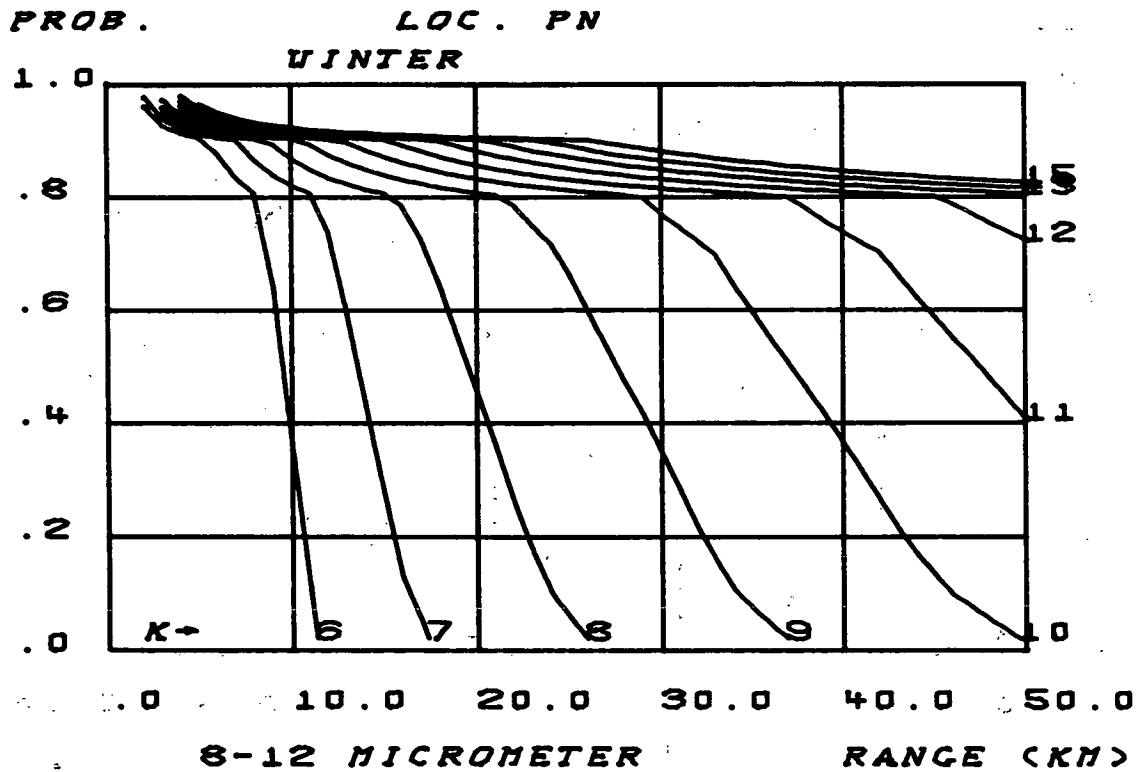
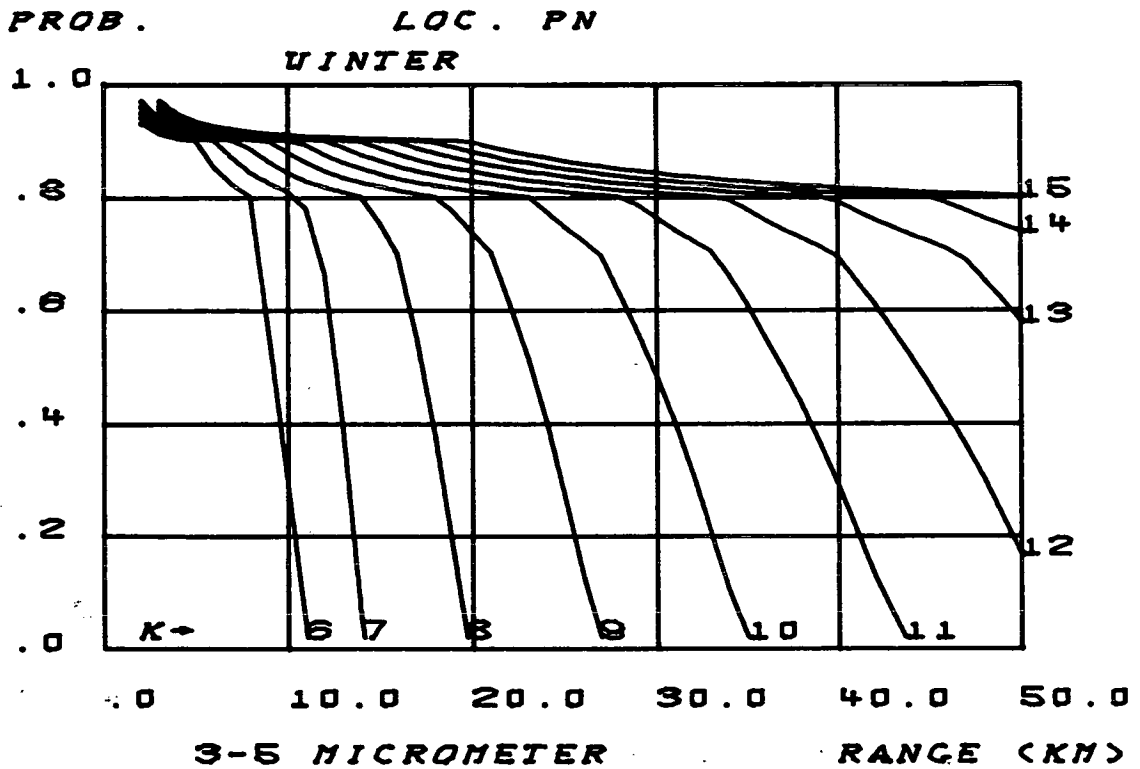


FIGURE - 71

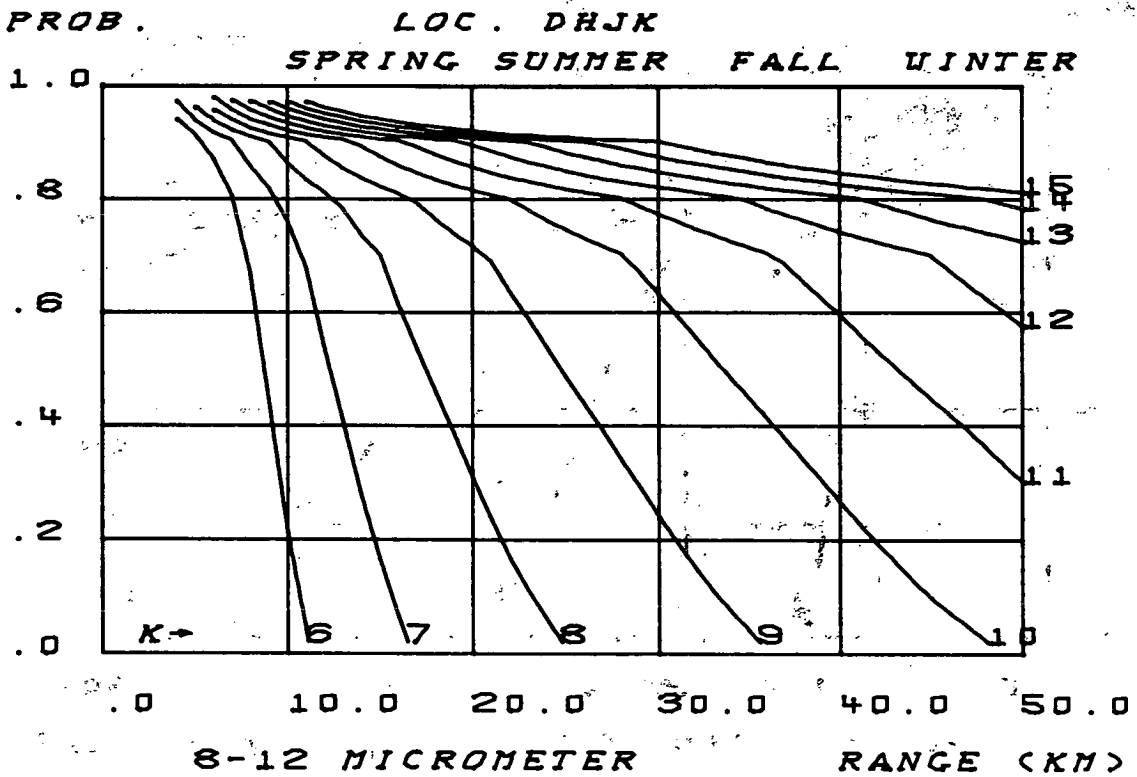
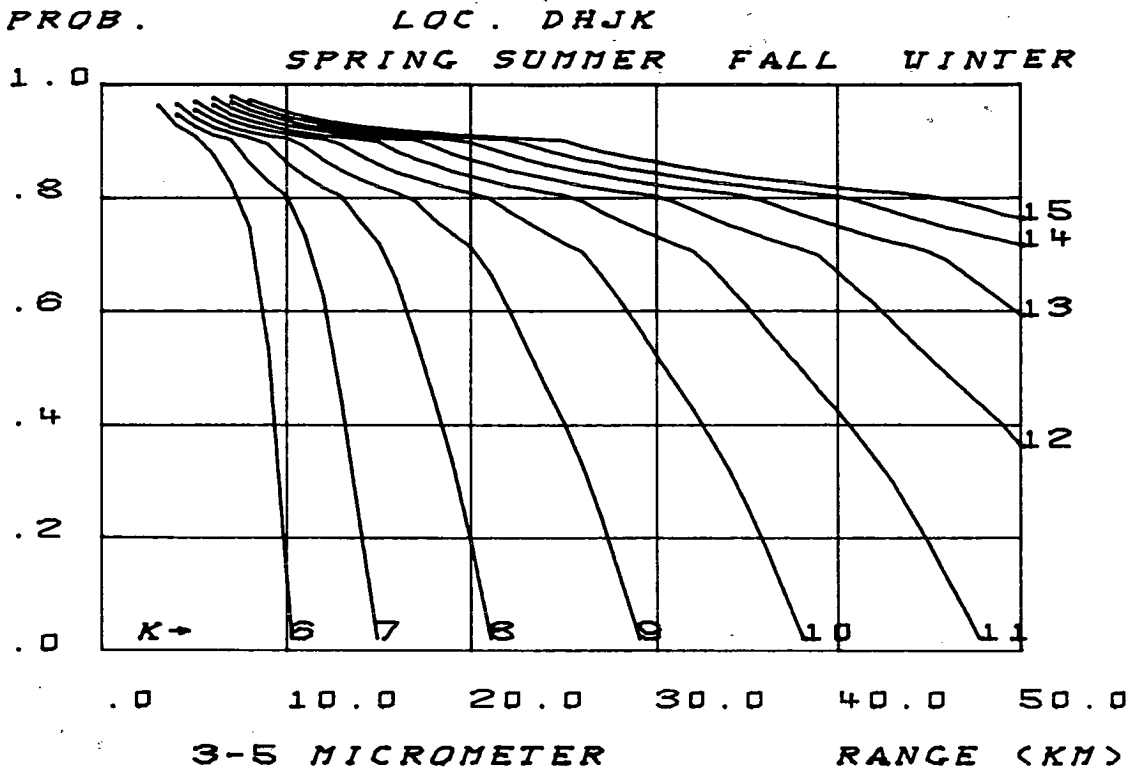


FIGURE - 73

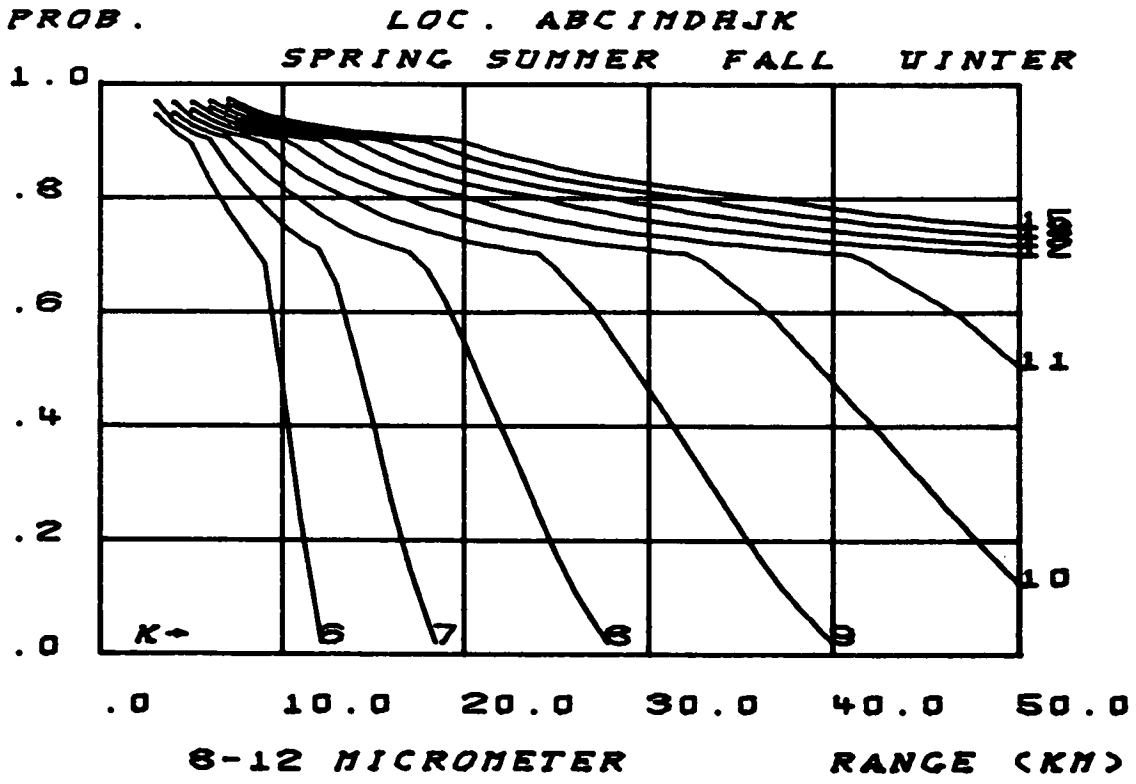
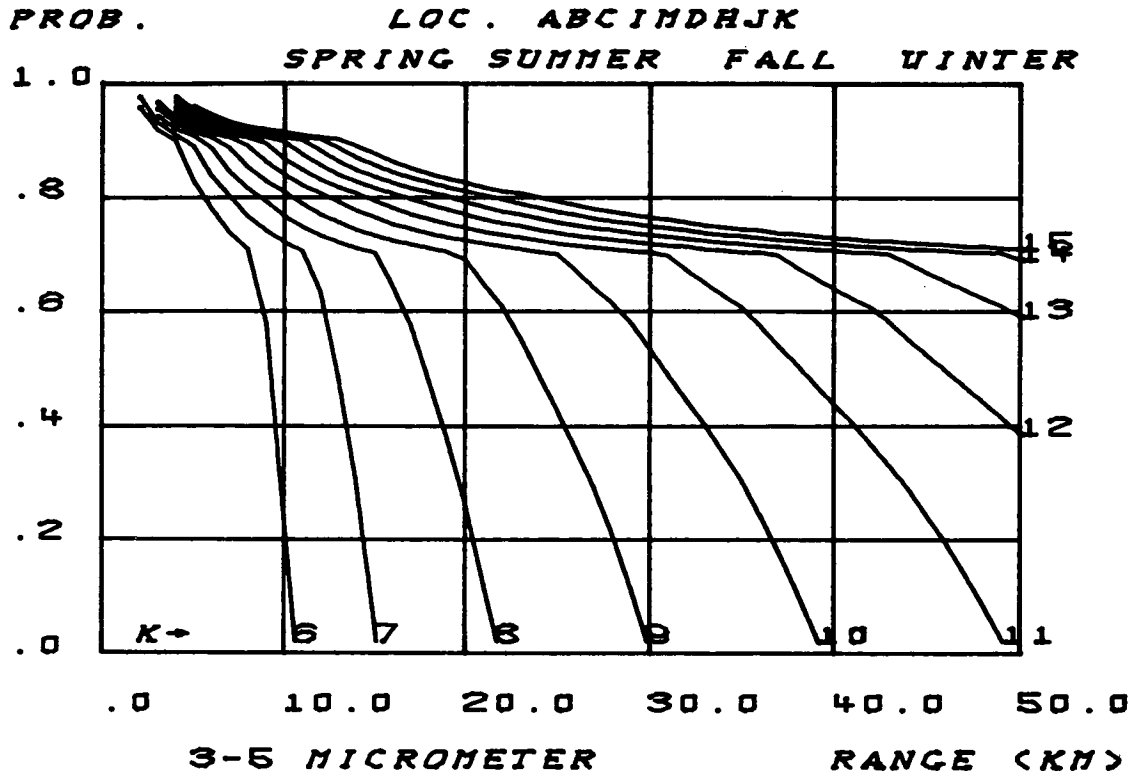


FIGURE - 74

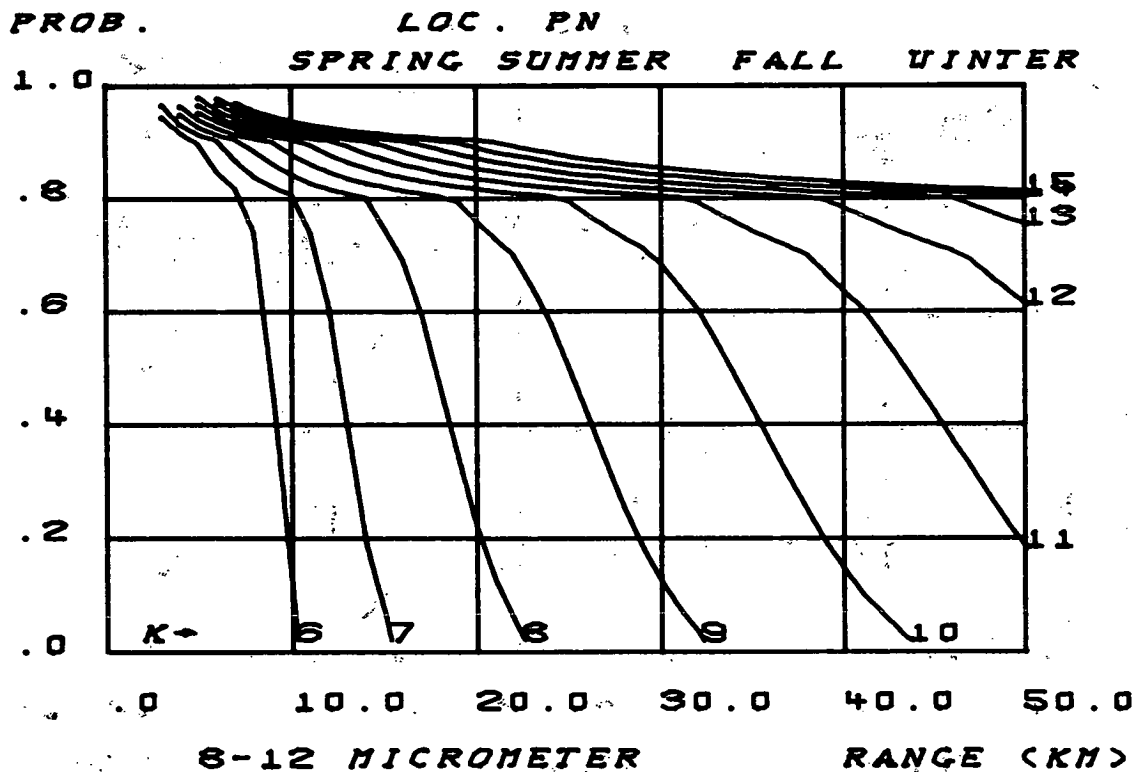
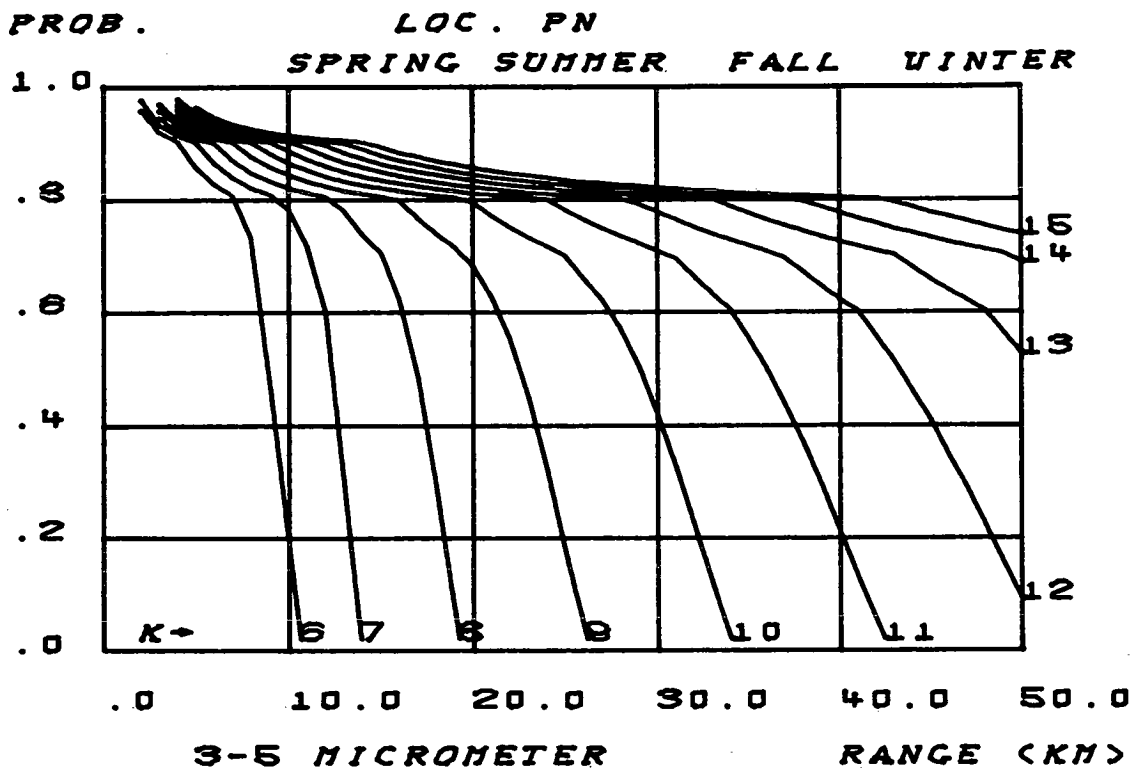


FIGURE - 75